

Novel Nonlinear Sliding Mode Observers for State and Parameter Estimation

by
Sagar Mehta

B.Tech., PES Institute of Technology, 2015

Thesis Submitted in Partial Fulfillment of the
Requirements for the Degree of
Master of Applied Science

in the
School of Mechatronic Systems Engineering
Faculty of Applied Sciences

© Sagar Mehta 2018
SIMON FRASER UNIVERSITY
Spring 2018

Approval

Name: Sagar Mehta

Degree: Master of Applied Science

Title: Novel Nonlinear Sliding Mode Observers for State and Parameter Estimation

Examining Committee:

Chair: Jiacheng Wang
Assistant Professor

Krishna Vijayaraghavan
Senior Supervisor
Associate Professor

Mehrdad Moallem
Supervisor
Professor

Siamak Arzanpour
Examiner
Associate Professor

Date Defended/Approved: [April 16th, 2018]

Abstract

Interest in the area of state and parameter estimation in nonlinear systems has grown significantly in recent years. The use of sliding mode observers promises superior robustness characteristics that make them very attractive for noisy uncertain systems. In this thesis, a novel Time-Averaged Lyapunov functional (TAL) is proposed that examines the effect of Gaussian noise on the stability of a sliding mode observer. The TAL averages the Lyapunov analysis over a small finite time interval, allowing for intuitive analysis of noises and disturbances affecting the system. Initially, a sliding mode observer for a linear system is analysed using the proposed functional. Later, the results are extended to various classes of nonlinear systems. The necessary and sufficient conditions for the existence of the observer are presented in the form of Linear Matrix Inequality (LMI), which can be explicitly solved offline using commercial LMI solvers. The types of nonlinearity examined are fairly general and embodies Lipschitz, bounded Jacobian, Sector bounded and Dissipative nonlinearities. All the system models considered are highly nonlinear and consist of system disturbances and sensor noise. The proposed sliding mode observer provides less conservative conditions to verify the existence and stability of the observer. The observer can also be effectively used for unknown parameter estimation as outlined in the final chapter of this report. Various examples are provided throughout the premise to support the proposed observer design and demonstrate its effectiveness.

Keywords: Sliding mode observers; Time Averaged Lyapunov functional; Unknown Parameter estimation; State estimation; Sector Bounded Nonlinearities

To My Parents, Friends and Family

Acknowledgements

Firstly, I would like to express my sincere gratitude to my supervisor, Dr. Krishna Vijayaraghavan for his continuous help and support throughout the course of my program. He has been a constant source of knowledge and inspiration. Without his guidance and persistent motivation, this dissertation would not have been possible. Further, I would also like to sincerely thank my co-supervisor Dr. Mehrdad Moallem who has been very supportive and welcoming with my work. Also, my deep gratitude goes to Dr. Siamak Arzanpour for examining this dissertation.

Furthermore, I would also like to take this opportunity to acknowledge and thank all my professors, Dr. Jason Wang, Dr. Kevin Oldknow, Dr. Woo Soo Kim and Dr. Daniel Lee for their support and motivation to take my academic steps so far. Their advice and support have been highly motivational and inspiring in my academic life.

Lastly, I would like to thank my parents, friends and family for providing me with unfailing support and continuous encouragement throughout my years of study and through the process of researching and writing this thesis. This accomplishment would not have been possible without them.

Table of Contents

Approval.....	ii
Abstract.....	iii
Dedication.....	iv
Acknowledgements.....	v
Table of Contents.....	vi
List of Figures.....	viii
List of Synonyms.....	ix
Chapter 1. Introduction.....	1
1.1. Nonlinear observers.....	2
1.2. Nonlinear adaptive observers.....	4
1.3. Sliding mode observers.....	6
1.4. Time averaged Lyapunov.....	9
1.5. Purpose and Motivation of this work.....	10
Chapter 2. Analysis of Sliding Mode Observers Using a Novel Time-Averaged Lyapunov Functional.....	12
2.1. Time averaged Lyapunov.....	15
2.2. Sliding mode using the time averaged Lyapunov (TAL) function on a simple diagonal system.....	16
2.2.1. Sliding mode observer design.....	20
2.3. Numerical Example.....	24
2.3.1. Example 1: Rössler Attractor System.....	24
Chapter 3. Sliding Mode Observer Design for a Lipschitz Nonlinear System.....	31
3.1. System Model.....	31
3.2. Observer design.....	32
3.3. Comparing Luenberger-like observer design using TAL with sliding mode observers.....	40
3.4. Illustrative examples.....	44
3.4.1. Example 1: Double Spring-Mass System.....	44
3.4.2. Example 2: Rössler Attractor System.....	47
Chapter 4. Adaptive Sliding Mode Observers for Sector-Bounded Nonlinear Systems.....	52
4.1. System Model.....	52
4.2. Observer Design.....	54
4.2.2. Example 1: 4th order nonlinear system.....	62
4.2.3. Comparing EKF based observers with proposed observer design.....	66
4.2.4. Dissipative nonlinear case.....	71
4.2.5. Example 2: Dissipative nonlinear system.....	76
Chapter 5. Conclusion and Future work.....	81

References.....83

List of Figures

Figure 2.1. Response of 1-D system with $\rho = 10$ and $Q = 0.01$	18
Figure 2.2. Response of 1-D system with $\rho = 10$ and $Q = 1$	19
Figure 2.3. Response of 1-D system with $\rho = 10$ and $Q = 100$	19
Figure 2.4. Response of 1-D system with $\rho = 100$ and $Q = 100$	20
Figure 2.5. Rössler Attractor	25
Figure 2.6. State $X1$ and its estimation	27
Figure 2.7. State $X2$ and its estimation	28
Figure 2.8. State $X3$ and its estimation	28
Figure 2.9. State Estimation error	29
Figure 2.10. System (Plant) Output	30
Figure 2.11. Observer Output	30
Figure 3.1. Double Spring-Mass System	44
Figure 3.2. Convergence of State $x1$	45
Figure 3.3. Convergence of State $x2$	46
Figure 3.4. Convergence of State $x3$	46
Figure 3.5. Convergence of State $x4$	47
Figure 3.6. Rössler Attractor	48
Figure 3.7. Convergence of State $x1$	50
Figure 3.8. Convergence of State $x2$	50
Figure 3.9. Convergence of State $x3$	51
Figure 4.1. Two-mass spring system	62
Figure 4.2. Convergence of State $x1$	64
Figure 4.3. Convergence of State $x2$	64
Figure 4.4. Convergence of State $x3$	65
Figure 4.5. Convergence of State $x4$	65
Figure 4.6. Unknown Parameter ' μ ' Estimation	66
Figure 4.7. Estimation error in state $x1$	68
Figure 4.8. Estimation error in state $x2$	69
Figure 4.9. Estimation error in state $x3$	69
Figure 4.10. Estimation error in state $x4$	70
Figure 4.11. Unknown Parameter ' μ ' Estimation using EKF	70
Figure 4.12. Gear train dissipative system	76
Figure 4.13. Estimation of state $X1$	78
Figure 4.14. Estimation of state $X2$	78
Figure 4.15. Estimation of state $X2$	79
Figure 4.16. Unknown Parameter ' μ ' Estimation	80

List of Synonyms

A	System matrix
B	Direction vector along which the unknown parameter and component of states affect the system dynamics
C	Output matrix
D	Direction matrix from which the state interacts with the unknown parameter
E	Direction vector for the nonlinearity
F	Direction matrix for the disturbance vector
G	Matrix used to bound the nonlinearity ϕ
H	Input Matrix
w	Unknown process disturbance noise
x	State vector
y	Output state vector
v	Measurement noise vector
\hat{x}	State estimate vector
\tilde{x}	State estimation error vector
ϕ	System nonlinearity
$sign(o)$	Signum function
ρ	Sliding mode gain
$\bar{\tilde{x}}_1$	State vector of the autonomous sub-system
$\bar{\tilde{x}}_{1-i}$	i th component of the state vector ($\bar{\tilde{x}}_1$)
$erf(\circ)$	Error function
$\mathcal{E}(\circ)$	Expected value function
$\Lambda(\circ)$	Eigenvalue function
$u_{\tilde{y}-eq}$	Equivalent output injection signal
$\rho_{c-i}(\bar{\tilde{x}}_1)$	Appropriate correction term
$\mathcal{P}(\circ)$	Probability of the event
$\Psi_c(\bar{\tilde{x}}_1)$	$diag(\rho_{c-i}(\bar{\tilde{x}}_1))$
subscript 1	States of the system in the non-null space of C
subscript 2	States of the system in the null space of C

Chapter 1.

Introduction

In order to completely analyze a control system, one needs to have full information of all the states that define the system. The states define the internal dynamics of the physical system in the form of variables and parameters. However, in practical situations it is not always possible to measure all the states of the system because of various technical or economic constraints. The use of sensors to measure every state is expensive and can induce significant errors such as stochastic noise and cyclical noises [1]. Additionally, the limited responsiveness of some sensors can introduce phase lag in the control system, thereby reducing the margin of stability [1]. Observers can reduce the sensor requirements and may improve disturbance rejection in such systems. An observer or a state-estimator is used to obtain an estimate of the system's internal states, given measurements of the input and output of the system. The chief consideration in the design of the observer is that the state estimate should be able to converge to the true state value of the observed system. This state estimate can also be used for many different observer-based applications like unknown parameter estimation, fault estimation and fault reconstruction [2], [3].

Most of the real world systems are complex in nature, and thus have some kind of uncertainty associated to them. Therefore, it is always challenging to transform these physical systems into their mathematical models without introducing any uncertainty. In addition, other uncertainties/disturbance may also originate from the system's operating environment. These disturbances may be in the form of unknown system disturbances and sensor noise. The sensor noise that appears in many control systems is in the form of additive white Gaussian noise. Also, for systems where the exact form of sensor noise is not known, the noise can be approximated to be Gaussian in nature [4]. This is because the sensor noise is nondeterministic in nature and can be characterised by a zero mean Gaussian distribution. The Gaussian approximation of these errors, makes it fairly easy to determine their effect on the system by analysing its distribution (normal distribution). The sensor noise can show up in systems because of temperature changes (thermal noise), transmission (electronic circuit noise), and black body radiation

(electromagnetic radiation). These additive sensor noises can have a severe effect on the observer's state estimate and controller signals, especially for cases with large sensor noise [5], [6]. Further, in many cases the system dynamics along with the actual states of the system are unknown and have to be reconstructed from the output data. Modelling errors often arise from the approximation of these system dynamics, especially in the presence of uncertainty. Hence, the observer design needs to be highly robust in order to be stable in the presence of such modeling uncertainties[7].

1.1. Nonlinear observers

The complex nature of nonlinear systems makes it challenging to design observers, largely because there is no defined method that works for all classes of nonlinearities. Plenty of research has been carried out in order to develop effective observers for various classes of nonlinear systems [8]–[26].

Many physical systems can be expressed as a linear system with an additive nonlinearity in the form $\dot{x} = Ax + \phi(x) + w, y = Cx + v$. Here, a linear feedback observer in the form $\dot{\hat{x}} = A\hat{x} + \phi(\hat{x}) + L(y - C\hat{x})$ can be designed. For cases where the nonlinearity satisfies a Lipschitz condition ($|\phi(x_2) - \phi(x_1)| < \gamma|x_2 - x_1|$), linear feedback observers have been developed for disturbance-free nonlinear systems ($w = 0, v = 0$) (DFNS)[27]–[31]. These observers utilize the robustness of the linear observer to satisfy the algebraic Riccati equation (ARE), $(A - LC)^T P + P(A - LC) + \epsilon\gamma^2 I + \epsilon^{-1}PP < 0$ and there is an inherent limit on the size of the Lipschitz constant. Observers for DFNS Lipschitz systems have even been extended to sensor fault detection[32], to actuator fault detection [33]and to unknown parameter estimation[34], [35]. DFNS observer design has been extended to nonlinearities with bounded Jacobian (Matrix Lipschitz) condition ($|\phi(x_2) - \phi(x_1)| < |G(x_2 - x_1)|$) [36], [37] wherein the observer is able to accommodate an equivalent Lipschitz constant particularly when G is a sparsely populated. For DFNS with a monotonically increasing nonlinearity ($[(x_2 - x_1)^T G[\phi(x_2) - \phi(x_1)]] > 0$), observers have been designed using an extension of the circle criterion[38], [39]. In the presence of sensor noise and input disturbances, observers cannot guarantee stability in the traditional sense. Some nonlinear observers in the presence of noise rely on linearizing the system dynamics about their estimates.

A variety of methods are available for the design of nonlinear observers, of which some of the most popular are: Geometric, Lie-Algebraic, Backstepping, Unscented Kalman filter approach, Lyapunov-based, High gain and sliding mode observers. Various cases of Lyapunov-based observers are discussed in literature [8], [9], [11], [17], [20], [22], [23], [40], [41]. Thau [40], presents a method to analyze the stability of the state estimation error, however, it fails to suggest a correct approach to design the observer gain for the system. Thus, making it infeasible for higher-order systems since selecting the appropriate gain makes it a trial and error process. Kou et al [42] provides conditions for the existence of a Lyapunov like function, although they are very difficult to satisfy. This method is further generalized in [9], nonetheless the system fails to satisfy some fundamental restrictive conditions. A design algorithm is proposed in [22] to develop an appropriate observer gain by using Lyapunov auxiliary theorem, but it is restricted to the condition that the system should be locally asymptotically stable at the origin. Further, Deutscher [8] provides a Linear matrix equation to solve for the conditions provided in [22] numerically. The authors in [17] provide a solution to solve for a special class of nonlinear systems (where the nonlinearity satisfies a certain multivariable sector condition) using convex optimization. Similarly, an observer design for a class of nonlinear discrete-time systems is presented in [23].

In many cases, geometric methods [12]–[14], [19], [43] are used where the observer design is achieved by transforming the nonlinear system into a linear one. An extended linearization technique for observer design is proposed in [14]. It uses a method of linearizing in which the nonlinear system is specified by constant operating points. An extended Luneberger observer is proposed in [19] where the system is transformed into the nonlinear observer canonical form and an extended linearization technique is implemented on a MIMO (Multiple-Input Multiple-Output) system.

Another eminent technique known as the Lie Algebraic approach [10], [24], [44], [45] is also used to design observers for nonlinear systems. The main objective of this approach is to transform the nonlinear system to a linear system and then design a suitable linear observer for the new system. Also, an alternative approach [44] is to transform the nonlinear system into a system where all the nonlinearities are measurable. Hence, for a case where the nonlinearity solely depends on the output, the observer is fairly easy to design by using various output injection and pole placement

techniques. Although, there are some shortcomings to this approach since the nonlinearity is assumed to be precisely known. This may introduce various modelling errors, which may in turn affect the state estimation error. It is also very complex to calculate the appropriate transformation for the system. Also, using this [44] approach for higher order systems is impractical since it introduces various partial differential equations. The results of [44] are extended in [10], making it simpler to solve, although some restrictions still exist. Also the results of [44] are further extended to a multi-input multi-output systems in [24]. The authors of [45] present an approach for the transformation of Single-Input Single-Output systems for designing adaptive observers.

In addition to the various classes of observers discussed above, High gain observers are utilized for their robust nature in error and disturbance rejection [46]. Here, the gain matrix is switched between two gain values. By using a higher gain value during the transient phase, the state estimates are quickly recovered. Once the state estimation error reaches to its minimum, the gain is switched to smaller value to reduce the effect of sensor noise. Khalil in [47] provides a detailed study on high-gain observer and their implementation in robust controller design. It also explicitly examines the peaking phenomenon in high gain observers which is observed to eliminate disturbances in the form of modelling errors. However, this phenomenon can also make the closed loop system unstable by directly transforming the erratic behavior from the observer to the actual system. Hence, the controller needs to be globally bounded in order to remain unaffected by the peaking behavior while designing the high gain observer. These observers are further explored in the domain of adaptive nonlinear observer which are discussed below.

1.2. Nonlinear adaptive observers

Many adaptive observer design techniques have been proposed to deal with unknown inputs to systems. Some of the earliest research was based on viewing the uncertainty in parameters as nonlinearities [48], [49] (other types of system uncertainties are not weighed). Polycarpou et al. [50] developed a robust adaptive observer for nonlinear uncertain systems, where the uncertainty was a result of both

unknown nonlinear functions and parameters. The observer is based on the assumption that the unknown function satisfies a certain triangular bounds condition homologous to the ones seen in [51][52]. Here, the unknown nonlinearities conform to some conditions defined by 'bounding' functions ($\dot{x} = f_o(x) + g_o(x)u + \phi * \zeta(x) + \Delta(x, y)$) which consist of the product of known functions ($\zeta(x)$) and unknown parameters (ϕ). Later Bastin et al. [53] presented an adaptive observer for a noise-free system of the form $\dot{x} = Ax + B(t)\mu$, where the unknown parameter μ is unaffected by the system states and measurements. Besançon et al. [54] presents a stable adaptive observer for noise free systems where the nonlinearity is a function of input and measurable outputs and transformable to an output nonlinear form given by $\dot{x} = Ax + B(y, t)u$. The results are further extended to systems with an input disturbance (w), $\dot{x} = Ax + B(y, t)\mu + w$ by Jung et al.[55]. Rajamani et al. [56] study systems where the nonlinearity depends on the entire state vector. These results have been further extended by Cho and Rajamani [57] for a noise-free Lipschitz nonlinear system of the form $\dot{x} = Ax + B(u, x)\mu + \Phi(x, u)$; $y = Cx$, where the nonlinearity isn't necessarily a stringent function of the measurement. These results are further expanded to include bounded input noise and other disturbances affecting the observer gain in [58]. However, most of the literature presented above [56][28][55], requires the Lyapunov matrix used in establishing the Lyapunov stability and uncertain parameters to fulfil a strictly positive-real type condition, $P > 0$, $b^T P C^\perp = 0$. Subsequently, the design of the observer error dynamics is confined to systems where b lies in the range space of C^T (since $P \neq 0$, $b \in \mathcal{R}(C^T)$), which is a strict condition for finding a P such that $b^T P C^\perp = 0$. Vijayaraghavan [59] addresses this issue by proposing an observer design for simultaneous state and multiple unknown parameter estimation but limited to classes of Lipschitz nonlinearity with no measurement noise. Vijayaraghavan et al [60] has also developed an adaptive observer based on H_∞ observer for the simultaneous estimation of state and unknown parameters by minimizing a cost function composed of a sum of the square integrals of the estimation error.

Elsewhere, observers have been developed to deal with parameter estimation in noisy systems. Many observers have used Extended Kalman Filter (EKF) based methods [61][62], unscented kalman filter(UKF) based methods [63][64][65] and some other recursive least squares method [66][67]. However, EKF and UKF observers are computationally intensive since they require an online calculation to solve the Riccati

equation and Jacobian. These observers also need to consider a virtual disturbance parameter (VPD) for the Kalman filter, for which the observers do not provide any suitable methods. Also, EKF and UKF require initial parameter and state estimates to generate precise estimates. However, it still does not yield any conditions that can guarantee the existence of the observer. Ahrens et al. [68] presents a high-gain observer design that transitions between two gain values to retrieve the system states and to minimize the effect of measurement noise in the neighborhood of the estimation error. Also, Esfandiari et al [69] presents the appropriate choice of the observer gain H in order to stabilize the homogenous error. This allows for the output feedback control to redeem the performance achieved by the state feedback control. However, high gain observers are not ideal for noisy systems since these observers become very sensitive to noise as the gain increases. Additionally, they also suffer from the 'peaking phenomenon' as mentioned in Khalil et al [69], [70]. This 'phenomenon' is a result of the high gain which causes an initial spike in the response of the state estimates. This results in high instability in certain types of systems. It is important to note that adaptive observers are usually only efficient for overcoming linear parametric uncertainty whereas recent geometric approaches tend to require strict geometric conditions on the systems considered.

1.3. Sliding mode observers

Sliding mode control is more suitable for disturbance rejection particularly when the disturbance vector lies in the range space of the output. Observers utilizing sliding mode control tend to be more robust and are completely insensitive to the nominal matched uncertainty [71][72]. A discontinuous feedback signal is added to the observer dynamics to drive it onto a sliding manifold (a subspace of the state-space) within a finite amount of time[71]. Once a suitable sliding manifold is designed, the closed loop system is nearly insensitive to external disturbances and parametric uncertainties because of the confined motion of the state trajectories within the sliding surface, which eventually is directed to the origin.

Previously, Edwards et al [73] presented an approach using the notion of equivalent output injection in which the observer signal can estimate the fault to a desired level of accuracy. The results were later extended to include sensor faults [74]. However, these early results do not account for any uncertainties. Since sliding mode observers force the observer error in the range space of the output to converge to zero in finite time, this transforms some classes of non-Lipschitz nonlinearities into Lipschitz nonlinearities. Additionally, for some Lipschitz systems, sliding mode observers will alter the Jacobian of the nonlinearity and aid with the observer design. Hence compared to linear finite gain observers such as H_∞ observers, sliding mode observer can extend the observer design. Alessandri [75] proposed a sliding mode observer for a Lipschitz nonlinear systems. When the disturbance and the noise are bounded, the observer is shown to be non-divergent. It must be noted that the paper fails to clearly identify the advantage of using both continuous and sliding mode feedback terms. The paper makes use of the Lyapunov criterion to demonstrate the feasibility of the observer. It determines an upper bound on the sliding mode feedback term and designs the linear gain to compensate this upper bound. Hence, the sliding mode term would serve to restrict rather than aid the observer design. Further, the existence of the observer cannot be established for Gaussian noise. Elsewhere sliding mode is used to estimate faults [76], [77], reject unknown input [78] and design observer for high relative degree nonlinear systems with no sensor noise [79]. However previous sliding mode observers have not adequately considered unknown inputs and sensor noises.

For a simple linear system given by:

$$\begin{aligned}\dot{x} &= Ax + Hu \\ y &= Cx\end{aligned}\tag{1.1}$$

where $A \in \mathbb{R}^{n \times n}$, $H \in \mathbb{R}^{n \times q}$, $C \in \mathbb{R}^{m \times n}$ are the system matrices of the appropriate dimensions and where $m \leq n$. $x \in \mathbb{R}^n$, $y \in \mathbb{R}^m$ and $u \in \mathbb{R}^q$ are the state vector, system output and control input respectively,

The sliding mode observer is written as:

$$\dot{\hat{x}} = A\hat{x} + Hu + Du_{\hat{y}} \quad (1.2)$$

$$u_{\hat{y}} = \rho \times \text{sign}(y - C\hat{x}) \quad (1.3)$$

Where \hat{x} represents the estimated state of the observer and $u_{\hat{y}}$ is a sliding mode input. The discontinuous sliding mode signal given by $u_{\hat{y}}$ is typically analyzed using the average value of the applied observer injection signal. This average value of injection signal contains useful information about the mismatch between the model used to define the observer and the actual plant[80].

Previous research on sliding mode observers has only considered a bounded disturbance to the system. We will examine Walcott et.al. [81] to illustrate this approach. The system model is of the form

$$\begin{aligned} \dot{x} &= Ax + Hu + Dd(x, u, t) \\ y &= Cx \end{aligned} \quad (1.4)$$

where $D \in \mathbb{R}^{n \times p}$ is the direction matrix thorough which the disturbances acts on the system and $d(x, u, t) \in \mathbb{R}^p$, is the unknown disturbance vector with $p \leq m$. When d is bounded with $|d(x, u, t)| \leq \bar{d}, \forall x, u, t > 0$ and $\text{rank}(CD) = p$. Hence, a sliding mode observer can be constructed as

$$\dot{\hat{x}} = A\hat{x} + Hu + L(y - C\hat{x}) + Du_{\hat{y}} \quad (1.5)$$

$$u_{\hat{y}} = -\rho(C_1 D)^{-1} \times \text{sign}(C_1(\hat{x} - x)) \quad (1.6)$$

Where L is the linear feedback gain, $u_{\hat{y}}$ is a sliding mode input, $C_1 \in \mathbb{R}^{m \times (n-p)}$ represents the matrix in the transformed space where the output measurements are available. The resulting observer dynamics are given by

$$\dot{\hat{x}} = (A - LC)\hat{x} + D(d - u_{\hat{y}}) \quad (1.7)$$

Using a Lyapunov function $V = \frac{1}{2}(C_1\hat{x})^T(C_1\hat{x})$ the authors demonstrated that the observer rejects the disturbance d when $\rho > \|C_1(A - LC)e - C_1Dd\|$ [82].

However, previous literature does not analyze the effect of Gaussian noise on a sliding mode observer when the error approaches zero. The first part of this thesis analyzes the effect of Gaussian noise on sliding mode observer over the entire error state space using an alternative Lyapunov candidate defined as a “Time-averaged Lyapunov function”. A similar concept had been proposed in Michel et al. [83] for scalar switched system. However, the author averages out the derivative and further does not consider the effect of noise.

1.4. Time averaged Lyapunov

The TAL provides a procedure for analysing the stability of the observer that is in line with the traditional concept of Lyapunov stability. The TAL averages the Lyapunov analysis over a small finite time interval, allowing for intuitive analysis of noises and disturbances. While similar time-averaging is proposed in the form of time-averaged Lyapunov function derivatives (TALFD) in Michel et al.[83], the TALFD requires the system to be continuous and the results do not apply to noisy sliding mode observer systems. The TAL bears some resemblance to Lyapunov–Krasovskii (LK) functionals [84], [85]. LK functionals analysis has been limited to analyzing stability of time delay functions. Here LK functionals have a quadratic term and a term that is integrated over the delay period. When the time derivative of the LK is calculated, the integral term is integrated by parts and an additional matrix product gets appended to the quadratic term. The analysis then requires both the augmented quadratic term as well as the term within the integral to be negative. Unlike LK analysis, the TAL aims to analyze the time-averaged stability of the observer. To the best of the authors’ knowledge, LK functionals have not been used to average the effect of the sensor noise or input disturbance.

1.5. Purpose and Motivation of this work

This thesis presents a sliding mode observer design that uses a novel Time-Averaged Lyapunov functional to analyse the effect of external Gaussian noise on the system. The observer also serves as a state and unknown parameter estimator based on an optimal approach as demonstrated in the upcoming chapters. The proposed observer is further developed for different types of nonlinear systems which include Lipschitz, Bounded Jacobian, Sector Bounded and Dissipative nonlinearities. An extensive method for checking the existence conditions and computing the observer gains is presented in the form of Linear Matrix Inequality (LMI).

In chapter 2, a novel Time Averaged Lyapunov functional is proposed. The TAL is shown to satisfy all the requirements of a Lyapunov candidate function. To utilise the idea of the proposed functional on a sliding mode observer, a simple autonomous system is developed. The convergence rate of the system error dynamics is determined and later plotted with respect to different values of covariance ρ and Q . Later, a sliding mode observer is developed for a linear system in the presence of system and external sensor disturbances. The conditions for existence of the observer are provided and supported by a numerical example.

In chapter 3, the results of the previous chapter are extended to a nonlinear case with an additive nonlinearity ϕ . A sliding mode observer design for a Lipschitz nonlinear system is presented. The observer is developed by taking into consideration the effect of covariance (noise) affecting the system. A systematic approach to design the appropriate observer gains and existence conditions are presented. The minimum performance conditions are presented in the form of LMIs which can be solved offline using MATLAB. The conditions provided are less conservative and are compared with other linear gain observer designs to further demonstrate its effectiveness. The robust and less conservative behaviour of this observer are established using various numerical examples.

In chapter 4, the observer design is extended to a wider class of nonlinear systems which include sector bounded and dissipative nonlinearities. The design also estimates unknown system parameters along with the system states. A systematic approach to design the appropriate observer gains which also include the unknown

parameter gain values is developed. The minimum performance conditions are presented in the form of LMIs which can be solved offline using MATLAB. Later, conditions for the existence of the observer for a dissipative case are presented. Numerical examples are provided to demonstrate the effectiveness of the observer for each case.

Finally, the thesis is concluded in chapter 5 followed by future recommendations that will extend the scope of the work presented here.

Chapter 2.

Analysis of Sliding Mode Observers Using a Novel Time-Averaged Lyapunov Functional

Sliding mode observers are desirable for their robust nature towards parameter uncertainty, parameter variation, disturbance rejection and simple implementation. As compared to other observers, the sliding mode observer utilizes a signum function of the state estimate error in the feedback correction term. This allows for error dynamics to be confined along the sliding surface where the motion of the state trajectories are restricted within the sliding manifold. As seen in literature, previous work on sliding mode observers does not take into account the effect of external Gaussian noise on a nonlinear system [75], [79], [81], [82]

Hence, we first introduce a novel scheme to examine the stability of a linear system in the presence of such external disturbance on the system using a Time-averaged Lyapunov functional. Then, we develop a sliding mode observer for this linear system using the same functional and observe its stability. Later, an illustrative example is presented to show the effectiveness of the proposed observer.

The stability of a system in the presence of noise cannot be determined using traditional Lyapunov methods. To demonstrate this, we consider the following general linear system with input disturbance and sensor noise, which is assumed to be Gaussian in nature

$$\begin{aligned}\dot{x} &= Ax + Fw + Hu \\ y &= Cx + v\end{aligned}\tag{2.1}$$

In this system, $x \in \mathbb{R}^n$ is the state vector, $u \in \mathbb{R}^q$ is the vector of known inputs, w is a vector of unknown input disturbances, $y \in \mathbb{R}^m$ is the output vector and v is a vector of unknown measurement noise. A, F, H, C are known system matrices of appropriate dimensions. Without loss of generality, we can partition the system into two subsystems such that,

$$\dot{x} = \begin{bmatrix} \dot{x}_1 \\ \dot{x}_2 \end{bmatrix}, \quad C = [I_m \quad 0], \quad A = \begin{bmatrix} A_{11} & A_{12} \\ A_{21} & A_{22} \end{bmatrix} \quad (2.2)$$

Where the 1-subspace given by \dot{x}_1 , represents the set of states that have an output measurement available, whereas the 2-subspace given by \dot{x}_2 spans the other states of the system that have no measurements available at the output. I_m is a $m \times m$ identity matrix.

The observer is constructed as

$$\dot{\hat{x}} = A\hat{x} + Hu + \begin{bmatrix} I_m \\ L_2 \end{bmatrix} u_{\hat{y}} \quad (2.3)$$

With a sliding observer signal given by

$$u_{\hat{y}} = \rho \times \text{sign}(y - c\hat{x}) \quad (2.4)$$

The dynamics of the estimation error for this observer becomes

$$\dot{\tilde{x}} = A\tilde{x} + Fw - [I_m \quad L_2]^T u_{\hat{y}} \quad (2.5)$$

Where, $\tilde{x} = x - \hat{x}$

In the absence of noise (i.e $w = 0$ and $v = 0$) the system can be written as

$$\begin{aligned} \dot{x} &= Ax + Hu \\ y &= Cx \end{aligned} \quad (2.6)$$

The dynamics of the estimation error for this observer becomes

$$\dot{\tilde{x}} = A\tilde{x} - \begin{bmatrix} I_m \\ L_2 \end{bmatrix} u_{\tilde{y}} \quad (2.7)$$

Where L_2 is the observer gain that acts on the 2-subspace of the system.

The \tilde{x}_1 -dynamics of the observer can be written as,

$$\dot{\tilde{x}}_1 = A_{11}\tilde{x}_1 + A_{12}\tilde{x}_2 - u_{\tilde{y}} \quad (2.8)$$

If we choose a sufficiently large ρ , s.t $\rho > \max(A_{11}\tilde{x}_1 + A_{12}\tilde{x}_2)$, by using an appropriate sliding mode input, we can drive $\tilde{x}_1 \rightarrow 0$, $\dot{\tilde{x}}_1 \rightarrow 0$ and $u_{\tilde{y}} \rightarrow u_{\tilde{y}-eq}$, in finite time with the equivalent average value of $u_{\tilde{y}}$ given by [72], [82]

$$u_{\tilde{y}-eq} = A_{12}\tilde{x}_2 \quad (2.9)$$

Hence, the \tilde{x}_2 - dynamics can be written as

$$\dot{\tilde{x}}_2 = (A_{22} - L_2A_{12})\tilde{x}_2 \quad (2.10)$$

If we begin with a quadratic Lyapunov candidate function

$$V = \tilde{x}^T P \tilde{x} > 0 \quad (2.11)$$

The derivative of the function is given by

$$\dot{V} = 2\tilde{x}_2^T P_{22}(A_{22} - L_2A_{12})\tilde{x}_2 \quad (2.12)$$

Hence, the Lyapunov can be made negative by making $A_{22} - L_2A_{12}$ Hurwitz. However, in the presence of noise,

$$\begin{aligned} \dot{V} = & \tilde{x}^T (A^T P + PA) \tilde{x} + 2\rho \tilde{x}^T P \begin{bmatrix} I_m \\ L_2 \end{bmatrix} \text{sign}(y - c\hat{x}) \\ & + 2\tilde{x}^T P F w \end{aligned} \quad (2.13)$$

As seen from Eq(2.13), an additional terms gets appended to the original Lyapunov derivative where the noise term given by: $2\tilde{x}^T P F w$, cannot be ensured to be negative. Therefore, the system cannot be shown to be stable. Hence, we introduce a time averaged Lyapunov (TAL).

2.1. Time averaged Lyapunov

We will introduce a time-averaged Lyapunov function (TAL) candidate as follows $P > 0$

$$V := \frac{1}{T} \int_{t-T}^t V_l(\tau) d\tau = \frac{1}{T} \int_{t-T}^t \tilde{x}^T(\tau) P \tilde{x}(\tau) d\tau \quad (2.14)$$

where T is an arbitrary time window. Notice that for a constant dt ,

$$V(t + dt) = \frac{1}{T} \int_{(t+dt)-T}^{t+dt} V_l(\tau) d\tau \quad (2.15)$$

By replacing τ with $\tau + dt$ inside the integral, and noting that dt is constant we find

$$\begin{aligned}
\dot{V} &= \frac{V(t+dt) - V(t)}{dt} \\
&= \frac{1}{T} \int_t^{t+T} \frac{V_I(\tau+dt) - V_I(\tau)}{dt} d\tau \\
&= \frac{1}{T} \int_t^{t+T} \dot{V}_I d\tau
\end{aligned} \tag{2.16}$$

Hence, the derivative of the TAL is equal to the time-averaged derivative of the underlying Lyapunov function. Compared to a quadratic Lyapunov function, the TAL is also positive definite. Hence if we can show that $\dot{V} < 0, \forall \tilde{x} \notin \mathbb{D}, \dot{V} = 0, \forall \tilde{x} \in \mathbb{D}$, then the system converges to a subspace in \mathbb{D} . Further, like the quadratic Lyapunov function, the TAL is radially unbounded as $V(\tilde{x}) \rightarrow \infty$ when $\|\tilde{x}\| \rightarrow \infty$. The quadratic Lyapunov function has a zero value only when $\tilde{x} = 0$. However, the TAL is zero only when $\tilde{x}(\tau) = 0 \forall \tau \in [t-T, t]$. Hence the TAL may impose a stronger constraint on \tilde{x} . The TAL will be used to study observer stability in the presence of sensor noise and input disturbances.

2.2. Sliding mode using the time averaged Lyapunov (TAL) function on a simple diagonal system

From eq(2.8) and eq(2.10) it can be seen that the time scale of the \tilde{x}_1 -dynamics of the observer is significantly faster than the time scale of the \tilde{x}_2 -dynamics. To better understand the observer (2.3), we will first consider a simple autonomous system corresponding to the \tilde{x}_1 -dynamics. Consider

$$\dot{\chi}_i = -\rho \text{sign}(\chi_i + v_i), v_i \sim (0, Q_i) \tag{2.17}$$

Where, v_i is the zero mean Gaussian noise with a covariance defined by Q_i

If we define

$$V_I = \chi^T \chi \quad (2.18)$$

Then

$$\dot{V}_I = -2\rho \chi^T \text{sign}(\chi + v) \quad (2.19)$$

Notice that

$$\begin{aligned} & \frac{1}{T} \int_t^{t+T} \chi_i \text{sign}(\chi_i + v_i) d\tau \\ &= \frac{1}{T} \int_t^{t+T} \chi_i (1 - 2p_{\chi_i}) \text{sign}(\chi_i) d\tau \end{aligned} \quad (2.20)$$

Where, p_{χ_i} denotes the probability of an event given by $p_{\chi_i} = P(v_i > |\chi_i|) = 1/2 [1 - \text{erf}(|\chi_i|/\sqrt{2Q_i})]$.

Hence,

$$\dot{V}_I = -2\rho \sum (1 - 2p_{\chi_i}) |\chi_i| \quad (2.21)$$

Since $p_{\chi_i} > 0.5 \forall \chi_i > 0$, $\dot{V}_I < 0 \forall \chi > 0$. To determine the convergence rate in the neighbourhood of $|\chi_i| = 0$, we expand p_{χ_i} in this neighbourhood $|\chi_i| = 0$ using Taylor expansion and find

$$p_{\chi_i} = \frac{1}{2} - \frac{|\chi_i|}{\sqrt{2\pi Q_i}} \quad (2.22)$$

Hence

$$\dot{V}_I \approx \frac{2\rho}{\sqrt{2\pi}} \chi^T Q^{-\frac{1}{2}} \chi = 2 \times 0.3989 \rho \chi^T Q^{-1/2} \chi \quad (2.23)$$

Hence, in the neighbourhood of $|\chi_i| = 0$ the system behaves as

$$\dot{\chi} \approx -0.3989 \rho Q^{-1/2} \chi \quad (2.24)$$

This behaviour is illustrated using Figure 2.1- Figure 2.4 (using $dt = 10^{-6}$)

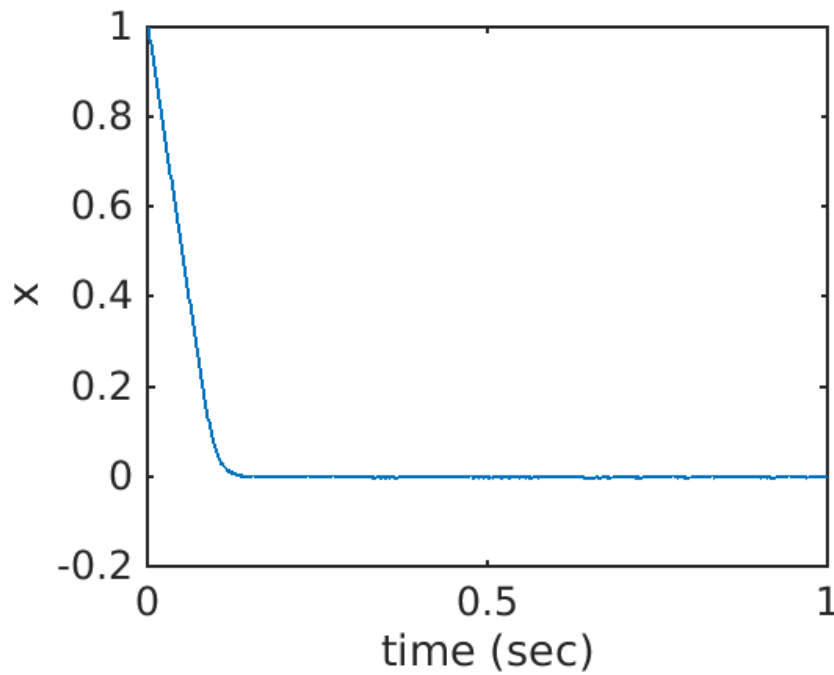


Figure 2.1. Response of 1-D system with $\rho = 10$ and $Q = 0.01$

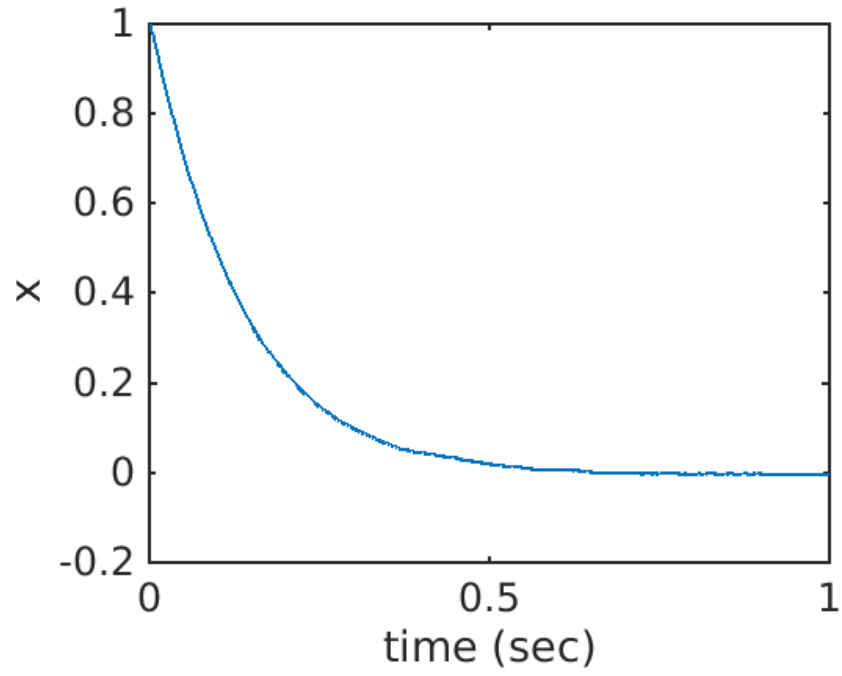


Figure 2.2. Response of 1-D system with $\rho = 10$ and $Q = 1$

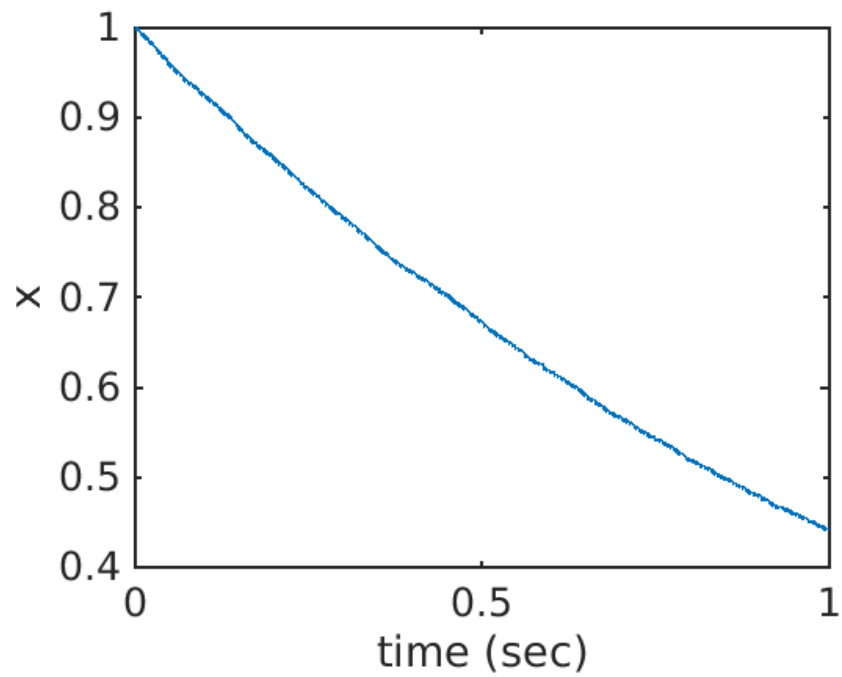


Figure 2.3. Response of 1-D system with $\rho = 10$ and $Q = 100$

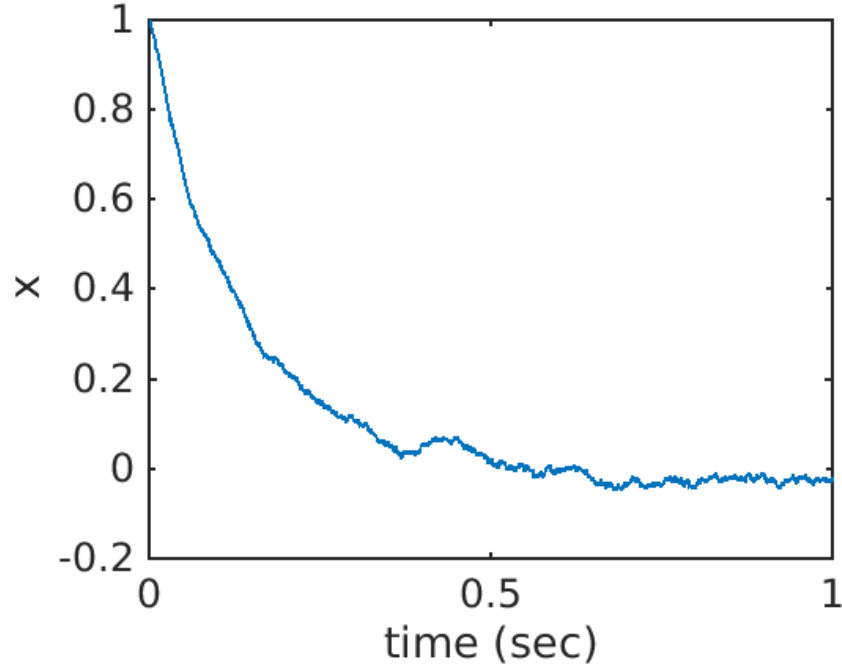


Figure 2.4. Response of 1-D system with $\rho = 100$ and $Q = 100$

Theoretically, the effect of noise which shows up in the form of v_i , gets averaged out over a period of time, such that the effect is reduced significantly.

2.2.1. Sliding mode observer design

Based on the covariance of the noise, we will need to make ρ sufficiently large. Hence the system time scale can be made arbitrarily small and therefore the system exhibits a dual time scale problem. Using Singular perturbation analysis, the slower sub-system can be viewed as a frozen [46].

$$u_{\bar{y}-eq} = A_{12}\tilde{x}_2 + F_1w \quad (2.25)$$

It must be noted that $u_{\tilde{y}-eq}$ would be a filtered version with a time constant $(0.3989\rho Q^{-1/2})^{-1}$. Since ρ is sufficiently large, we can ignore this filter time constant. Hence the \tilde{x}_2 -dynamics can be written as

$$\dot{\tilde{x}}_2 = (A_{22} - L_2 A_{12})\tilde{x}_2 + (F_2 - L_2 F_1)w \quad (2.26)$$

Theorem 2.1

For a system (2.1) in the form of the observer (2.3), for a choice of $\rho > 0$ with $\rho Q^{-1/2}/\sqrt{2\pi} \gg A_{11}$ and time scale of \tilde{x}_2 -dynamics, and $\rho > A_{11}\tilde{x}_1 + A_{12}\tilde{x}_2$, the \tilde{x}_1 -dynamics of the observer can be approximated as

$$\tilde{x}_1 \approx \frac{\sqrt{2\pi}}{\rho} Q^{1/2} [A_{12}\tilde{x}_2] + w_{\text{filt}} \quad (2.27)$$

Where w_{filt} is the filtered noise

$$\dot{w}_{\text{filt}} + \frac{1}{\sqrt{2\pi}} \rho Q^{-1/2} w_{\text{filt}} = F_1 w \quad (2.28)$$

and on the time scale of the \tilde{x}_2 -dynamics,

$$u_{\tilde{y}} := u_{\tilde{y}-eq} = A_{12}\tilde{x}_2 \quad (2.29)$$

Proof: Now the \tilde{x}_1 -dynamics is given by

$$\dot{\tilde{x}}_1 = A_{11}\tilde{x}_1 + A_{12}\tilde{x}_2 + F_1 w - u_{\tilde{y}} \quad (2.30)$$

Since $\rho > A_{11}\tilde{x}_1$, the system will be driven towards the origin. Now in the neighbourhood of $|\tilde{x}_1| = 0$, the effective \tilde{x}_1 -dynamics becomes

$$\begin{aligned} \dot{\tilde{x}}_1 &= A_{11}\tilde{x}_1 + A_{12}\tilde{x}_2 + F_1 w \\ &\quad - \rho / \sqrt{2\pi} Q^{-1/2} \tilde{x}_1 \end{aligned} \quad (2.31)$$

Since ρ is arbitrarily large, we can choose $\rho / \sqrt{2\pi} Q^{-1/2}$ to be much larger than the time scale of \tilde{x}_2 -dynamics. Using Singular perturbation analysis, the slower \tilde{x}_2 -subsystem can be viewed as a frozen (constant) system from the time scale of the \tilde{x}_1 -dynamics [70]. Further since $\rho / \sqrt{2\pi} Q^{-1/2} \gg A_{11}$,

$$u_{\tilde{y}} := u_{\tilde{y}-eq} \approx \frac{1}{\sqrt{2\pi}} \rho Q^{-1/2} \tilde{x}_1 \quad (2.32)$$

And

$$\dot{\tilde{x}}_1 + \frac{1}{\sqrt{2\pi}} \rho Q^{-1/2} \tilde{x}_1 \approx [A_{12}\tilde{x}_2 + F_1 w] \quad (2.33)$$

The solution of (2.33) yields

$$\tilde{x}_1 \approx \frac{\sqrt{2\pi}}{\rho} Q^{1/2} [A_{12}\tilde{x}_2] + w_{\text{filt}} \quad (2.34)$$

From the time scale of the \tilde{x}_2 -dynamics,

$$u_{\tilde{y}-eq} = A_{12}\tilde{x}_2 + F_1 w \quad (2.35)$$

Q.E.D. ■

Theorem 2.2

For a system (2.1) in the form (2.3) for a choice of $\rho > 0$ with $\rho/\sqrt{2\pi}Q^{-1/2} \gg A_{11}$ and $A_{22} - L_2A_{12}$, and $\rho > A_{11}\tilde{x}_1 + A_{12}\tilde{x}_2$, if $\exists P_{22} > 0$, $W_{22} \geq 0$ and X_2 such that

$$\begin{bmatrix} (2W_{22} + P_{22}A + A^T P_{22} & P_{22}F - X_2F \\ -X_2A_{12} - A_{12}^T X_2^T) & \\ F^T P_{22} - F^T X_2^T & R^{-1} \end{bmatrix} < 0 \quad (2.36)$$

by choosing $L_2 = P_{22}^{-1}X_2$, the observer (2.3) drives the states to $\exists W_\infty$

$$\frac{1}{T} \int_{t-T}^t \tilde{x}_2^T W_{22} \tilde{x}_2 d\tau \rightarrow W_\infty < 1 \quad (2.37)$$

Proof: Using (2.29)(2.28) from Theorem 2.2 in the \tilde{x}_2 -dynamics, Eq(2.5) can be written as,

$$\dot{\tilde{x}}_2 = (A_{22} - L_2 A_{12})\tilde{x}_2 + (F_2 - L_2 F_1)w \quad (2.38)$$

If we consider a TAL candidate function

$$V := \frac{1}{T} \int_t^{t+T} V_1 d\tau = \frac{1}{T} \int_t^{t+T} \tilde{x}_2^T(\tau) P_{22} \tilde{x}_2(\tau) d\tau > 0 \quad (2.39)$$

It is evident that $\dot{V}_1 < 0$ if

$$\frac{1}{T} \int_{t-T}^t \tilde{x}_2^T W_{22} \tilde{x}_2 d\tau > 1 \quad (2.40)$$

Hence, the observer drives the states

$$\frac{1}{T} \int_{t-T}^t \tilde{x}_2^T W_{22} \tilde{x}_2 d\tau \rightarrow 1 \quad (2.41)$$

Q.E.D.

■

2.3. Numerical Example

2.3.1. Example 1: Rössler Attractor System

To demonstrate the broad implementation of the proposed system, we consider the Rössler Attractor System, which is a highly nonlinear system with chaotic system

dynamics corresponding to its fractal properties [86], [87]. The system is defined using the following set of equations:

$$\dot{x} = -y - z \quad (2.42)$$

$$\dot{y} = x + ay \quad (2.43)$$

$$\dot{z} = bx - cz + xz \quad (2.44)$$

Where x, y and z are the three variables that evolve in continuous time and a, b and c are the variable parameters. Oscillations in variables x and y are generated by the linear terms present in the first two equations (2.42)(2.43) of the system. Now, if $a > 0$, then these oscillations are amplified which results in a spiraling-out motion in x and y . This motion is coupled with variable z from eq(2.44) which contains the nonlinear term 'xz'. This brings about the reinjection back to the beginning of the spiraling-out motion[88] as seen in Figure 2.5. This system is formed from another set of Navier-Stokes equation which is found in chemical reactions in the form of oscillations. It is similar to a Lorenz attractor, however, it has only one manifold.

Using parameters from earlier literature[89], $a = 0.2, b = 0.2$ and $c = 5.7$ (Standard Rössler Attractor), we model the linearized dynamics of the Rössler system.

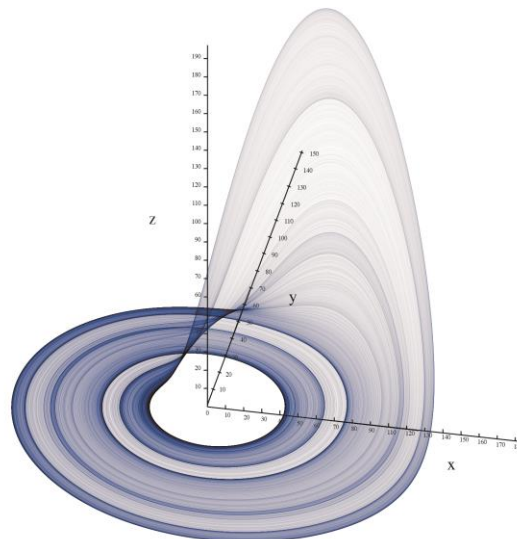


Figure 2.5. Rössler Attractor

The system is defined as:

$$\begin{aligned} \dot{x} &= \begin{bmatrix} 0 & -1 & -1 \\ 1 & 0.2 & 0 \\ 0 & 0 & -5.7 \end{bmatrix} x + \begin{bmatrix} 1 \\ 0 \\ 0 \end{bmatrix} u \\ y &= \begin{bmatrix} 1 & 0 & 0 \\ 0 & 1 & 0 \end{bmatrix} x \end{aligned} \quad (2.45)$$

Hence, the system matrices are given by:

$$A = \begin{bmatrix} 0 & -1 & -1 \\ 1 & 0.2 & 0 \\ 0 & 0 & -5.7 \end{bmatrix}, F = H = \begin{bmatrix} 1 \\ 0 \\ 0 \end{bmatrix}, C = \begin{bmatrix} 1 & 0 & 0 \\ 0 & 1 & 0 \end{bmatrix}, E = \begin{bmatrix} 0 \\ 0 \\ 0 \end{bmatrix}$$

For the simulation, the system is divided into different subsystems to satisfy the proposed LMI (2.36). The above mentioned system matrices are divided into the following subsystems:

$$\begin{aligned} A_{12} &= \begin{bmatrix} -1 \\ 0 \end{bmatrix}, A_{22} = [-5.7], E_1 = \begin{bmatrix} 0 \\ 0 \end{bmatrix}, E_2 = [0], \\ F_1 &= \begin{bmatrix} 1 \\ 0 \end{bmatrix}, F_2 = [0] \end{aligned}$$

Using an initial condition $x(0) = [5 \ 5 \ 5]^T$ and an input $u = \sin(6\pi t)$, we model the Rössler system dynamics in the presence of an external disturbance v with covariance $Q = 1$ and $R = 1$. The system is simulated in MATLAB to solve for \bar{L}_2 using LMI (2.36). The given observer design yields:

$$\begin{aligned} \bar{L}_2 &= [-1.0614 \quad -4.1573] \\ X_2 &= [-0.3647 \quad -1.4328] \\ P_{22} &= 0.3436 \end{aligned} \quad (2.46)$$

The sub gain matrix \bar{L}_2 is used as we are only observing the effect on the 22 subsystem. Using Simulink the above system is modeled and simulated for a time period of $T_{end} = 10$ secs. Figures Figure 2.6 to Figure 2.9 explicitly demonstrate the convergence of the estimated states and the parameters to their true values. The timescale for each plot is suitably adjusted to give comprehensive information about the state behaviour. The plots given below, demonstrate how the estimated state converges to its actual/true state value.

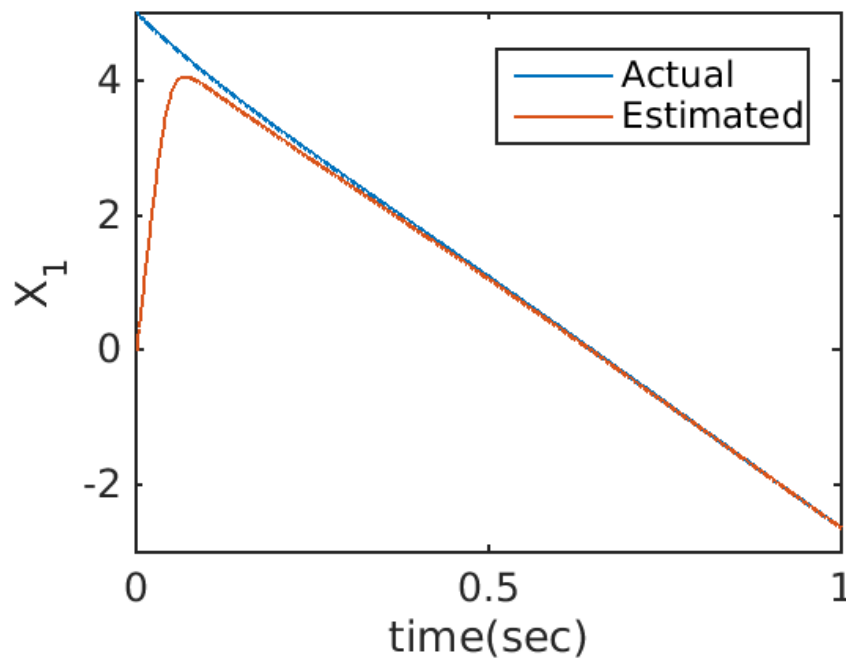


Figure 2.6. State X_1 and its estimation

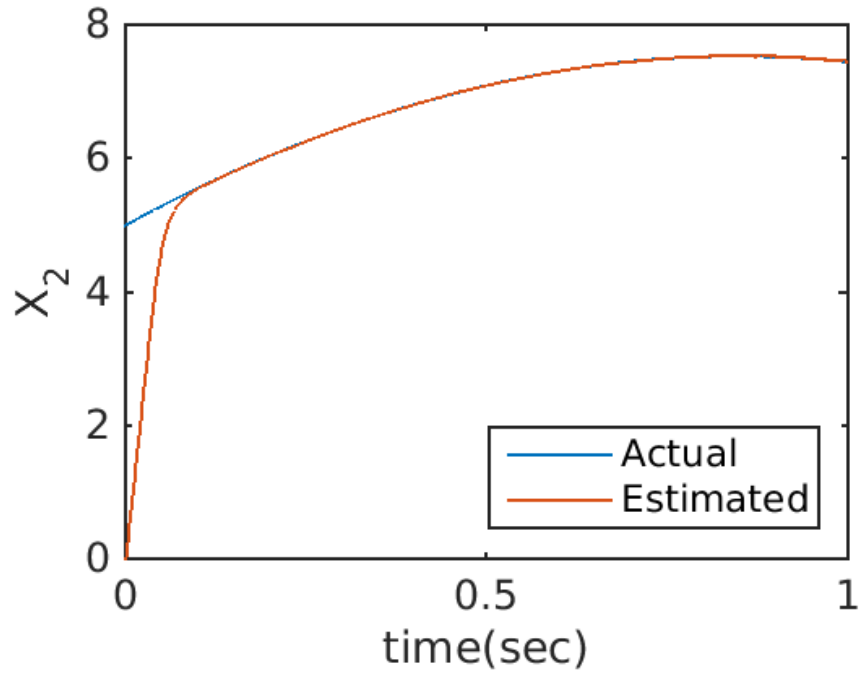


Figure 2.7. State X_2 and its estimation

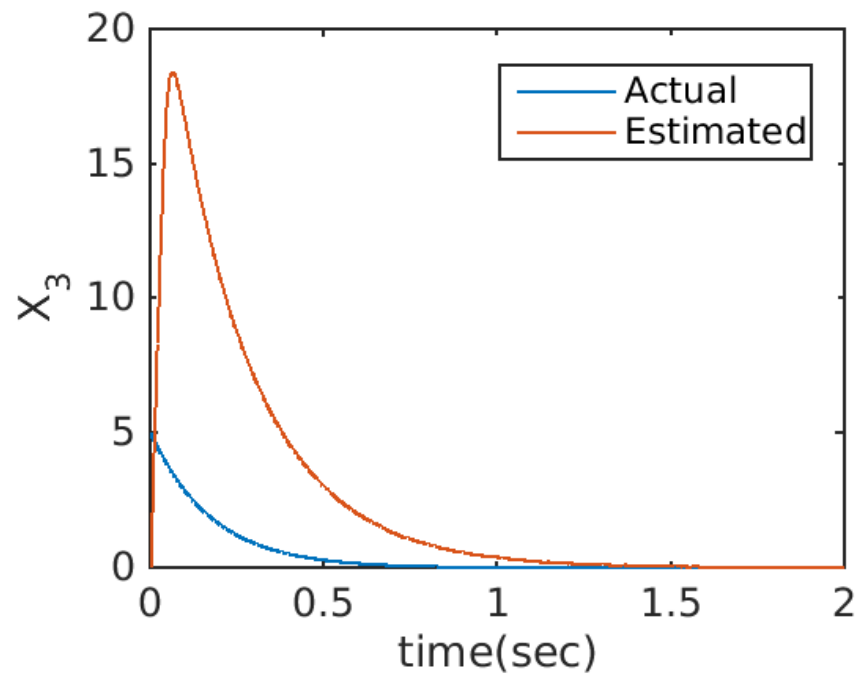


Figure 2.8. State X_3 and its estimation

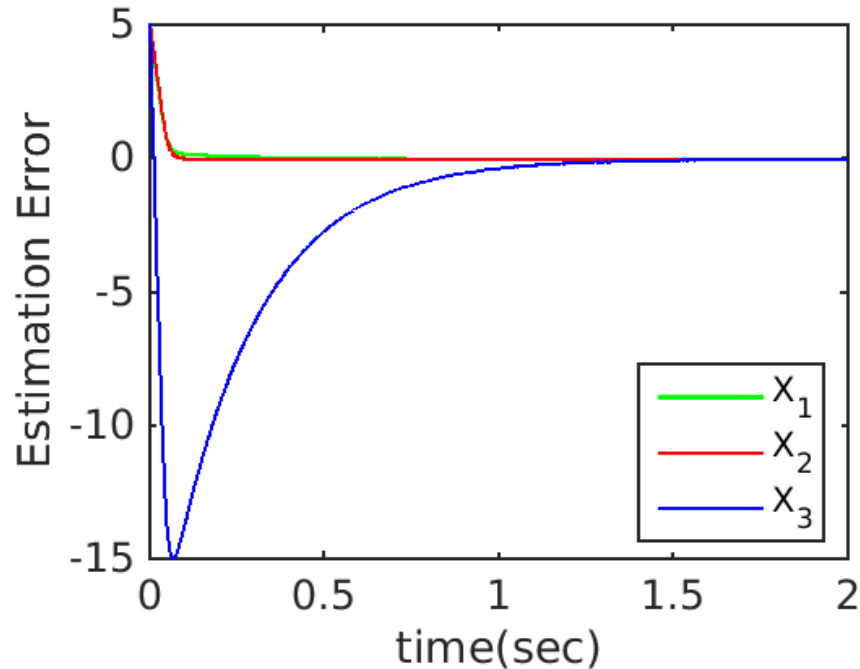


Figure 2.9. State Estimation error

Hence, the TAL function helps analyze the choice of covariance and sliding mode gain parameters so that the convergence rate can be improved. The effectiveness of the proposed observer is shown above in the form of state convergence plots and an estimation error plot.

To see the effect of the sensor noise ' v ' on the system, we plot figures for the system and observer outputs (y and \hat{y} respectively). The outputs represent the values at the sensors of the system (plant) and observer respectively. Figure 2.10 and Figure 2.11 represent the values of outputs of the plant and the observer of the system respectively. The Rössler Attractor system analysed here has two sensors at the output. Hence, the figures represent the values of the two sensors of the system, which give us the measurement of states x_1 and x_2 of the system. Figure 2.11 demonstrates the effectiveness of the proposed observer on the sensor noise affecting the system. The effect of the noise is significantly reduced as compared to the plant. Hence, the state estimates of the observer are not affected by the external sensor noise acting on the system, which makes the observer design robust to external disturbances.

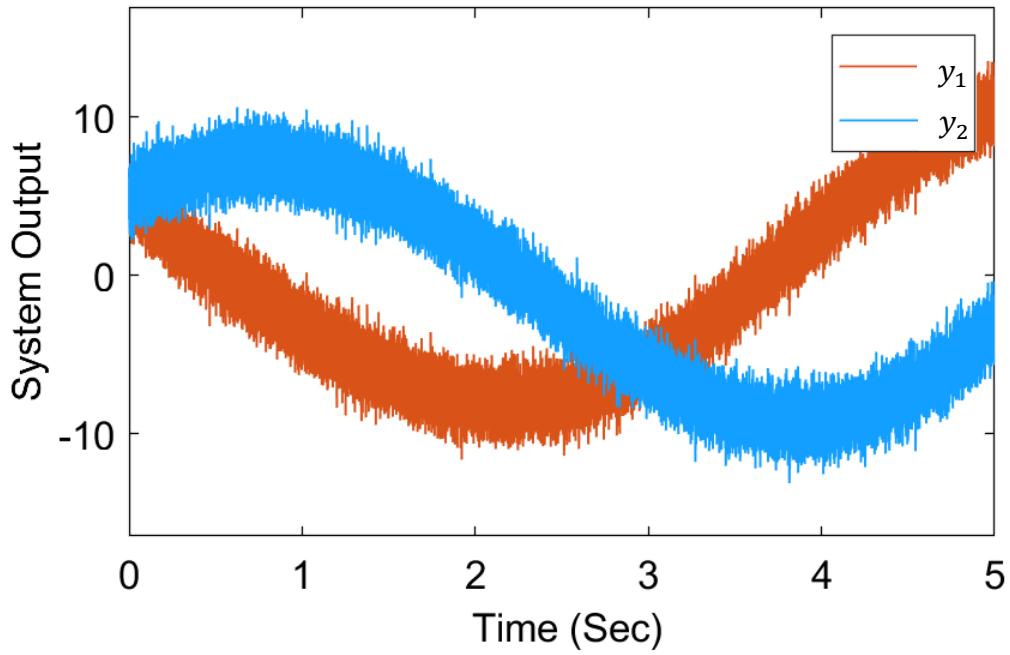


Figure 2.10. System (Plant) Output

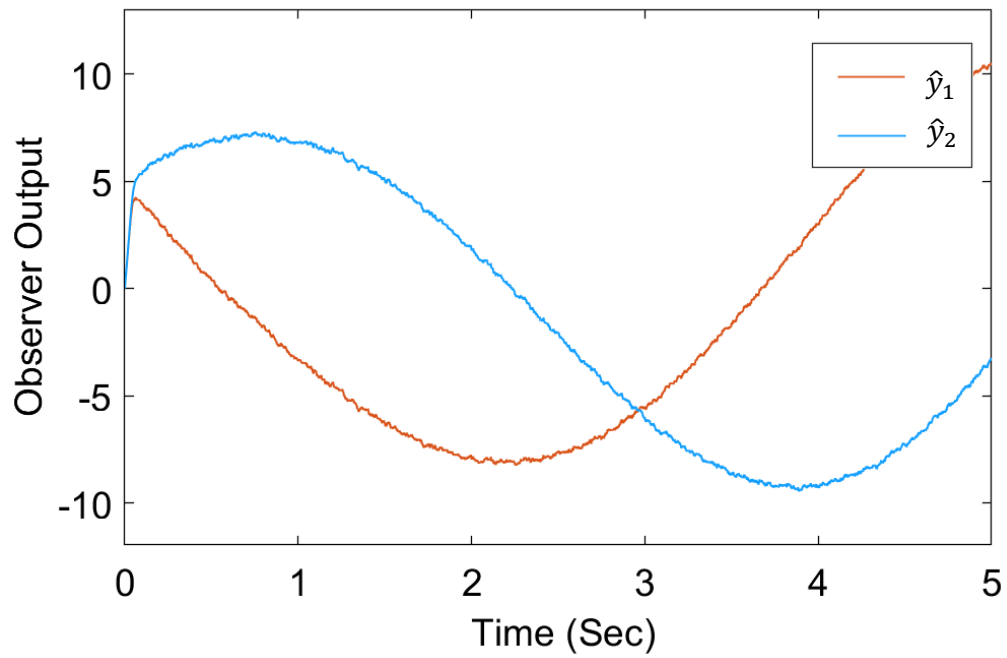


Figure 2.11. Observer Output

Chapter 3.

Sliding Mode Observer Design for a Lipschitz Nonlinear System

Typically, complex real world systems are nonlinear in nature and hence in order to estimate the states of these systems, a nonlinear observer is necessary. Furthermore, these real world systems are also subject to system noise and external disturbances. This chapter serves as an extension of the previous chapter. It explains the design of a sliding mode observer for a system with an added Lipschitz nonlinearity.

The chapter initially presents the design of the observer dynamics using the TAL functional as discussed previously, followed by various existence conditions to ensure the stability of the nonlinear system. A systematic approach to design the appropriate observer and sliding mode gains is presented. Furthermore, the LMI conditions presented here are less conservative and hence the observer functions robustly even in the presence of large Lipschitz constants. Later, the LMI conditions are compared to that of a Luenberger-like observer designed using the TAL technique. Finally, various results are presented and conclusions are made regarding its conservativeness.

3.1. System Model

Consider a general nonlinear system

$$\begin{aligned} \dot{x} &= Ax + E\phi(u, x) + Fw + Hu \\ y &= Cx + v \\ w &\sim (0, R), \quad v \sim (0, Q) \end{aligned} \tag{3.1}$$

In this system, $x \in \mathbb{R}^n$ is the state vector, $u \in \mathbb{R}^q$ is the vector of known inputs, w is a vector of unknown input disturbances, $y \in \mathbb{R}^m$ is the output vector and v is a vector of unknown measurement noise (zero mean Gaussian noise). A, H, C, E, F are known system matrices of appropriate dimensions. We consider all the nonlinearities in the system as a whole and represent it in terms of an additive nonlinearity $\phi(u, x) \in (\mathbb{R}^q \times \mathbb{R}^n) \rightarrow \mathbb{R}^p$, which is assumed to satisfy a matrix Lipschitz condition, given by

$$|\phi(u, x) - \phi(u, \hat{x})| \leq \gamma |G(x - \hat{x})| \quad (3.2)$$

Where γ is a Lipschitz constant and G is assumed to be a sparsely populated matrix. Without loss of generality, we can also assume that,

$$C = [I_m \quad 0], A = \begin{bmatrix} A_{11} & A_{12} \\ A_{21} & A_{22} \end{bmatrix}, G = [G_1 \quad G_2], Q \text{ is a diagonal matrix} \quad (3.3)$$

Where the 1-subspace represents the outputs, and the 2-subspace spans the other states of the system and I_m is a $m \times m$ identity matrix.

3.2. Observer design

We will construct the sliding mode observer as

$$\dot{\hat{x}} = A\hat{x} + E\phi(u, \hat{x}) + Hu + [I_m \quad L_2]^T u_{\tilde{y}} \quad (3.4)$$

With a sliding observer signal given by

$$u_{\tilde{y}} = \rho \times \text{sign}(y - C\hat{x}) \quad (3.5)$$

Where ρ is an arbitrarily large sliding mode gain and $\text{sign}(\circ)$ is the sign function.

For this observer, the dynamics of the estimation error becomes

$$\dot{\tilde{x}} = A\tilde{x} + E\tilde{\phi} - [I_m \quad L_2]^T u_{\tilde{y}} + Fw \quad (3.6)$$

Where $\tilde{x} = x - \hat{x}$, $\tilde{\phi} = \phi - \hat{\phi}$ and L_2 is the observer gain.

The \tilde{x}_1 -dynamics of the observer can be written as,

$$\dot{\tilde{x}}_1 = A_{11}\tilde{x}_1 + A_{12}\tilde{x}_2 + E_1\tilde{\phi} + F_1w - u_{\tilde{y}} \quad (3.7)$$

Theorem 3.1

For a system (3.1) in the form (3.3) with a zero mean Gaussian sensor noise, the \tilde{x}_1 -dynamics of the observer (3.4) can be approximated as

$$\tilde{x}_1 \approx \frac{\sqrt{2\pi}}{\rho} Q^{1/2} [A_{12}\tilde{x}_2 + E_1\tilde{\phi}_2] + w_{\text{filt}} \quad (3.8)$$

for a choice of a sufficiently large $\rho > 0$. Where $\tilde{\phi}_2 = \tilde{\phi}|_{\tilde{x}_1=0} = \phi(u, [x_1^T \ x_2^T]^T) - \phi(u, [\hat{x}_1^T \ \hat{x}_2^T]^T)$ and w_{filt} is the filtered noise

$$\dot{w}_{\text{filt}} + \frac{1}{\sqrt{2\pi}} \rho Q^{-1/2} w_{\text{filt}} = F_1 w \quad (3.9)$$

and on the time-scale of the \tilde{x}_2 -dynamics, the equivalent control

$$u_{\tilde{y}-eq} = A_{12}\tilde{x}_2 + E_1\tilde{\phi}_2 + F_1 w \quad (3.10)$$

Proof: We shall begin by first examining the stability of an autonomous system

$$\dot{\tilde{x}}_1 = A_{11}\tilde{x}_1 - \bar{u}_{\tilde{y}} + E_1\bar{\phi} \quad (3.11)$$

Where \bar{x}_1 are the states \tilde{x}_1 in (3.10)(3.7) when $\tilde{x}_2 = 0$ and $w = 0$, $\bar{u}_{\tilde{y}} = \rho \times \text{sign}(\bar{x}_1 + v)$ and $\bar{\phi} = \phi(u, [x_1^T \ x_2^T]^T) - \phi(u, [\hat{x}_1^T \ \hat{x}_2^T]^T)$. To analyse the stability of (3.10) we will treat \tilde{x}_2 and w as inputs to (3.11). From (3.2) we find

$$|\bar{\phi}| \leq |G_1\bar{x}_1| \quad (3.12)$$

Consider a TAL candidate for the above system with

$$\bar{V}_I = \bar{x}_1^T \bar{x}_1 \quad (3.13)$$

For an arbitrarily small Δt

$$\bar{V}_I(t + \Delta t) = \bar{x}_1^T(t + \Delta t)\bar{x}_1(t + \Delta t) \quad (3.14)$$

Or

$$\begin{aligned}
\bar{V}_I(t + \Delta t) &= \left(\bar{x}_1 + A_{11}\bar{x}_1 \Delta t - \rho \int_t^{t+\Delta t} \text{sign}(\bar{x}_1 + v_i) d\tau_1 + E_1 \bar{\phi} \Delta t \right)^T \\
&\quad \times \left(\bar{x}_1 + A_{11}\bar{x}_1 \Delta t - \rho \int_t^{t+\Delta t} \text{sign}(\bar{x}_1 + v_i) d\tau_2 + E_1 \bar{\phi} \Delta t \right) \\
&= \bar{V}_I + 2\bar{x}_1^T \left[A_{11}\bar{x}_1 \Delta t - \rho \int_t^{t+\Delta t} \text{sign}(\bar{x}_1 + v_i) d\tau + E_1 \bar{\phi} \Delta t \right] + \\
&\quad + \left(A_{11}\bar{x}_1 + E_1 \bar{\phi} \right)^T \left(A_{11}\bar{x}_1 + E_1 \bar{\phi} \right) \Delta t^2 \\
&\quad + \rho^2 \int_t^{t+\Delta t} \int_t^{t+\Delta t} \text{sign}(\bar{x}_1(\tau_1) + v_i(\tau_1)) \text{sign}(\bar{x}_1(\tau_2) + v_i(\tau_2)) d\tau_1 d\tau_2
\end{aligned} \tag{3.15}$$

Notice that $\text{sign}(\bar{x}_1 + v)$ is bounded. As a result

$$\int_t^{t+\Delta t} \int_t^{t+\Delta t} \text{sign}(\bar{x}_1(\tau_1) + v_i(\tau_1)) \text{sign}(\bar{x}_1(\tau_2) + v_i(\tau_2)) d\tau_1 d\tau_2 \sim \mathcal{O}(\Delta t^2) \tag{3.16}$$

Where $\mathcal{O}(\circ)$ indicates the order of magnitude of a term. Hence by taking the limit $\Delta t \rightarrow 0$, and noting that \bar{V}_I is averaged over a time window T we find

$$\dot{\bar{V}}_I = 2\bar{x}_1^T \left(A_{11}\bar{x}_1 - \rho \mathcal{E}[\text{sign}(\bar{x}_1 + v)] + E_1 \bar{\phi} \right) \tag{3.17}$$

Where $\mathcal{E}(\circ)$ denotes the expected value function. Hence, although \bar{x}_1 is driven by $\text{sign}(\bar{x}_1 + v)$, the term $\bar{x}_1^T u_y$ gets averaged over a time window T. Now let \bar{x}_{1-i} denote the the i-th component of \bar{x}_1 . When $|\bar{x}_{1-i}|$ is sufficiently large, $\mathcal{E}[\text{sign}(\bar{x}_{1-i} + v_i)] \approx \text{sign}(\bar{x}_{1-i})$, and when $|\bar{x}_{1-i}| = 0$, $\mathcal{E}[\text{sign}(\bar{x}_{1-i} + v_i)] = \mathcal{E}[\text{sign}(v_i)] = 0$. Since $\text{sign}(0) = 0$, we will define the correction term $0 < \rho_{c-i}(\bar{x}_{1-i}) \leq 1$

$$\mathcal{E}[\text{sign}(\bar{x}_{1-i} + v_i)] := \rho_{c-i}(\bar{x}_{1-i}) \text{sign}(\bar{x}_{1-i}) \tag{3.18}$$

Defining $\Psi_c(\bar{x}_1) := \text{diag}(\rho_{c-i}(\bar{x}_{1-i}))$, (3.17) can be written as

$$\dot{\bar{V}}_I = 2\bar{x}_1^T \left(A_{11}\bar{x}_1 - \rho \Psi_c(\bar{x}_1) \text{sign}(\bar{x}_1) + E_1 \bar{\phi} \right) \tag{3.19}$$

Using (3.12),

$$\dot{\bar{V}}_I \leq 2\bar{x}_1^T \left(A_{11}\bar{x}_1 - \rho \Psi_c(\bar{x}_1) \text{sign}(\bar{x}_1) + E_1^T E_1 \bar{x}_1 + G_1^T G_1 \bar{x}_1 \right) \tag{3.20}$$

Suppose $\rho > |A_{11}\bar{x}_1 + E_1^T E_1 \bar{x}_1 + G_1^T G_1 \bar{x}_1|$, notice that $\dot{\bar{V}}_1 < 0$. Hence the system gets driven to the origin. As \bar{x}_1 approaches $\bar{x}_1 = 0$,

$$\dot{\bar{V}}_1 \approx -2\rho\bar{x}_1^T \Psi_c(\bar{x}_1) \text{sign}(\bar{x}_1) \quad (3.21)$$

From the perspective of convergence, the system (3.11) is equivalent to

$$\dot{\bar{x}}_{1-i} = -\rho\rho_{c-i}(\bar{x}_{1-i}) \times \text{sign}(\bar{x}_{1-i}) \quad (3.22)$$

To determine the convergence rate near $|\bar{x}_1| = 0$, we will consider the first term in the Taylor series expansion of $\rho_{c-i}(\bar{x}_{1-i})$ giving

$$\dot{\bar{x}}_{1-i} \approx -\rho\rho_{c-i}^{0'}\bar{x}_{1-i} \quad (3.23)$$

Where,

$$\rho_{c-i}^{0'} = \left. \frac{d}{d\bar{x}_{1-i}} \rho_{c-i}(\bar{x}_{1-i}) \right|_{\bar{x}_{1-i}=0^+} \quad (3.24)$$

To determine $\rho_{c-i}^{0'}$, we will first determine an expression for $\rho_{c-i}(\bar{x}_{1-i})$. Notice that

$$\text{sign}(|\bar{x}_{1-i}| + v_i) = \begin{cases} +1 & \text{if } v_i > -|\bar{x}_{1-i}| \\ -1 & \text{if } v_i < -|\bar{x}_{1-i}| \end{cases} \quad (3.25)$$

If $\mathcal{P}(\circ)$ denotes probability of an event,

$$\begin{aligned} \rho_{c-i}(\bar{x}_{1-i}) &= \mathcal{E}[\text{sign}(|\bar{x}_{1-i}| + v_i)] \\ &= \mathcal{P}(v_i > -|\bar{x}_{1-i}|) - \mathcal{P}(v_i < -|\bar{x}_{1-i}|) \\ &= [1 - \mathcal{P}(v_i < -|\bar{x}_{1-i}|)] - \mathcal{P}(v_i < -|\bar{x}_{1-i}|) \\ &= 1 - 2 \times \mathcal{P}(v_i < -|\bar{x}_{1-i}|) \end{aligned} \quad (3.26)$$

Since the sensor noise is Gaussian,

$$\begin{aligned}
\mathcal{P}(v_i < -|\bar{x}_{1-i}|) &= P(v_i > |\bar{x}_{1-i}|) \\
&= \frac{1}{\sqrt{2Q_i\pi}} \int_{v=|\bar{x}_{1-i}|}^{v=\infty} \exp(-v^2/2Q_i) dv \\
&= \frac{1}{\sqrt{\pi}} \int_{v=\frac{|\bar{x}_{1-i}|}{\sqrt{2Q_i}}}^{v=\infty} \exp(-v^2) dv \\
&= \frac{1}{2} - \frac{1}{\sqrt{\pi}} \int_0^{v=\frac{|\bar{x}_{1-i}|}{\sqrt{2Q_i}}} \exp(-v^2) dv \\
&= \frac{1}{2} (1 - \operatorname{erf}(|\bar{x}_{1-i}|/\sqrt{2Q_i}))
\end{aligned} \tag{3.27}$$

Where $\operatorname{erf}(\circ)$ denotes the error function. This yields

$$\rho_{c-i}(\chi_{1-i}) = \operatorname{erf}\left(\frac{|\bar{x}_{1-i}|}{\sqrt{2Q_i}}\right) \tag{3.28}$$

Hence

$$\rho_{c-i}^{0'} = \frac{d}{d\bar{x}_{1-i}} \operatorname{erf}\left(\frac{|\bar{x}_{1-i}|}{\sqrt{2Q_i}}\right) \Big|_{\bar{x}_{1-i}=0^+} = \frac{2}{\sqrt{\pi}} \times \sqrt{\frac{1}{2Q_i}} = \sqrt{\frac{2}{\pi}} Q_i^{-1/2} \tag{3.29}$$

Hence, in the neighborhood of $|\bar{x}_{1-i}| = 0$ the system behaves as

$$\dot{\tilde{x}}_1 \approx -u_{\tilde{y}} \tag{3.30}$$

$$u_{\tilde{y}} \approx \rho \sqrt{\frac{2}{\pi}} Q^{-1/2} \tilde{x}_1 \tag{3.31}$$

Applying (3.30) to (3.10) in the neighborhood of $|\tilde{x}_1| = 0$, the effective \tilde{x}_1 -dynamics becomes

$$\begin{aligned}
\dot{\tilde{x}}_1 &= A_{11}\tilde{x}_1 - \rho \sqrt{\frac{2}{\pi}} Q^{-1/2} \tilde{x}_1 + A_{12}\tilde{x}_2 + F_1 w \\
&E_1 \left\{ [\phi(u, [x_1^T \ x_2^T]^T) - \phi(u, [\hat{x}_1^T \ \hat{x}_2^T]^T)] + \frac{\partial \phi}{\partial x_1} \tilde{x}_1 \right\}
\end{aligned} \tag{3.32}$$

Since ρ is arbitrarily large, we can choose $\rho\sqrt{2/\pi}Q^{-1/2}$ to be much larger than the time scale of \tilde{x}_2 -dynamics. Using Singular perturbation analysis [90], the slower \tilde{x}_2 -subsystem can be viewed as a frozen (constant) system from the time scale of the \tilde{x}_1 -dynamics. We can further assume $\rho\sqrt{2/\pi}Q^{-1/2} \gg |A_{11} + E_1 \partial\phi/\partial x_1|$ giving,

$$\dot{\tilde{x}}_1 + \rho\sqrt{\frac{2}{\pi}}Q^{-1/2}\tilde{x}_1 \approx [A_{12}\tilde{x}_2 + E_1\tilde{\phi}_2 + F_1w] \quad (3.33)$$

Where $\tilde{\phi}_2 = \tilde{\phi}|_{\tilde{x}_1=0} = \phi(u, [x_1^T x_2^T]^T) - \phi(u, [\hat{x}_1^T \hat{x}_2^T]^T)$. The solution of (3.33) yields

$$\tilde{x}_1 \approx \rho^{-1}\sqrt{\frac{\pi}{2}}Q^{1/2}[A_{12}\tilde{x}_2 + E_1\tilde{\phi}_2] + F_1w_{\text{filt}} \quad (3.34)$$

If $u_{\tilde{y}-eq}$ is the equivalent control from the time scale of the \tilde{x}_2 -dynamics,

$$u_{\tilde{y}-eq} = A_{12}\tilde{x}_2 + E_1\tilde{\phi}_2 + F_1w \quad (3.35)$$

Note 1: In order to ensure \tilde{x}_1 approaches the origin when $|\tilde{x}_1|$ is large, we would require $\rho \gg |A_{11}\tilde{x}_1 + A_{12}\tilde{x}_2 + E_1\tilde{\phi}|$. In order to ensure Singular perturbation analysis is valid, we would require $\rho/\sqrt{2\pi}Q^{-1/2} \gg$ the time scale of \tilde{x}_2 -dynamics.

We will now formulate a linear matrix inequality to solve for the observer gain.

Lemma 3.2 (S-Procedure Lemma[67]): If $V_1: \mathbb{R}^r \rightarrow \mathbb{R}$ and $V_2: \mathbb{R}^s \rightarrow \mathbb{R}$ be such that $V_2 \leq 0$, then $V_1 < 0$ iff $\exists \varepsilon > 0$ such that

$$V_1 - \varepsilon V_2 < 0 \quad (3.36)$$

Theorem 3.3

For a system (3.1) in the form (3.3) with a Gaussian sensor noise, suppose $\exists T$ such that zero mean Gaussian processes $w \sim (0, R)$ satisfies

$$\frac{1}{T} \int_{t-T}^t w^T R^{-1} w d\tau = 1 \quad (3.37)$$

Let $\rho > 0$ with $\rho \sqrt{2/\pi} Q^{-1/2} \gg \Lambda(A_{22} - L_2 A_{12})$, $\rho \sqrt{2/\pi} Q^{-1/2} \gg |A_{11} + E_1 \partial \phi / \partial x_1|$ and $\rho \gg A_{11} \tilde{x}_1 + A_{12} \tilde{x}_2 + E_1 \tilde{\phi}$, (where $\Lambda(\circ)$ denotes the eigenvalue function). The error dynamics (3.6) is stable iff $\exists P_{22} > 0, W_{22} \geq 0, \epsilon > 0$ and X_2 such that

$$\begin{bmatrix} (W_{22} + P_{22} A_{22} + A_{22}^T P_{22} & P_{22} E_2 - X_2 E_1 & P_{22} F_2 - X_2 F_1 \\ -X_2 A_{12} - A_{12}^T X_2^T + \epsilon \gamma^2 G_2^T G_2) & -\epsilon I & 0 \\ E_2^T P_{22} - E_1^T X_2^T & 0 & R^{-1} \\ F_2^T P_{22} - F_1^T X_2^T & 0 & R^{-1} \end{bmatrix} < 0 \quad (3.38)$$

By choosing the observer gain as $L_2 = P_{22}^{-1} X_2$, the observer (3.4) drives the states to

$$\frac{1}{T} \int_{t-T}^t \tilde{x}_2^T W_{22} \tilde{x}_2 d\tau \leq 1 \quad (3.39)$$

Proof: Notice that by using (3.10) from Theorem 3.1, the \tilde{x}_2 -dynamics from (3.6) can be written as,

$$\dot{\tilde{x}}_2 = (A_{22} - L_2 A_{12}) \tilde{x}_2 + (E_2 - L_2 E_1) \tilde{\phi}_2 + (F_2 - L_2 F_1) w \quad (3.40)$$

Where, $\tilde{\phi}_2 = \tilde{\phi}|_{\tilde{x}_1=0} = \phi(u, [x_1^T \ x_2^T]^T) - \phi(u, [\hat{x}_1^T \ \hat{x}_2^T]^T)$.

Consider a TAL candidate with $P_{22} > 0$,

$$V := \frac{1}{T} \int_{t-T}^t V_I d\tau = \frac{1}{T} \int_{t-T}^t \tilde{x}_2^T(\tau) P_{22} \tilde{x}_2(\tau) d\tau \quad (3.41)$$

Hence

$$\begin{aligned} \dot{V}_I = & \tilde{x}_2^T [(A_{22} - L_2 A_{12})^T P_{22} + P_{22} (A_{22} - L_2 A_{12})] \tilde{x}_2 \\ & + 2 \tilde{x}_2^T P_{22} [(E_2 - L_2 E_1) \tilde{\phi}_2 + (F_2 - L_2 F_1) w] \end{aligned} \quad (3.42)$$

Since ϕ satisfies (3.2), we choose

$$V_\phi := \frac{1}{T} \int_{t-T}^t (\tilde{\phi}_2^T \tilde{\phi}_2 - \gamma^2 \tilde{x}_2^T G_2^T G_2 \tilde{x}_2) d\tau \leq 0 \quad (3.43)$$

From Lemma 3.2 (ie S-Procedure Lemma [67]), $\dot{V} < 0$ iff $\exists \epsilon > 0, V_\phi \leq 0$ such that

$$\dot{V} - \epsilon V_\phi < 0 \quad (3.44)$$

Using the equality (3.37), we conclude that $\dot{V} < 0$ iff

$$\begin{aligned} & \frac{1}{T} \int_{t-T}^t \{ \tilde{x}_2^T [(A_{22} - L_2 A_{12})^T P_{22} + P_{22} (A_{22} - L_2 A_{12})] \tilde{x}_2 \\ & \quad + 2 \tilde{x}_2^T P_{22} [(E_2 - L_2 E_1) \tilde{\phi}_2 + (F_2 - L_2 F_1) w] \\ & \quad + \epsilon \gamma^2 \tilde{x}_2^T G_2^T G_2 \tilde{x}_2 - \epsilon \tilde{\phi}_2^T \tilde{\phi}_2 - w^T R^{-1} w + 1 \} d\tau < 0 \end{aligned} \quad (3.45)$$

Suppose $\exists P_{22} > 0, W_{22} \geq 0, \epsilon > 0$ and X_2 such that

$$\begin{bmatrix} (W_{22} + P_{22} A_{22} + A_{22}^T P_{22} & P_{22} E_2 - X_2 E_1 & P_{22} F_2 - X_2 F_1 \\ -X_2 A_{12} - A_{12}^T X_2^T + \epsilon \gamma^2 G_2^T G_2) & -\epsilon I & 0 \\ E_2^T P_{22} - E_1^T X_2^T & 0 & R^{-1} \\ F_2^T P_{22} - F_1^T X_2^T & 0 & 0 \end{bmatrix} < 0 \quad (3.46)$$

Then, by taking $L_2 = P_{22}^{-1} X_2$,

$$\begin{aligned} & \tilde{x}_2^T [(A_{22} - L_2 A_{12})^T P_{22} + P_{22} (A_{22} - L_2 A_{12})] \tilde{x}_2 \\ & \quad + 2 \tilde{x}_2^T P_{22} [(E_2 - L_2 E_1) \tilde{\phi}_2 + (F_2 - L_2 F_1) w] \\ & \quad + \epsilon \gamma^2 \tilde{x}_2^T G_2^T G_2 \tilde{x}_2 - \epsilon \tilde{\phi}_2^T \tilde{\phi}_2 - w^T R^{-1} w < -\tilde{x}_2^T W_{22} \tilde{x}_2 \end{aligned} \quad (3.47)$$

Comparing (3.45) and (3.47) we can conclude that $\dot{V} < 0$ if

$$\frac{1}{T} \int_{t-T}^t \tilde{x}^T W_{22} \tilde{x} d\tau > 1 \quad (3.48)$$

Hence, the observer drives the states to

$$\frac{1}{T} \int_{t-T}^t \tilde{x}^T W_{22} \tilde{x} d\tau \leq 1 \quad (3.49)$$

Notice that for every choice of L_2 that stabilizes the observer, $\exists X_2 = P_{22} L_2$. Hence if $\nexists P_{22} > 0, W_{22} \geq 0, \epsilon > 0$ and X_2 such that (3.38) is satisfied, then there is no stable observer. Hence the condition is also necessary. ■

Hence, by minimizing $|W_{22}|$ we can find the tightest bound on the observer error.

3.3. Comparing Luenberger-like observer design using TAL with sliding mode observers

In this section, we will use the TAL to design a linear gain observer for a nonlinear system using a TAL function. This will serve both, to demonstrate the utility of the TAL, as well as allow this work to compare the sliding mode observer design with the linear gain observer. The observer is assumed to be of the form

$$\dot{\hat{x}} = A\hat{x} + E\phi(u, \hat{x}) + L(y - C\hat{x}) + Bu \quad (3.50)$$

Theorem 3.4

For the system (3.1) with zero mean Gaussian white noise $v \sim (0, Q)$ and $w \sim (0, R) \exists T$ such that

$$\begin{aligned} \frac{1}{T} \int_{t-T}^t w^T R^{-1} w d\tau &= 1 \\ \frac{1}{T} \int_{t-T}^t v^T Q^{-1} v d\tau &= 1 \end{aligned} \quad (3.51)$$

the observer of the form (3.50) drives the observer error $\tilde{x} := x - \hat{x}$ to

$$\frac{1}{T} \int_{t-T}^t \tilde{x}^T W \tilde{x} d\tau \leq 1 \quad (3.52)$$

iff $\exists P > 0$, $W \geq 0$ and X such that

$$\begin{bmatrix} 2W + PA + A^T P - XC - C^T X^T + \epsilon \gamma^2 G^T G & PE & PF & X \\ E^T P & -\epsilon I & 0 & 0 \\ F^T P & 0 & -R^{-1} & 0 \\ X^T & 0 & 0 & -Q^{-1} \end{bmatrix} < 0 \quad (3.53)$$

and the observer gain is given by $L = P^{-1}X$.

Proof: The proof follows along the lines of the proof of Theorem 3.3. We would consider a TAL candidate with $P > 0$,

$$V := \frac{1}{T} \int_{t-T}^t V_I d\tau = \frac{1}{T} \int_{t-T}^t \tilde{x}^T(\tau) P \tilde{x}(\tau) d\tau \quad (3.54)$$

Then the error dynamics can be written as

$$\dot{\tilde{x}} = (A - LC)\tilde{x} + E\tilde{\phi} + Fw + Lv \quad (3.55)$$

where, $\tilde{\phi} = \phi(u, \hat{x}) - \phi(u, x)$.

When compared to the proof of Theorem 3.3, notice that the error dynamics (3.55) resembles (3.40) when $E_1 = 0$, $F_1 = 0$, $A_{12} = C$, the subscripts 2 and 22 are dropped, and the term Lv is added. Using the equality (3.51), we conclude that $\dot{V} < 0$ iff

$$\begin{aligned} & \frac{1}{T} \int_{t-T}^t \{ \tilde{x}^T [(A - LC)^T P + P(A - LC)] \tilde{x} + 2\tilde{x}^T P [E\tilde{\phi} + Fw + Lv] \\ & + \epsilon \gamma^2 \tilde{x}^T G^T G \tilde{x} - \epsilon \phi \tilde{x}^T \tilde{\phi} - w^T R^{-1} w + 1 - v^T Q^{-1} v + 1 \} d\tau < 0 \end{aligned} \quad (3.56)$$

Defining $PL := X$ we can conclude that if (3.53) is satisfied, the error dynamics is driven to (3.52). ■

Note: The above observer would correspond to a H_∞ filter with

$$J = \frac{\int_{t_0}^{t_1} \tilde{x}^T W \tilde{x} d\tau}{\int_{t_0}^{t_1} w^T R^{-1} w \tau + \int_{t_0}^{t_1} v^T Q^{-1} v d\tau} \leq \frac{1}{2} \quad (3.57)$$

Maximizing the smallest singular value of W would minimize the effect of the noise.

While the sliding mode observer reduces the size of the state-space, it adds terms to the off-diagonal elements of the LMI. We will now show that the sliding mode observer design is indeed less conservative than the linear gain observer.

Lemma 3.5: In the absence of sensor noise, (3.53), the LMI for the existence of a linear observer, is equivalent to (3.38), the LMI for the existence of a sliding mode observer.

Proof: In the absence of sensor noise, (3.45) in Theorem 3.4 would become

$$\begin{aligned} \frac{1}{T} \int_{t-T}^t \{ \tilde{x}^T [(A - LC)^T P + P(A - LC)] \tilde{x} + 2\tilde{x}^T P [E\tilde{\phi} + Fw] \\ + \epsilon\gamma^2 \tilde{x}^T G^T G \tilde{x} - \epsilon\phi \tilde{x}^T \tilde{\phi} - w^T R^{-1} w + 1 \} d\tau < 0 \end{aligned} \quad (3.58)$$

Hence, (3.53) would become

$$\begin{bmatrix} W + PA + A^T P - XC - C^T X^T + \epsilon\gamma^2 G^T G & PE & PF \\ E^T P & -\epsilon I & 0 \\ F^T P & 0 & -R^{-1} \end{bmatrix} < 0 \quad (3.59)$$

Or

$$W + PA + A^T P - XC - C^T X^T + \epsilon\gamma^2 G^T G + \frac{1}{\epsilon} PEE^T P + PFRF^T P < 0 \quad (3.60)$$

Following the argument made in Theorem 2 in Phanomchoeng et al. (Phanomchoeng & Rajamani, 2010), we can show an observer exists iff $\exists \beta$, $X = PL = \beta^2/2 \times C^T$. Notice that

$$PA = \begin{bmatrix} P_{11}A_{11} + P_{12}A_{21} & P_{11}A_{12} + P_{12}A_{22} \\ P_{21}A_{11} + P_{22}A_{21} & P_{21}A_{12} + P_{22}A_{22} \end{bmatrix} \quad (3.61)$$

$$CX = \begin{bmatrix} \beta^2/2 C_1^T C_1 & 0 \\ 0 & 0 \end{bmatrix} \quad (3.62)$$

$$G^T G = \begin{bmatrix} G_1^T G_1 & G_1^T G_2 \\ G_2^T G_1 & G_2^T G_2 \end{bmatrix} \quad (3.63)$$

$PEE^T P$

$$= \begin{bmatrix} (P_{11}E_1E_1^T P_{11} + P_{12}E_2E_1^T P_{11}) & (P_{12}E_1E_1^T P_{11} + P_{12}E_2E_1^T P_{12}) \\ + (P_{11}E_1E_2^T P_{21} + P_{12}E_2E_2^T P_{21}) & + (P_{11}E_1E_2^T P_{22} + P_{12}E_2E_2^T P_{22}) \\ * & (P_{12}E_1E_1^T P_{21} + P_{12}E_2E_1^T P_{22}) \\ & + (P_{21}E_1E_2^T P_{22} + P_{22}E_2E_2^T P_{22}) \end{bmatrix} \quad (3.64)$$

$PFRF^T P$

$$= \begin{bmatrix} (P_{11}F_1R F_1^T P_{11} + P_{12}F_2R F_1^T P_{11}) & (P_{12}F_1R F_1^T P_{11} + P_{12}F_2R F_1^T P_{12}) \\ + (P_{11}F_1R F_2^T P_{21} + P_{12}F_2R F_2^T P_{21}) & + (P_{11}F_1R F_2^T P_{22} + P_{12}F_2R F_2^T P_{22}) \\ * & (P_{12}F_1R F_1^T P_{21} + P_{12}F_2R F_1^T P_{22}) \\ & + (P_{21}F_1R F_2^T P_{22} + P_{22}F_2R F_2^T P_{22}) \end{bmatrix} \quad (3.65)$$

Since β is arbitrary, we can set $\beta \rightarrow \infty$. Hence (3.60) can be written as

$$\begin{aligned} & W_{22} + (P_{21}A_{12} + P_{22}A_{22})^T + (P_{21}A_{12} + P_{22}A_{22}) + \epsilon\gamma^2 G_2^T G_2 + \\ & \epsilon^{-1}(P_{21}E_1E_1^T P_{12} + P_{22}E_2E_1^T P_{12}) + \epsilon^{-1}(P_{21}E_1E_2^T P_{22} + P_{22}E_2E_2^T P_{22}) \\ & (P_{12}F_1R F_1^T P_{21} + P_{12}F_2R F_1^T P_{22}) + (P_{21}F_1R F_2^T P_{22} + P_{22}F_2R F_2^T P_{22}) < 0 \end{aligned} \quad (3.66)$$

Or

$$\begin{bmatrix} (W_{22} + P_{22}A + A^T P_{22} \\ -P_{21}A_{12} - A_{12}^T P_{21} + \epsilon\gamma^2 G_2^T G_2) & P_{22}E_2 + P_{21}E_1 & P_{22}F_2 + P_{21}F_1 \\ E_2^T P_{22} + E_1^T P_{21} & -\epsilon I & 0 \\ F_2^T P_{22} + F_1^T P_{21} & 0 & R^{-1} \end{bmatrix} < 0 \quad (3.67)$$

The above equation is identical to (3.38) with $X_2 = P_{22}L_2 = -P_{21}$. ■

Note 2: For a given Lipchitz constant, the sliding mode observer offers the performance as a noise-free linear gain observer. In the presence of noise, it will not be possible to set $\beta \rightarrow \infty$ in (3.62). Since LMI (3.53) uses $\epsilon\gamma^2 G^T G$ compared to $\epsilon\gamma^2 G_2^T G_2$ in LMI (3.38), we can conclude that the sliding mode observer makes the design less conservative.

Note 3: When the nonlinearity has an unbounded Jacobian (for instance $\phi = x_1 x_3$ as in the Rössler Attractor System [86], [87] discussed later in the paper) an equivalent Lipschitz constants is chosen based on the maximum anticipated values of $\hat{x}_1, \hat{x}_3, \tilde{x}_1$ and \tilde{x}_3 . In such cases, the sliding mode observer will only need to consider the \hat{x}_1 which can

reduce the effective equivalent Lipschitz constants and make the observer design significantly less conservative.

3.4. Illustrative examples

3.4.1. Example 1: Double Spring-Mass System

We consider a variant of the robotic arm as used in Vijayaraghavan et al [60] originally discussed by Spong [91]. Originally, the system is a flexible link robot where the elasticity of the arm is represented by a linear torsional spring. The states of this system represent the motor position and velocity (defined by x_1 and x_2), link position and velocity (x_3 and x_4). Vijayaraghavan et al [60] uses a simplified version of this system in the form of a double spring-mass system to implement the observer design. The system is illustrated in Figure 3.1 as given below:

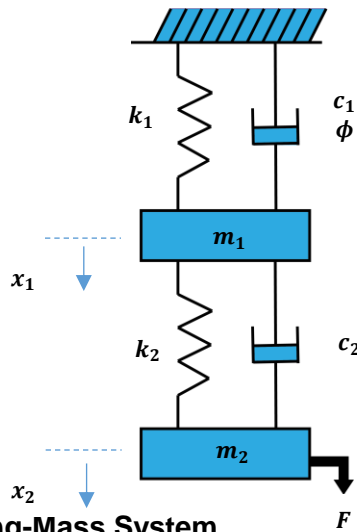


Figure 3.1. Double Spring-Mass System

The system is a simple second order system with

$$A = \begin{bmatrix} 0 & 1 & 0 & 0 \\ -25 & -1 & 15 & 0.3 \\ 0 & 0 & 0 & 1 \\ 15 & 0.3 & -15 & -0.3 \end{bmatrix}, \quad F = B = \begin{bmatrix} 0 \\ 0 \\ 0 \\ 1 \end{bmatrix}, \quad C = \begin{bmatrix} 1 & 0 \\ 0 & 0 \\ 0 & 1 \\ 0 & 0 \end{bmatrix}^T, \quad E = \begin{bmatrix} 0 \\ 1 \\ 0 \\ 0 \end{bmatrix}, \quad \phi = 0.1\sin(x_2),$$

Using covariance $R=1$; $Q=1$ and the assuming $W=0$. Notice that the nonlinearity satisfies (3.2) with $G = [0 \ 1 \ 0 \ 0]$ and $\gamma = 0.1$. In order to get the system in the form (3.3), we apply a state transformation matrix of the form

$$T = \begin{bmatrix} 1 & 0 & 0 & 0 \\ 0 & 0 & 1 & 0 \\ 0 & 1 & 0 & 0 \\ 0 & 0 & 0 & 1 \end{bmatrix}, \bar{A} = T^{-1}AT, \bar{F} = \bar{B} = T^{-1}B, \bar{C} = CT, \bar{E} = T^{-1}E \text{ and } \bar{G} = GT$$

Given the above system, MATLAB is used to solve the LMI (3.38) and determine the value of \bar{L}_2 . The calculations yield,

$$\bar{L}_2 = \begin{bmatrix} 0.5110 & 0.0203 \\ 0.3550 & 0.7210 \end{bmatrix} \quad (3.68)$$

Using Simulink, the above system is simulated for a period of $T_{end} = 10$ seconds.

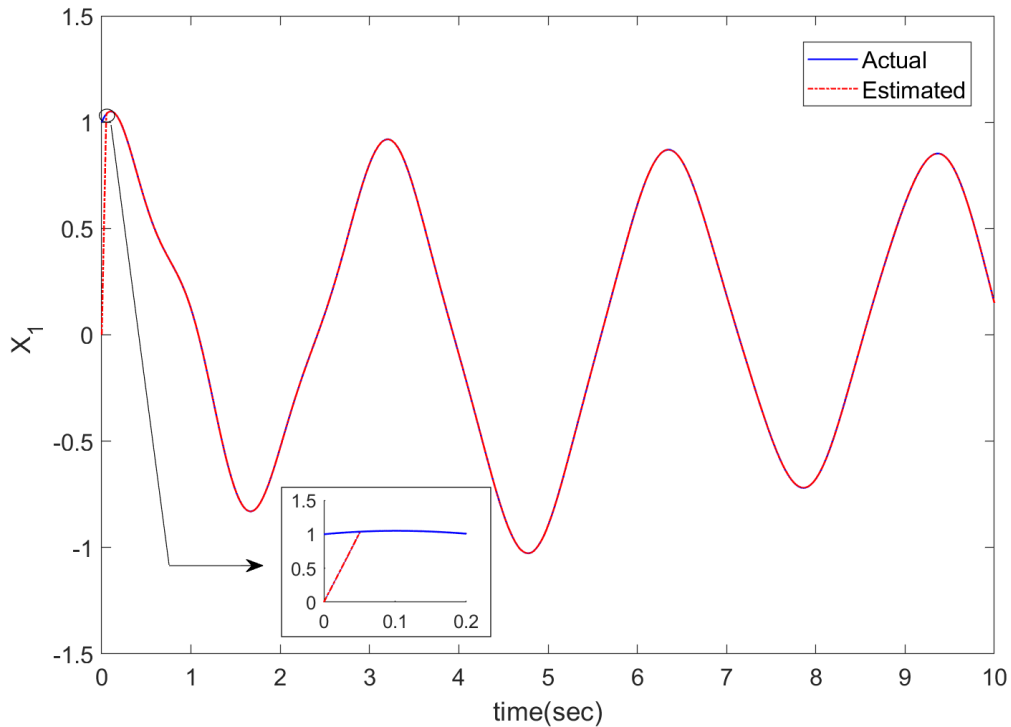


Figure 3.2. Convergence of State x_1

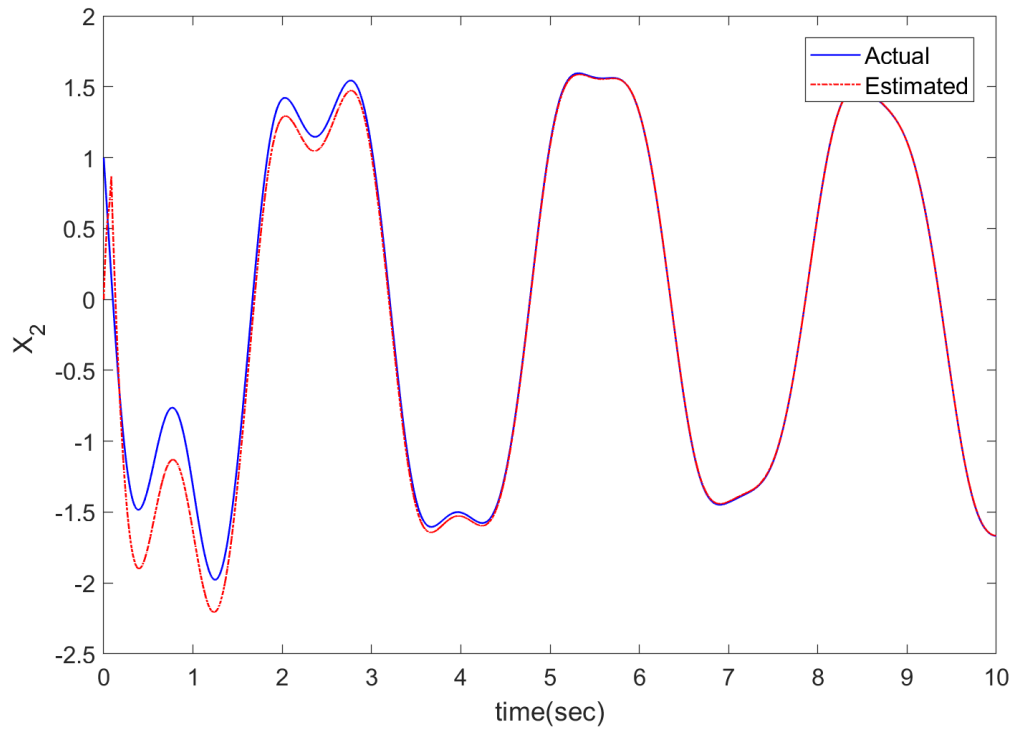


Figure 3.3. Convergence of State x_2

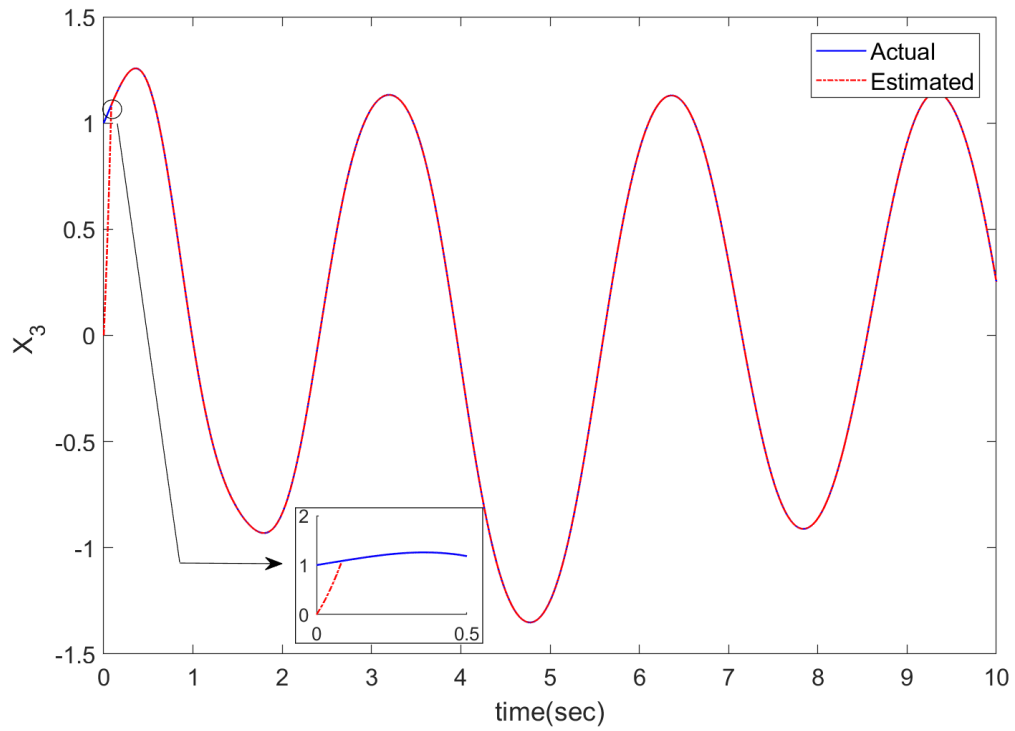


Figure 3.4. Convergence of State x_3

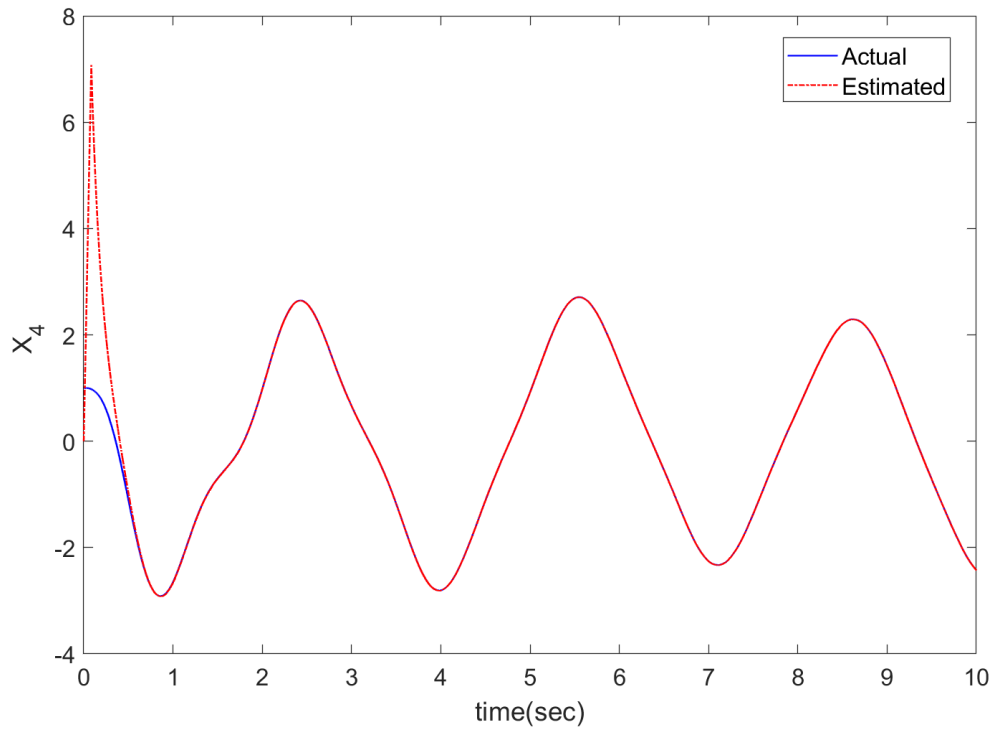


Figure 3.5. Convergence of State x_4

As seen in Figure 3.2-Figure 3.5, the states (in the original basis) are unaffected by the sensor noise, and they converge to their true state values. The sensor noise is minimized to such an extent that it doesn't show up in the plots unless one were to enlarge the y-axis to the order of 10^{-4} . Hence, the proposed observer is seen to significantly reduce the external sensor noise such that its effect on the system is negligible, and the system converges effectively.

3.4.2. Example 2: Rössler Attractor System

To demonstrate the broad implementation of the proposed system, we again consider the Rössler Attractor System from Section 2.3.1 of Chapter 2,

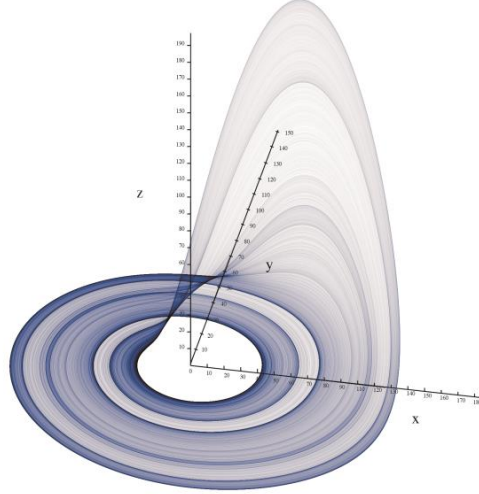


Figure 3.6. Rössler Attractor

The system is defined using the following set of equations:

$$\dot{x} = -y - z \quad (3.69)$$

$$\dot{y} = x + ay \quad (3.70)$$

$$\dot{z} = bx - cz + xz \quad (3.71)$$

The system is defined as:

$$\dot{x} = \begin{bmatrix} 0 & -1 & -1 \\ 1 & a & 0 \\ 0 & 0 & -c \end{bmatrix} x + \begin{bmatrix} 1 \\ 0 \\ 0 \end{bmatrix} u + \begin{bmatrix} 0 \\ 0 \\ 1 \end{bmatrix} (x_1 x_3 + b)$$

$$y = [1 \quad 0 \quad 0]x$$

The nonlinear conditions, given by $\phi = x_1 x_3 + b$, can be expressed in terms of its nonlinear error dynamics as

$$\tilde{\phi} = x_1 x_3 - (\hat{x}_1 \hat{x}_3) = -[x_1 \tilde{x}_3 + x_3 \tilde{x}_1 + \tilde{x}_1 \tilde{x}_3] \quad (3.72)$$

Using parameters from earlier literature [89], we dynamics of the Rössler system using parameters $a = 0.2$, $b = 0.2$ and $c = 5.7$.

Taking

$$A = \begin{bmatrix} 0 & -1 & -1 \\ 1 & a & 0 \\ 0 & 0 & -c \end{bmatrix}, H = \begin{bmatrix} 1 \\ 0 \\ 0 \end{bmatrix}, C = [1 \ 0 \ 0], E = \begin{bmatrix} 0 \\ 0 \\ 1 \end{bmatrix} \text{ and a disturbance matrix } F = \begin{bmatrix} 1 \\ 0 \\ 0 \end{bmatrix}$$

By assuming $|x_1|, |x_3| < 10, |\tilde{x}_1|, |\tilde{x}_3| < 10$, one can choose $G = [1 \ 0 \ 1]$ and assume $\gamma = 15$ for the design of Luenberger-like observer. We assume $W = 0$ for this system. We find that the general observer design is not feasible as the maximum value of γ for which LMI (3.53) is feasible, is found to be 5.72. However for the sliding mode observer, the value of the Lipchitz constant we use is $\gamma = 10$ since the maximum value of γ for which LMI (3.38) is feasible is found to be 10.88. Hence the observer design becomes more feasible as the sliding mode observer has the dual advantage of increasing the maximum allowable γ while simultaneously reducing the maximum effective γ .

Using an initial condition $x(0) = [5 \ 5 \ 5]^T$ and an input $u = \sin(6\pi t)$, we model the Rössler system dynamics in the presence of an external disturbance v with covariance $Q = 1$ and $R = 1$. The system is simulated in MATLAB to solve for \bar{L}_2 using LMI (3.38). The calculations yield the following,

$$\bar{L}_2 = [-0.9445 \quad -3.7780] \quad (3.73)$$

The sub gain matrix \bar{L}_2 is then used to formulate the observer gain matrix L given as,

$$L = \begin{bmatrix} 1 & 0 \\ 0 & 1 \\ -0.9445 & -3.7780 \end{bmatrix}, \text{ as we are only observing its effect on the 22-subsystem.}$$

Using Simulink the above system is modeled and simulated for a time-period of $T_{end} = 5$ secs. Figure 3.7- Figure 3.9 explicitly demonstrate the convergence of the estimated states and the parameters to their true values. This illustrates how the proposed observer works with highly nonlinear chaotic systems even in the presence of external disturbances.

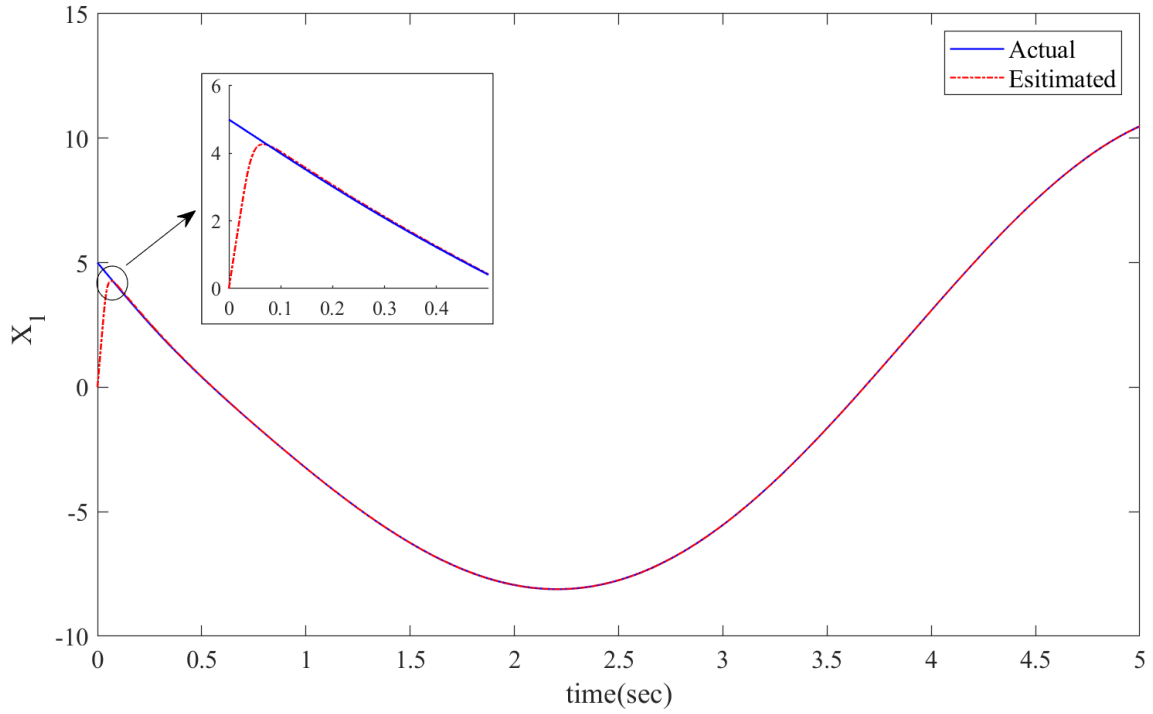


Figure 3.7. Convergence of State x_1

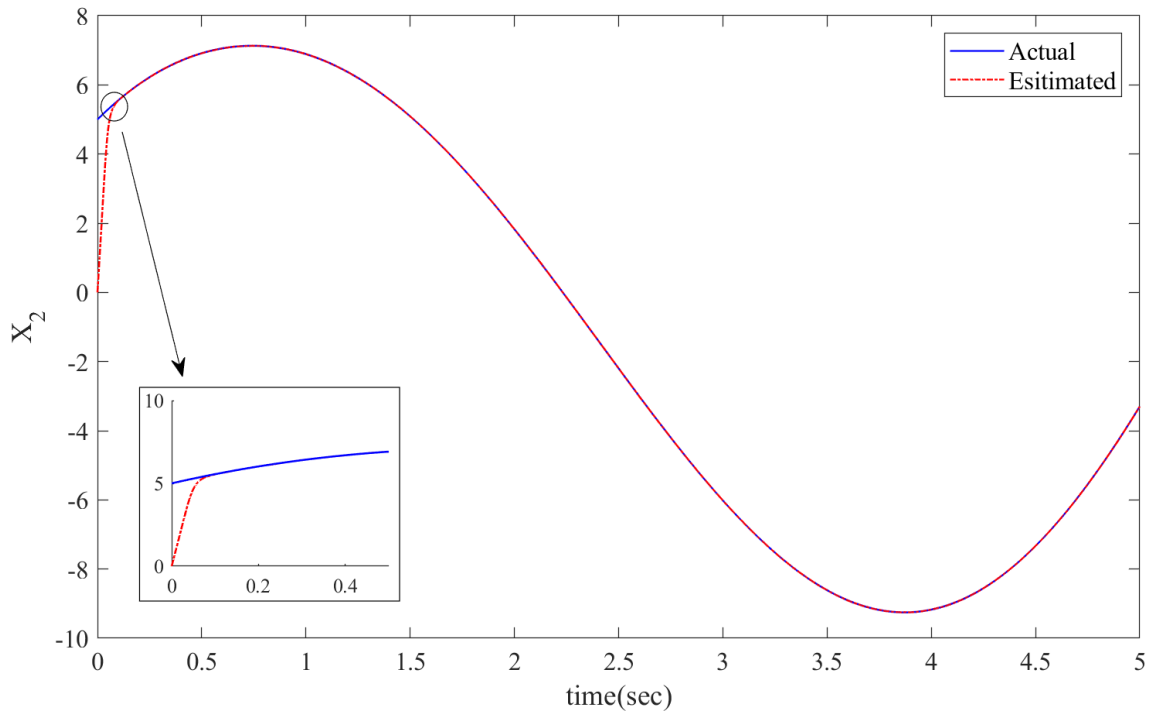


Figure 3.8. Convergence of State x_2

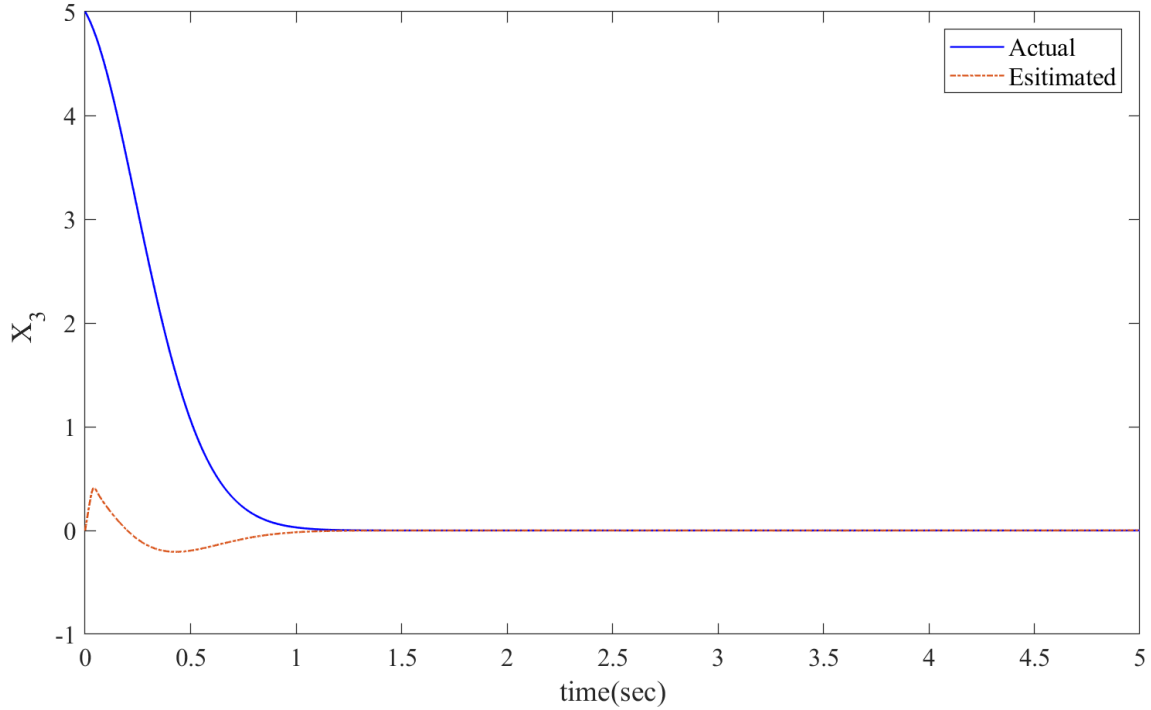


Figure 3.9. Convergence of State x_3

Hence, this demonstrates that the effect of a Gaussian noise can be effectively reduced by utilizing a sliding mode observer and that the LMI used for the design of the observer can be made less conservative. It also additionally applies the TAL function to analyze the stability of linear gain Lipschitz nonlinear observer, the results of which are used to compare the LMIs for the two observers. The illustrative examples demonstrate the effectiveness of the proposed observer and its ability to discard the external sensor noise.

Chapter 4.

Adaptive Sliding Mode Observers for Sector-Bounded Nonlinear Systems

When modelling certain dynamic systems, whilst the various elementary dynamics of the system may be established, some of the parameters of the model are not readily available. For example, while modelling a mechanical spring mass system, the nonlinear model for damping can be assumed with sufficient accuracy. However, the actual value of the damping parameter used in that nonlinear model is unknown. Hence, the observer for the system should be capable of estimating these unknown parameter along with the states simultaneously. Furthermore, the observer should also be robust. This chapter expands on the design of a robust sliding mode observer which is capable of estimating unknown system parameters whilst simultaneously estimating the system states. To further extend the design, we consider a nonlinear system that satisfies a generalized sector bounded (GSB) condition as proposed in [92] given as,

$$\tilde{\Phi}^T \tilde{\Phi} + (\gamma_1 - \gamma_2) \tilde{\Phi}^T G \tilde{x} - \gamma_1 \gamma_2 \tilde{x}^T G^T G \tilde{x} \leq 0 \quad (4.1)$$

The GSB condition encircles a broad range of nonlinearities that include dissipative, Lipschitz and positive real nonlinearity. Hence, the proposed observer encompasses a large area of nonlinear systems.

4.1. System Model

We begin with the following general nonlinear system without input disturbance and sensor noise

$$\begin{aligned} \dot{x} &= Ax + \mu B D x + E \phi(u, x) + F w + H u \\ y &= C x + v \end{aligned} \quad (4.2)$$

In this system, $x \in \mathbb{R}^n$ is the state vector, $u \in \mathbb{R}^q$ is the vector of known inputs, w is a vector of unknown input disturbances, $y \in \mathbb{R}^m$ is the output vector and v is a vector of unknown measurement noise. A, E, F, H, C are known system matrices of appropriate dimensions. The unknown parameter of the system is denoted by μ and matrices B, D represent the direction matrix of the parameter in which it affects the states of the system. The nonlinearity $\phi(u, x) \in (\mathbb{R}^q \times \mathbb{R}^n) \rightarrow \mathbb{R}^p$, is assumed to satisfy a generalized sector bounded condition (4.1) as proposed in [92].

The modelling of the above system (4.2) using the unknown parameters ' μ ' is illustrated using the following example:

If we analyze a second order spring mass system given by,

$$F(t) = kx(t) + m \frac{d^2x(t)}{dt^2} + c \frac{dx(t)}{dt}$$

Where, k and c are the spring and damping constants respectively.

This can also be represented by the following state space model:

$$\begin{bmatrix} \dot{x}_1 \\ \dot{x}_2 \end{bmatrix} = \begin{bmatrix} 0 & 1 \\ -k/m & -c/m \end{bmatrix} \begin{bmatrix} x_1 \\ x_2 \end{bmatrix} + \begin{bmatrix} 0 \\ 1/m \end{bmatrix} F$$

If we assume the damping constant c to be the uncertain parameter in the system, then, c is replaced by $c^* + \Delta c$. Here, c^* is the nominal value of the parameter and Δc is the deviation of the true damping value from its nominal value. Therefore, the above system can be rewritten as:

$$\begin{bmatrix} \dot{x}_1 \\ \dot{x}_2 \end{bmatrix} = \begin{bmatrix} 0 & 1 \\ -k/m & -c^*/m \end{bmatrix} \begin{bmatrix} x_1 \\ x_2 \end{bmatrix} + \Delta c \begin{bmatrix} 0 \\ -1/m \end{bmatrix} \begin{bmatrix} 0 & 1 \end{bmatrix} \begin{bmatrix} x_1 \\ x_2 \end{bmatrix} + \begin{bmatrix} 0 \\ 1/m \end{bmatrix} F$$

Now, this new representation gives us the values for matrices B and D . Where Δc denotes our unknown parameter of the system ' μ ' as given in our system model, and the direction matrix $B = \begin{bmatrix} 0 \\ -1/m \end{bmatrix}$ and matrix $D = [0 \ 1]$.

4.2. Observer Design

We will construct the observer as

$$\begin{aligned}\dot{\hat{x}} &= A\hat{x} + \hat{\mu}BD\hat{x} + E\phi(u, G\hat{x}) + Hu + [I_m \ L_2]^T u_{\hat{y}} \\ \dot{\hat{\mu}} &= L_{\mu}u_{\hat{y}}\end{aligned}\tag{4.3}$$

The dynamics of the estimation error for this observer becomes

$$\begin{aligned}\dot{\tilde{x}} &= A\tilde{x} + BD_{\tilde{x}}\mu + BD_{\tilde{x}}\tilde{\mu} + E\tilde{\phi} - [I_m \ L_2]^T u_{\tilde{y}} + Fw \\ \dot{\tilde{\mu}} &= -L_{\mu}u_{\tilde{y}}\end{aligned}\tag{4.4}$$

Where, L_{μ} denotes the gain for the unknown parameter estimate.

With a sliding observer signal given by

$$u_{\hat{y}} = \rho \times \text{sign}(y - c\hat{x})\tag{4.5}$$

Where $D_x := Dx$

Without loss of generality, we can assume that,

$$C = [I_m \ 0], A = \begin{bmatrix} A_{11} & A_{12} \\ A_{21} & A_{22} \end{bmatrix}, G = [G_1 \ G_2]\tag{4.6}$$

If we examine the dynamics,

$$\dot{\tilde{x}}_1 = A_{11}\tilde{x}_1 + A_{12}\tilde{x}_2 + B_1\mathcal{D}_{\tilde{x}}\mu + B_1\mathcal{D}_{\tilde{x}}\tilde{\mu} + E_1\tilde{\phi} + F_1w - u_{\tilde{y}} \quad (4.7)$$

Theorem 4.1

For a system (4.2) in the form (4.6) , for a choice of $\rho > 0$ with $\rho/\sqrt{2\pi}Q^{-1/2} \gg A_{11}$, G_1 and time scale of \tilde{x}_2 -dynamics, and $\rho > A_{11}\tilde{x}_1 + A_{12}\tilde{x}_2 + E_1\tilde{\phi}$, the \tilde{x}_1 -dynamics of the observer (4.3) can be approximated as

$$\dot{\tilde{x}}_1 \approx \frac{\sqrt{2\pi}}{\rho}Q^{1/2}[A_{12}\tilde{x}_2 + E_1\tilde{\phi}_2 + B_1\mathcal{D}_{\tilde{x}_2}\mu + B_1\mathcal{D}_{\tilde{x}_2}\tilde{\mu}] + w_{\text{filt}} \quad (4.8)$$

Where $\tilde{\phi}_2 = \tilde{\phi}|_{\tilde{x}_1=0} = \phi(u, [y^T \ x_2^T]^T) - \phi(u, [y^T \ \hat{x}_2^T]^T)$ and w_{filt} is the filtered noise

$$\dot{w}_{\text{filt}} + \frac{1}{\sqrt{2\pi}}\rho Q^{-1/2}w_{\text{filt}} = F_1w \quad (4.9)$$

and on the time scale of the \tilde{x}_2 -dynamics,

$$u_{\tilde{y}-eq} = A_{12}\tilde{x}_2 + E_1\tilde{\phi}_2 + B_1\mathcal{D}_{\tilde{x}_2}\mu + B_1\mathcal{D}_{\tilde{x}_2}\tilde{\mu} + F_1 \quad (4.10)$$

Proof: Now the \tilde{x}_1 error dynamics is given by

$$\dot{\tilde{x}}_1 = A_{11}\tilde{x}_1 + A_{12}\tilde{x}_2 + B_1\mathcal{D}_{\tilde{x}}\mu + B_1\mathcal{D}_{\tilde{x}}\tilde{\mu} + E_1\tilde{\phi} + F_1w - u_{\tilde{y}} \quad (4.11)$$

Since $\rho > A_{11}\tilde{x}_1 + E_1\tilde{\phi}$, the system will be driven towards the origin. Now in the neighbourhood of $|\tilde{x}_1| = 0$, the effective \tilde{x}_1 -dynamics becomes

$$\begin{aligned} \dot{\tilde{x}}_1 &= A_{11}\tilde{x}_1 + A_{12}\tilde{x}_2 + E_1 \left[\frac{\partial \phi}{\partial x_1} \tilde{x}_1 + \frac{\partial \phi}{\partial x_2} \tilde{x}_2 \right]_{\tilde{x}_1} \\ &+ B_1\mathcal{D}_{\tilde{x}_2}\mu + B_1\mathcal{D}_{\tilde{x}_2}\tilde{\mu} + F_1w - \rho/\sqrt{2\pi}Q^{-1/2} \end{aligned} \quad (4.12)$$

Since $\rho/\sqrt{2\pi}Q^{-1/2}$ is very large, the observer error dynamics exhibits dual time scale problem. Using Singular perturbation analysis, the slower \tilde{x}_2 -subsystem can be

viewed as a frozen system from the time scale of the \tilde{x}_1 -dynamics [92]. Further since $\rho/\sqrt{2\pi}Q^{-1/2} \gg A_{11}$ and G_1 ,

$$u_{\tilde{y}} := u_{\tilde{y}-eq} \approx \frac{1}{\sqrt{2\pi}}\rho Q^{-1/2}\tilde{x}_1 \quad (4.13)$$

and

$$\left(s + \frac{1}{\sqrt{2\pi}}\rho Q^{-1/2}\right)\tilde{x}_1 \approx [A_{12}\tilde{x}_2 + E_1\tilde{\phi}_2 + B_1\mathcal{D}_{\tilde{x}_2}\mu + B_1\mathcal{D}_{\tilde{x}_2}\tilde{\mu} + F_1w] \quad (4.14)$$

The solution of (4.14) yields

$$\tilde{x}_1 \approx \frac{\sqrt{2\pi}}{\rho}Q^{1/2}[A_{12}\tilde{x}_2 + E_1\tilde{\phi}_2 + B_1\mathcal{D}_{\tilde{x}_2}\mu + B_1\mathcal{D}_{\tilde{x}_2}\tilde{\mu}] + w_{\text{filt}} \quad (4.15)$$

From the time scale of the \tilde{x}_2 -dynamics,

$$u_{\tilde{y}-eq} = A_{12}\tilde{x}_2 + E_1\tilde{\phi}_2 + B_1\mathcal{D}_{\tilde{x}_2}\mu + B_1\mathcal{D}_{\tilde{x}_2}\tilde{\mu} + F_1w \quad (4.16)$$

Based on the covariance of the noise, we will need to make ρ sufficiently large. Hence, the system time scale can be made arbitrarily small, the system will exhibit dual time scale problem. Using Singular perturbation analysis, the slower sub-system can be viewed as a frozen [46].

$$u_{\tilde{y}-eq} = A_{12}\tilde{x}_2 + E_1\tilde{\phi}_2 + B_1\mathcal{D}_{\tilde{x}_2}\mu + B_1\mathcal{D}_{\tilde{x}_2}\tilde{\mu} + F_1 \quad (4.17)$$

It must be noted that $u_{\tilde{y}-eq}$ would be a filtered version with a time constant $(0.3989\rho Q^{-1/2})^{-1}$ as demonstrated in eq(3.30) and (3.31). Since ρ is sufficiently large, we can ignore this filter time constant.

For a general sector bounded nonlinear system, the LMI is formulated as follows:

Lemma 4.2: For the system (4.2) in the form (4.6), a stable observer exists given a choice of $\rho > 0$ with $\rho/\sqrt{2\pi}Q^{-1/2} \gg A_{11}$, $\rho > A_{11}\tilde{x}_1 + A_{12}\tilde{x}_2 + E_1\tilde{\phi}$, if $\exists P_{22} > 0$, $W_{22} \geq 0$, X_2 and $|D\hat{x}| < \sigma'|D\hat{x}| \forall \sigma'$ at every time instance, such that

$$\begin{bmatrix} \tilde{x}_2 \\ \mathcal{D}_{\tilde{x}_2}\tilde{\mu} \\ \tilde{\Phi}_2 \\ \mathcal{D}_{\tilde{x}_2}\mu \\ w \end{bmatrix}^T \begin{bmatrix} M_{11} & M_{12} & M_{13} & M_{14} & M_{15} \\ M_{21} & M_{22} & M_{23} & M_{24} & M_{25} \\ M_{31} & M_{32} & -\epsilon_\phi I & 0 & 0 \\ M_{41} & M_{42} & 0 & -\epsilon_i I & 0 \\ M_{51} & M_{52} & 0 & 0 & R^{-1} \end{bmatrix} \begin{bmatrix} \tilde{x}_2 \\ \mathcal{D}_{\tilde{x}_2}\tilde{\mu} \\ \tilde{\Phi}_2 \\ \mathcal{D}_{\tilde{x}_2}\mu \\ w \end{bmatrix} < 0 \quad (4.18)$$

Where,

$$X_2 = P_{22}L_2 + P_{2\mu}D_{\tilde{x}_2}L_\mu$$

$$X_\mu = \mathcal{D}_{\tilde{x}_2}P_{2\mu}^T L_2 + \mathcal{D}_{\tilde{x}_2}P_{\mu\mu}D_{\tilde{x}_2}L_\mu$$

$$M_{11} = P_{22}A_{22} + A_{22}^T P_{22} - A_{12}^T X_2^T - X_2 A_{12} - \mu_{i-max}^2 \epsilon_i D_{2-i}^T D_{2-i} + \epsilon_\phi \gamma_1 \gamma_2 G_2^T G_2$$

$$M_{12} = P_{22}B_2 + A_{22}^T P_{2\mu} - X_2 B_1 - A_{12}^T X_\mu^T + \sigma' P_{2\mu}$$

$$M_{13} = P_{22}E_2 - X_2 E_1 - (\gamma_1 - \gamma_2) \epsilon_\phi G_2$$

$$M_{14} = P_{22}B_2 - X_2 B_1$$

$$M_{15} = P_{22}F_2 - X_2 F_1$$

$$M_{22} = B_2^T P_{2\mu}^T + P_{2\mu}^T B_2 - B_2^T X_\mu^T - X_\mu B_1 + 2\sigma' P_{\mu\mu}$$

$$M_{23} = P_{2\mu}^T E_2 - X_\mu E_1$$

$$M_{24} = P_{2\mu}^T B_2 - X_\mu B_1$$

$$M_{25} = P_{2\mu}^T F_2 - X_\mu F_1$$

The observer can be chosen by using , the gains L_2 and L_μ given by :

$$L_2 = [P_{22} - P_{\mu 2}^T P_{\mu \mu}^{-1} P_{\mu 2}]^{-1} A_{12}^T Q \quad (4.19)$$

$$L_\mu = -[P_{22} - P_{\mu 2}^T P_{\mu \mu}^{-1} P_{\mu 2}]^{-1} P_{2\mu} P_{\mu \mu}^{-1} (\mathcal{D}_{\hat{x}_2})^{-1} A_{12}^T Q \quad (4.20)$$

Proof :

Equation (4.4) can be written as,

$$\begin{aligned} \dot{\tilde{x}}_2 &= (A_{22} - L_2 A_{12}) \tilde{x}_2 + (E_2 - L_2 E_1) \tilde{\Phi}_2 + (B_2 - L_2 B_1) \mathcal{D}_{\tilde{x}_2} \mu \\ &\quad + (B_2 - L_2 B_1) \mathcal{D}_{\tilde{x}_2} \tilde{\mu} + F_2 w - L_2 F_1 w \\ \dot{\tilde{\mu}} &= -L_\mu (A_{12} \tilde{x}_2 + E_1 \tilde{\Phi}_2 + B_1 \mathcal{D}_{\tilde{x}} \mu + B_1 \mathcal{D}_{\tilde{x}_2} \tilde{\mu} + F_1 w) \end{aligned} \quad (4.21)$$

Consider the Lyapunov candidate function,

$$V = \begin{bmatrix} \tilde{x}_2 \\ \tilde{\mu} \end{bmatrix}^T \begin{bmatrix} P_{22} & P_{2\mu} \mathcal{D}_{\tilde{x}_2} \\ P_{2\mu}^T \mathcal{D}_{\tilde{x}_2} & \mathcal{D}_{\tilde{x}} P_{\mu \mu} \mathcal{D}_{\tilde{x}_2} \end{bmatrix} \begin{bmatrix} \tilde{x}_2 \\ \tilde{\mu} \end{bmatrix} \quad (4.22)$$

Assuming $|D\hat{x}| < \sigma' |D\hat{x}| \forall \sigma'$ at every time instance

Now as per the Lyapunov stability theorem

$$\dot{V} < 0$$

Lemma 4.3 (S-procedure lemma[67])

$$\dot{V} < 0 \Leftrightarrow \bar{V} := \dot{V} - \epsilon_i V_i - \epsilon_\phi V_\phi < 0 \quad (4.23)$$

Assuming $\mu_i < \mu_{i-max}$, on the sliding surface

$$V_i = \mu_i^2 \tilde{x}^T D_i^T D_i \tilde{x} - \mu_{i-max}^2 \tilde{x}^T D_i^T D_i \tilde{x} \leq 0 \quad (4.24)$$

$$V_\phi = \tilde{\Phi}_2^T \tilde{\Phi}_2 + (\gamma_1 - \gamma_2) \tilde{\Phi}_2^T G \tilde{x}_2 - \gamma_1 \gamma_2 \tilde{x}_2^T G^T G \tilde{x}_2 \leq 0 \quad (4.25)$$

Now,

$$\begin{aligned}
\dot{V} = & \begin{bmatrix} \tilde{x}_2 \\ \tilde{\mu} \end{bmatrix}^T \begin{bmatrix} P_{22} & P_{2\mu} \mathcal{D}_{\hat{x}_2} \\ \mathcal{D}_{\hat{x}_2} P_{2\mu}^T & \mathcal{D}_{\hat{x}_2} P_{\mu\mu} \mathcal{D}_{\hat{x}_2} \end{bmatrix} \begin{bmatrix} \dot{\tilde{x}}_2 \\ \dot{\tilde{\mu}} \end{bmatrix} \\
& + \begin{bmatrix} \tilde{x}_2 \\ \tilde{\mu} \end{bmatrix}^T \begin{bmatrix} P_{22} & P_{2\mu} \dot{\mathcal{D}}_{\hat{x}_2} \\ \dot{\mathcal{D}}_{\hat{x}_2} P_{2\mu}^T & \dot{\mathcal{D}}_{\hat{x}_2} P_{\mu\mu} \mathcal{D}_{\hat{x}_2} + \mathcal{D}_{\hat{x}_2} P_{\mu\mu} \dot{\mathcal{D}}_{\hat{x}_2} \end{bmatrix} \begin{bmatrix} \tilde{x}_2 \\ \tilde{\mu} \end{bmatrix}
\end{aligned} \tag{4.26}$$

Hence, defining

$$\begin{bmatrix} P_{22} & P_{2\mu} \mathcal{D}_{\hat{x}_2} \\ \mathcal{D}_{\hat{x}_2} P_{2\mu}^T & \mathcal{D}_{\hat{x}_2} P_{\mu\mu} \mathcal{D}_{\hat{x}_2} \end{bmatrix} \times \begin{bmatrix} L_2 \\ L_\mu \end{bmatrix} = \begin{bmatrix} X_2 \\ X_\mu \end{bmatrix} \tag{4.27}$$

We find

$$\begin{aligned}
\begin{bmatrix} \tilde{x}_2 \\ \tilde{\mu} \end{bmatrix}^T \begin{bmatrix} P_{22} & P_{2\mu} \mathcal{D}_{\hat{x}_2} \\ \mathcal{D}_{\hat{x}_2} P_{2\mu}^T & \mathcal{D}_{\hat{x}_2} P_{\mu\mu} \mathcal{D}_{\hat{x}_2} \end{bmatrix} \begin{bmatrix} \dot{\tilde{x}}_2 \\ \dot{\tilde{\mu}} \end{bmatrix} = & \begin{bmatrix} \tilde{x}_2 \\ \tilde{\mu} \end{bmatrix}^T \begin{bmatrix} P_{22} & P_{2\mu} \mathcal{D}_{\hat{x}_2} \\ \mathcal{D}_{\hat{x}_2} P_{2\mu}^T & \mathcal{D}_{\hat{x}_2} P_{\mu\mu} \mathcal{D}_{\hat{x}_2} \end{bmatrix} \times \\
& \left(\begin{bmatrix} A_{22} & B_2 \mathcal{D}_{\hat{x}_2} \\ 0 & 0 \end{bmatrix} \begin{bmatrix} \tilde{x}_2 \\ \tilde{\mu} \end{bmatrix} + \begin{bmatrix} E_2 \tilde{\Phi}_2 + B_2 \mathcal{D}_{\hat{x}_2} \mu + F_2 w \\ 0 \end{bmatrix} \right) \\
& - \begin{bmatrix} X_2 \\ X_\mu \end{bmatrix} \left\{ \begin{bmatrix} A_{12} & B_1 \mathcal{D}_{\hat{x}_2} \end{bmatrix} \begin{bmatrix} \tilde{x}_2 \\ \tilde{\mu} \end{bmatrix} + E_1 \tilde{\Phi}_2 + B_1 \mathcal{D}_{\hat{x}_2} \mu + F_1 w \right\}
\end{aligned} \tag{4.28}$$

Hence,

$$\begin{aligned}
\begin{bmatrix} \tilde{x}_2 \\ \tilde{\mu} \end{bmatrix}^T \begin{bmatrix} P_{22} & P_{2\mu} \mathcal{D}_{\hat{x}_2} \\ \mathcal{D}_{\hat{x}_2} P_{2\mu}^T & \mathcal{D}_{\hat{x}_2} P_{\mu\mu} \mathcal{D}_{\hat{x}_2} \end{bmatrix} \begin{bmatrix} \dot{\tilde{x}}_2 \\ \dot{\tilde{\mu}} \end{bmatrix} = & \\
\begin{bmatrix} \tilde{x}_2 \\ \mathcal{D}_{\hat{x}_2} \tilde{\mu} \\ \tilde{\Phi}_2 \\ \mathcal{D}_{\hat{x}_2} \mu \\ w \end{bmatrix}^T \begin{bmatrix} P_{22} A_{22} & P_{22} B_2 & P_{22} E_2 & P_{22} B_2 & P_{22} F_2 \\ P_{2\mu}^T A_{22} & P_{2\mu}^T B_2 & P_{2\mu}^T E_2 & P_{2\mu}^T B_2 & P_{2\mu}^T F_2 \\ 0 & 0 & 0 & 0 & 0 \\ 0 & 0 & 0 & 0 & 0 \\ 0 & 0 & 0 & 0 & 0 \end{bmatrix} \begin{bmatrix} \tilde{x}_2 \\ \mathcal{D}_{\hat{x}_2} \tilde{\mu} \\ \tilde{\Phi}_2 \\ \mathcal{D}_{\hat{x}_2} \mu \\ w \end{bmatrix} \\
- \begin{bmatrix} \tilde{x}_2 \\ \mathcal{D}_{\hat{x}_2} \tilde{\mu} \\ \tilde{\Phi}_2 \\ \mathcal{D}_{\hat{x}_2} \mu \\ w \end{bmatrix}^T \begin{bmatrix} X_2 A_{12} & X_2 B_1 & X_2 E_1 & X_2 B_1 & X_2 F_1 \\ X_\mu A_{12} & X_\mu B_1 & X_\mu E_1 & X_\mu B_1 & X_\mu F_1 \\ 0 & 0 & 0 & 0 & 0 \\ 0 & 0 & 0 & 0 & 0 \\ 0 & 0 & 0 & 0 & 0 \end{bmatrix} \begin{bmatrix} \tilde{x}_2 \\ \mathcal{D}_{\hat{x}_2} \tilde{\mu} \\ \tilde{\Phi}_2 \\ \mathcal{D}_{\hat{x}_2} \mu \\ w \end{bmatrix}
\end{aligned} \tag{4.29}$$

Where,

$$X_2 = P_{22}L_2 + P_{2\mu}D_{\hat{x}_2}L_\mu \text{ and } X_\mu = \mathcal{D}_{\hat{x}_2}P_{2\mu}^TL_2 + \mathcal{D}_{\hat{x}_2}P_{\mu\mu}D_{\hat{x}_2}L_\mu$$

Hence,

$$\begin{aligned} & \begin{bmatrix} \tilde{x}_2 \\ \tilde{\mu} \end{bmatrix}^T \begin{bmatrix} P_{22} & P_{2\mu}D_{\hat{x}_2} \\ \mathcal{D}_{\hat{x}_2}P_{2\mu}^T & \mathcal{D}_{\hat{x}_2}P_{\mu\mu}D_{\hat{x}_2} \end{bmatrix} \begin{bmatrix} \dot{\tilde{x}}_2 \\ \dot{\tilde{\mu}} \end{bmatrix} \\ &= \begin{bmatrix} \tilde{x}_2 \\ \mathcal{D}_{\hat{x}_2}\tilde{\mu} \\ \tilde{\Phi}_2 \\ \mathcal{D}_{\hat{x}_2}\mu \\ w \end{bmatrix}^T \begin{bmatrix} M_{11} & M_{12} & M_{13} & M_{14} & M_{15} \\ M_{21} & M_{22} & M_{23} & M_{24} & M_{25} \\ M_{31} & M_{32} & -\epsilon_\phi I & 0 & 0 \\ M_{41} & M_{42} & 0 & -\epsilon_i I & 0 \\ M_{51} & M_{52} & 0 & 0 & R^{-1} \end{bmatrix} \begin{bmatrix} \tilde{x}_2 \\ \mathcal{D}_{\hat{x}_2}\tilde{\mu} \\ \tilde{\Phi}_2 \\ \mathcal{D}_{\hat{x}_2}\mu \\ w \end{bmatrix} \end{aligned}$$

(4.30)

Where,

$$X_2 = P_{22}L_2 + P_{2\mu}D_{\hat{x}_2}L_\mu$$

$$X_\mu = \mathcal{D}_{\hat{x}_2}P_{2\mu}^TL_2 + \mathcal{D}_{\hat{x}_2}P_{\mu\mu}D_{\hat{x}_2}L_\mu$$

$$M_{11} = P_{22}A_{22} + A_{22}^TP_{22} - A_{12}^TX_2^T - X_2A_{12} - \mu_{i-max}^2\epsilon_i D_{2-i}^TD_{2-i} + \epsilon_\phi\gamma_1\gamma_2G_2^TG_2$$

$$M_{12} = P_{22}B_2 + A_{22}^TP_{2\mu} - X_2B_1 - A_{12}^TX_\mu^T + \sigma'P_{2\mu}$$

$$M_{13} = P_{22}E_2 - X_2E_1 - (\gamma_1 - \gamma_2)\epsilon_\phi G_2$$

$$M_{14} = P_{22}B_2 - X_2B_1$$

$$M_{15} = P_{22}F_2 - X_2F_1$$

$$M_{22} = B_2^TP_{2\mu}^T + P_{2\mu}^TB_2 - B_2^TX_\mu^T - X_\mu B_1 + 2\sigma'P_{\mu\mu}$$

$$M_{23} = P_{2\mu}^TE_2 - X_\mu E_1$$

$$M_{24} = P_{2\mu}^TB_2 - X_\mu B_1$$

$$M_{25} = P_{2\mu}^TF_2 - X_\mu F_1$$

As seen from (4.30) , the LMI gives the complete condition for the convergence of observer (4.3).

Hence, the gains L_2 and L_μ can be calculated from (4.27) after solving the LMI above. However, this makes the gains functions of $\mathcal{D}_{\hat{x}_2}$. In order to simplify the solution and decouple the gains from $\mathcal{D}_{\hat{x}_2}$, we choose $PL = \begin{bmatrix} X_2 \\ X_\mu \end{bmatrix} = \begin{bmatrix} A_{12}^T \\ 0 \end{bmatrix} Q$ by extending Phanomchoeng et al [93].

$$\text{Now, if } P^I = \begin{bmatrix} P_{22} & P_{2\mu} \mathcal{D}_{\hat{x}_2} \\ \mathcal{D}_{\hat{x}_2}^T P_{2\mu}^T & \mathcal{D}_{\hat{x}_2}^T P_{\mu\mu} \mathcal{D}_{\hat{x}_2} \end{bmatrix}^{-1},$$

$$\begin{bmatrix} P_{22}^I & P_{\mu 2}^I \\ P_{\mu 2}^I & P_{\mu\mu}^I \end{bmatrix} \begin{bmatrix} A_{12}^T \\ 0 \end{bmatrix} Q = \begin{bmatrix} P_{22}^I A_{12}^T Q \\ P_{\mu 2}^I A_{12}^T Q \end{bmatrix} \quad (4.31)$$

Or

$$\bar{L} = \begin{bmatrix} P_{22}^I & P_{\mu 2}^I \\ P_{\mu 2}^I & P_{\mu\mu}^I \end{bmatrix} \begin{bmatrix} A_{12}^T \\ 0 \end{bmatrix} Q = \begin{bmatrix} P_{22}^I A_{12}^T Q \\ P_{\mu 2}^I A_{12}^T Q \end{bmatrix} \quad (4.32)$$

Since

$$P_{22}^I = [P_{22} - P_{\mu 2}^T P_{\mu\mu}^{-1} P_{\mu 2}]^{-1} \quad (4.33)$$

$$P_{\mu 2}^I{}^T = -[P_{22} - P_{\mu 2}^T P_{\mu\mu}^{-1} P_{\mu 2}]^{-1} P_{2\mu} P_{\mu\mu}^{-1} (\mathcal{D}_{\hat{x}_2})^{-1} \quad (4.34)$$

We find

$$L_2 = [P_{22} - P_{\mu 2}^T P_{\mu\mu}^{-1} P_{\mu 2}]^{-1} A_{12}^T Q \quad (4.35)$$

$$L_\mu = -[P_{22} - P_{\mu 2}^T P_{\mu\mu}^{-1} P_{\mu 2}]^{-1} P_{2\mu} P_{\mu\mu}^{-1} (\mathcal{D}_{\hat{x}_2})^{-1} A_{12}^T Q \quad (4.36)$$

Where the value of Q can be determined by solving the LMI (4.30)

Note 1 : Since, the observer design reduces the size of \mathcal{D} matrix, it presents an LMI which is more easier to solve mathematically as compared to the one proposed in [60] . This added advantage is very useful for solving complex systems where the unknown term affects more than one state. This is distinctly demonstrated in the example given below.

4.2.2. Example 1: 4th order nonlinear system

Consider the following 4th order nonlinear two-mass spring system with damping from Section 3.4.1 in Chapter 3 . The system is represented in Figure 4.1 as follows:

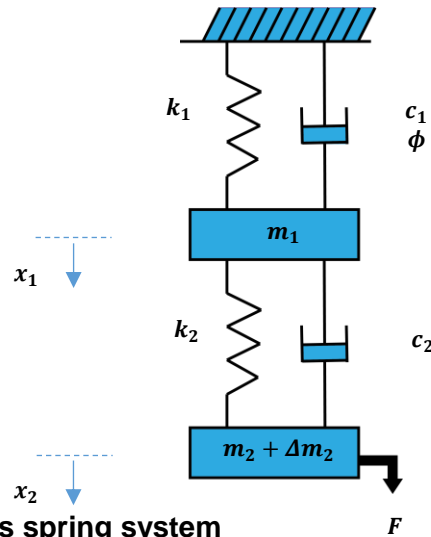


Figure 4.1. Two-mass spring system

The figure represents a two-mass spring system where k_1, k_2 are the spring constants, c_1, c_2 are the damping coefficients and m_1, m_2 are the masses suspended by the springs. In this system, the second mass ' m_2 ', is assumed to be unknown. Hence it is modeled as $m_2 = m_2 + \Delta m_2$, in order to represent it in the form of the proposed system model (4.2). Here, The m_2 is the nominal mass and Δm_2 represented the deviation of this nominal mass from the real value. The unknown parameter assumed, models some uncertainty to one of the masses. The system can be represented by the following general nonlinear state space model:

$$\dot{x} = Ax + \mu BDx + E\phi(u, x) + Fw + Hu$$

$$y = Cx + v$$

Where,

$$A = \begin{bmatrix} 0 & 1 & 0 & 0 \\ -25 & -1 & 15 & 0.3 \\ 0 & 0 & 0 & 1 \\ 15 & 0.3 & -15 & -0.3 \end{bmatrix}, B = [0 \ 0 \ 0 \ 1]^T,$$

$$C = \begin{bmatrix} 1 & 0 & 0 & 0 \\ 0 & 0 & 1 & 0 \end{bmatrix}, D = [-0.25 \ -0.0033 \ 0.25 \ 0.0033],$$

$$E = [0 \ 1 \ 0 \ 0]^T, F = [0 \ 0 \ 0 \ 1]^T, G = [0 \ 1 \ 0 \ 0],$$

$$H = [0 \ 0 \ 0 \ 1]^T, \phi = \sin(x_2), u = 35\sin(2\pi t)$$

The parameters provide the complete state space representation of the system. The observer proposed estimates the states and the unknown parameter of the system simultaneously.

Using an initial condition $x(0) = [10 \ 20 \ 20 \ 40]^T$ and an input $u = 35\sin(2\pi t)$, the mass spring system dynamics were modelled in the presence of an external disturbance v with covariance $Q = 1$ and $R = 1$. We choose the unknown parameter $\mu = 1$ and assume the Lipschitz constant $\gamma = 0.1$ for the simulation.

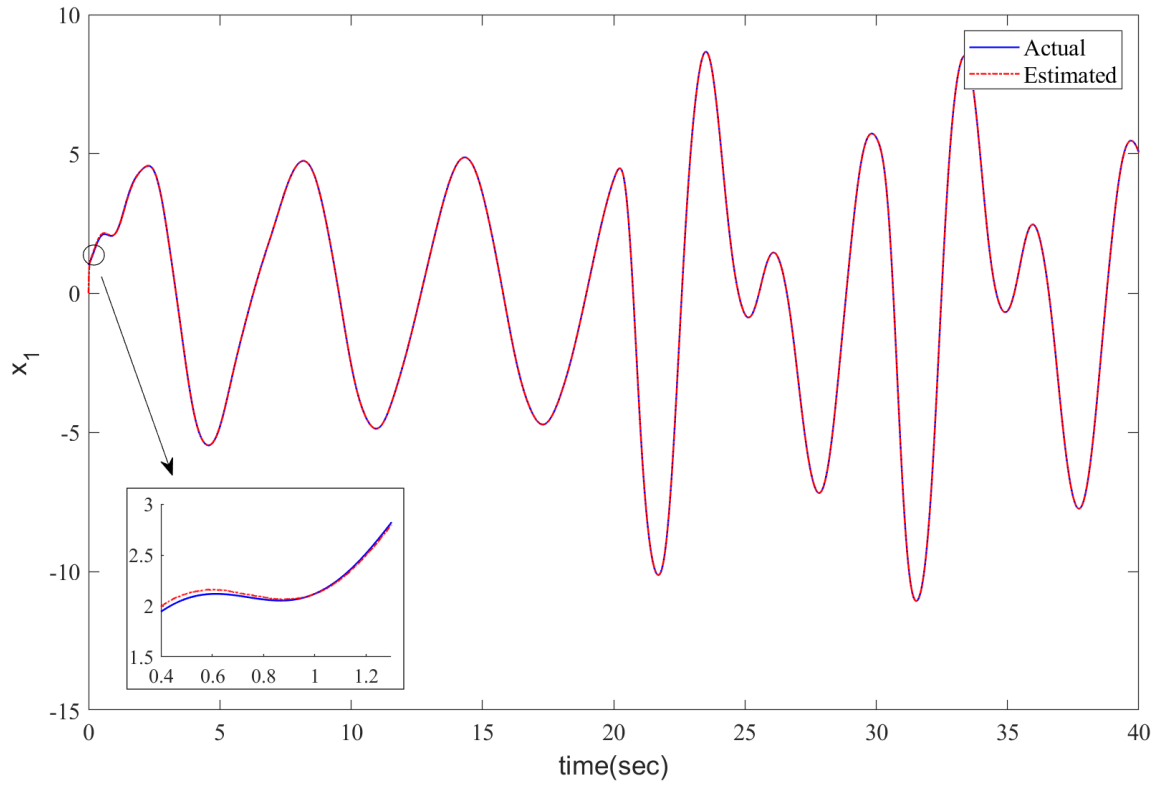


Figure 4.2. Convergence of State x_1

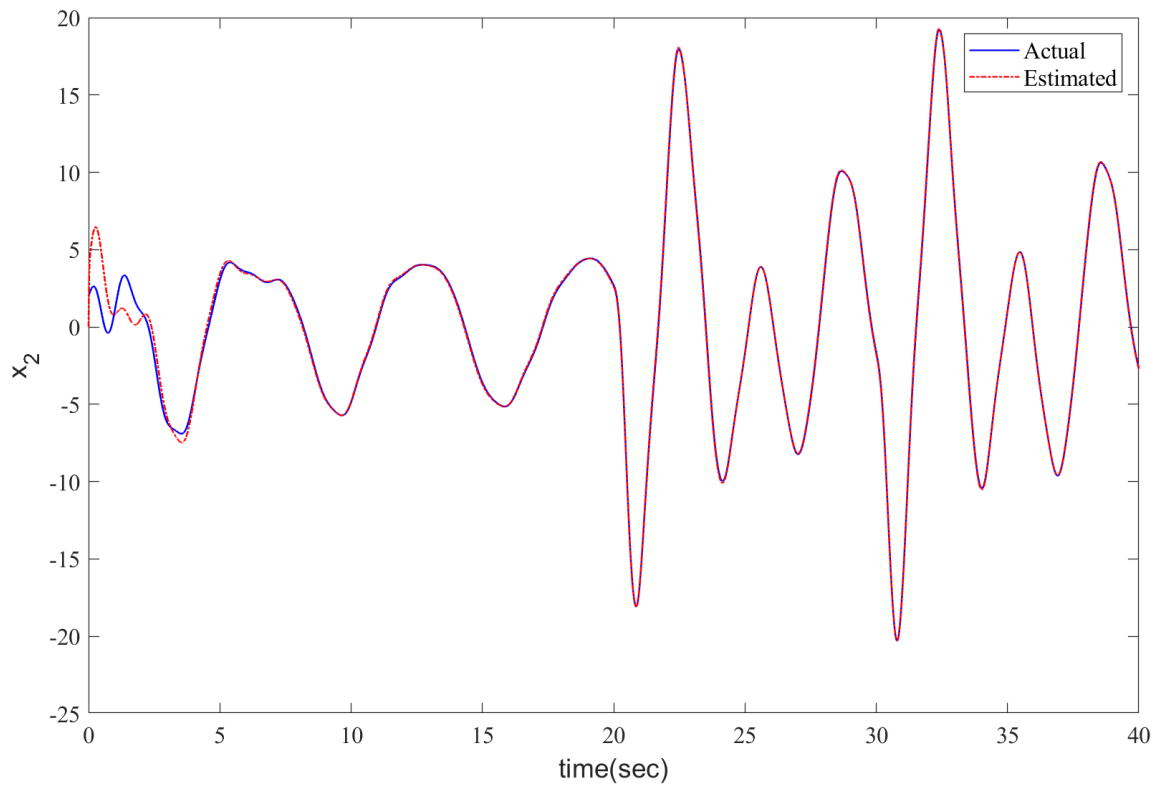


Figure 4.3. Convergence of State x_2

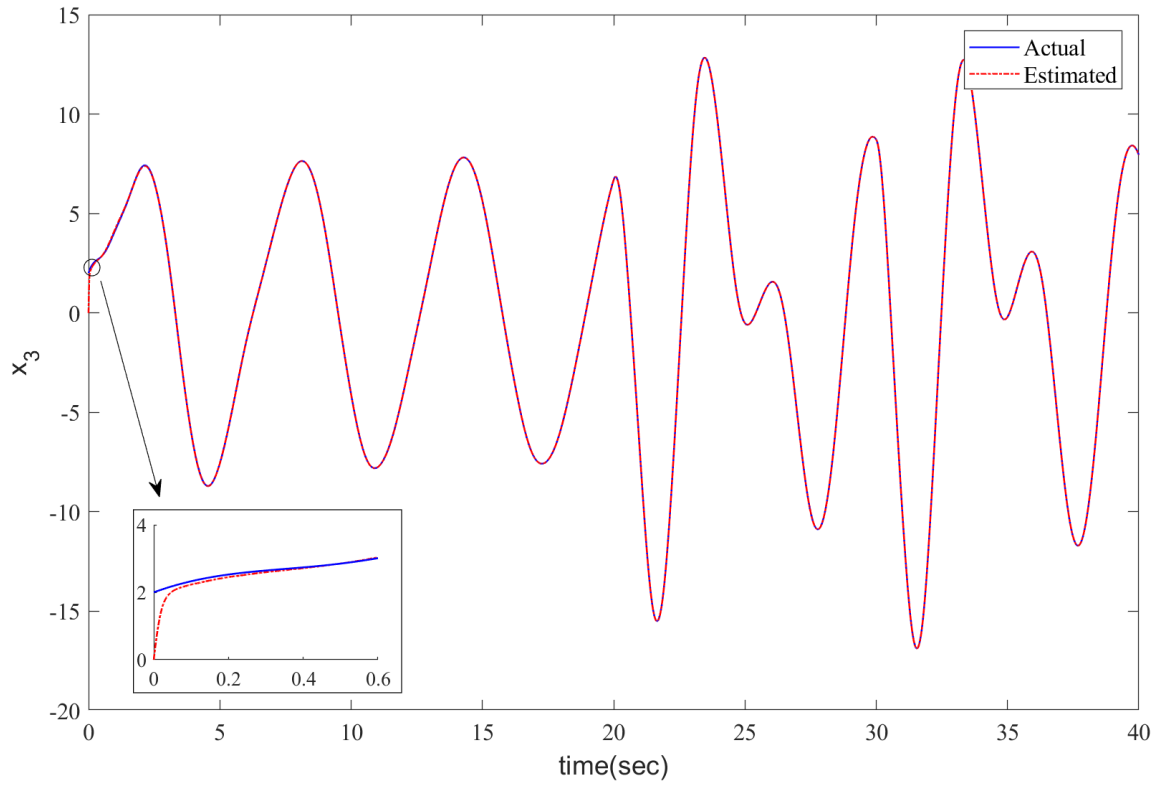


Figure 4.4. Convergence of State x_3

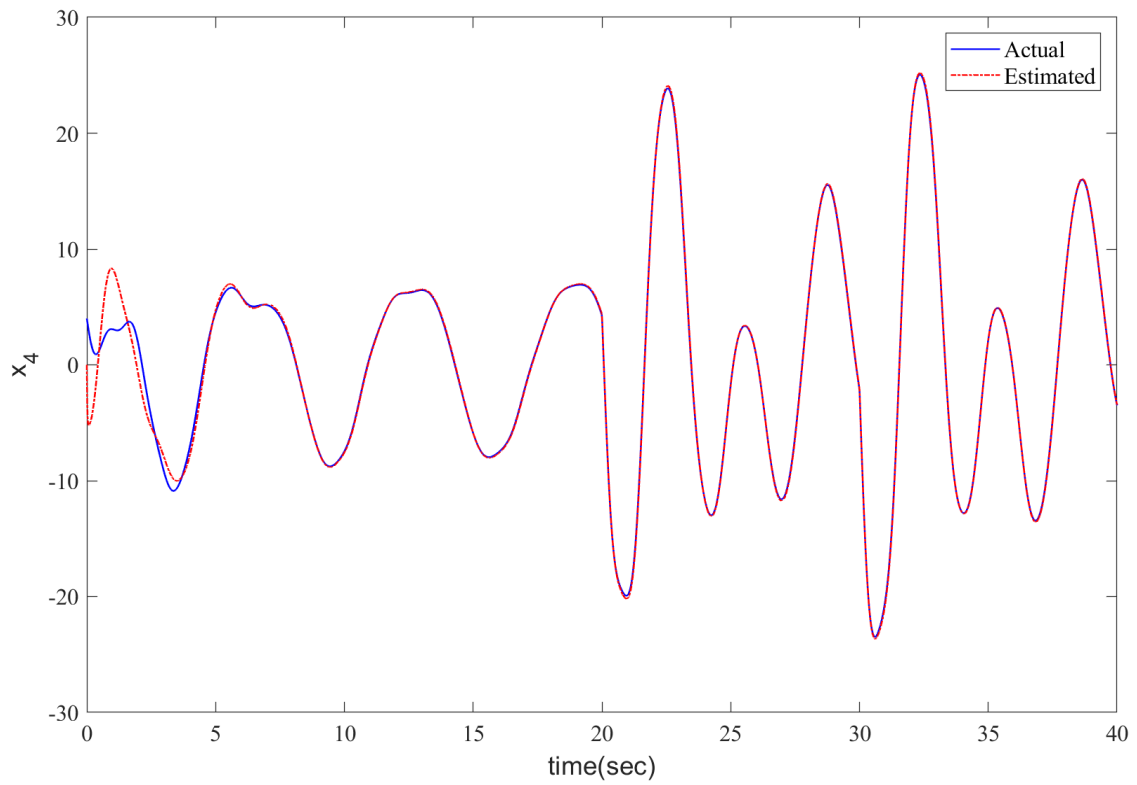


Figure 4.5. Convergence of State x_4

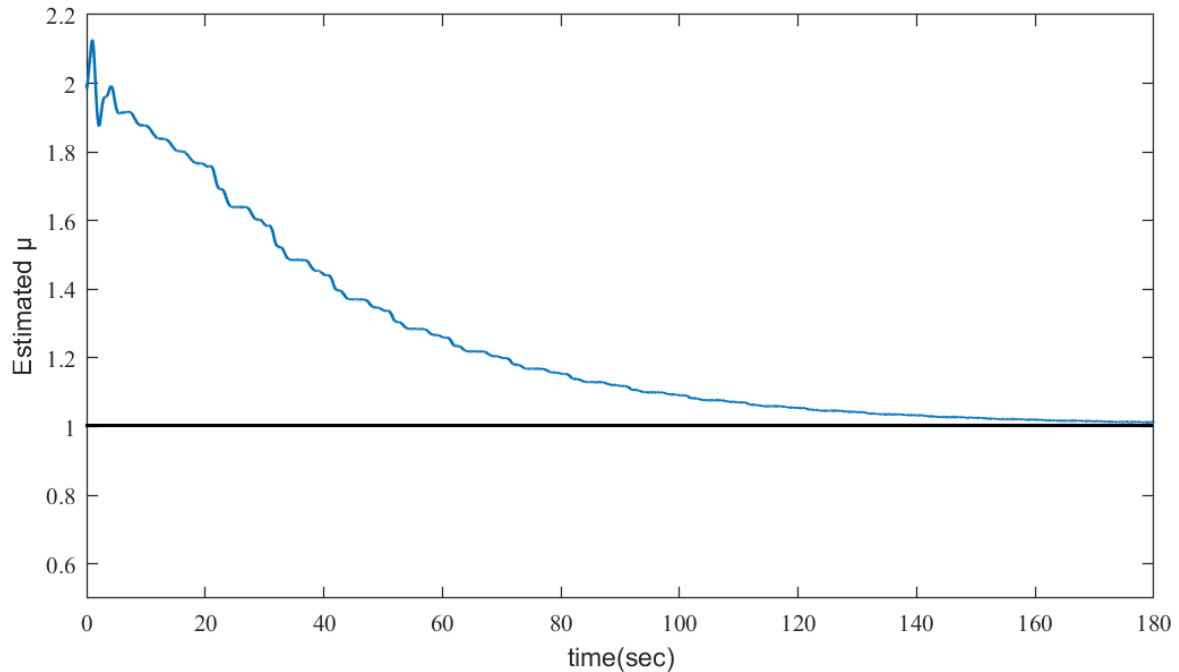


Figure 4.6. Unknown Parameter ' μ ' Estimation

Figure 4.2 - Figure 4.5 show the evolution of the actual state values and their estimations, while figure Figure 4.6 shows the evolution of the parameter estimate to its true value $\mu = 1$.

4.2.3. Comparing EKF based observers with proposed observer design

In order to compare the two observer designs, we construct an EKF based observer to evaluate its performance on the previous example (4.2.2).

In order to estimate the unknown parameters of the system, we augment the unknown parameters of the system to the states as seen in literature [61],[62]. Similarly, for our continuous time system we define the augmented state vector as:

$$\dot{\hat{x}} = f(\bar{x}, u) + w$$

$$y = h(\bar{x}) + v$$

The EKF is given by,

$$\hat{\dot{x}} = f(\hat{x}, u) + L(y - h(\hat{x}))$$

Where,

$$L = PH^T Q^{-1}$$

$$\dot{P} = FP + PF^T - LHP + \bar{R}$$

And

$$F = \left. \frac{\partial f}{\partial \bar{x}} \right|_{\hat{x}, u}, H = \left. \frac{\partial h}{\partial \bar{x}} \right|_{\hat{x}}$$

Hence for example 4.2.2, we can write the system as,

$$F = \left. \frac{\partial f}{\partial \bar{x}} \right|_{\hat{x}, u} = \begin{bmatrix} 0 & 1 & 0 & 0 & 0 \\ -25 & -1 + \cos(\hat{x}_2) & 15 & 0.3 & 0 \\ 0 & 0 & 0 & 1 & 0 \\ 15 - 0.25\mu_1 & 0.3 - 0.0033\mu_1 & -15 + 0.25\mu_1 & -0.3 + 0.0033\mu_1 & S \\ 0 & 0 & 0 & 0 & 0 \end{bmatrix}$$

Where, $S = -0.25\hat{x}_1 - 0.0033\hat{x}_2 + 0.25\hat{x}_3 + 0.0033\hat{x}_4$

$$\text{And } H = \left. \frac{\partial h}{\partial \bar{x}} \right|_{\hat{x}} = \begin{bmatrix} 1 & 0 & 0 & 0 & 0 \\ 0 & 0 & 1 & 0 & 0 \end{bmatrix}$$

In order for the EKF to estimate the unknown parameter of the system, it requires the knowledge of the Virtual Parameter Disturbance (VPD). However, since there is no

defined method to select the VPD-covariance, we assume the value to be equal to the VPD-covariance of the disturbance w .

Therefore,

$$\bar{R} = \begin{bmatrix} 0 & 0 & 0 & 0 & 0 \\ 0 & 0 & 0 & 0 & 0 \\ 0 & 0 & 0 & 0 & 0 \\ 0 & 0 & 0 & R & 0 \\ 0 & 0 & 0 & 0 & R \end{bmatrix}$$

Using the system parameters mentioned above, the system is simulated for a time period of $T=20$ seconds. The simulation is performed under the same initial conditions ($x(0) = [10 \ 20 \ 20 \ 40]^T$) as the previous example for the proposed observer design. The state estimation results obtained are plotted along side the proposed observer design to compare the convergence rate error of the two methods. Figure

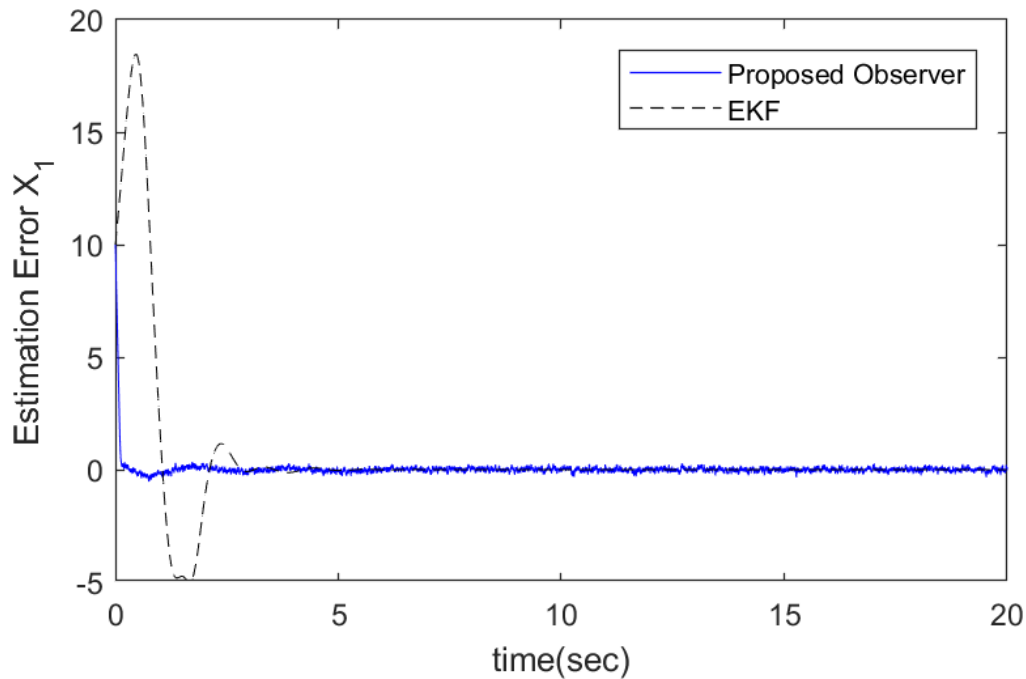


Figure 4.7. Estimation error in state x_1

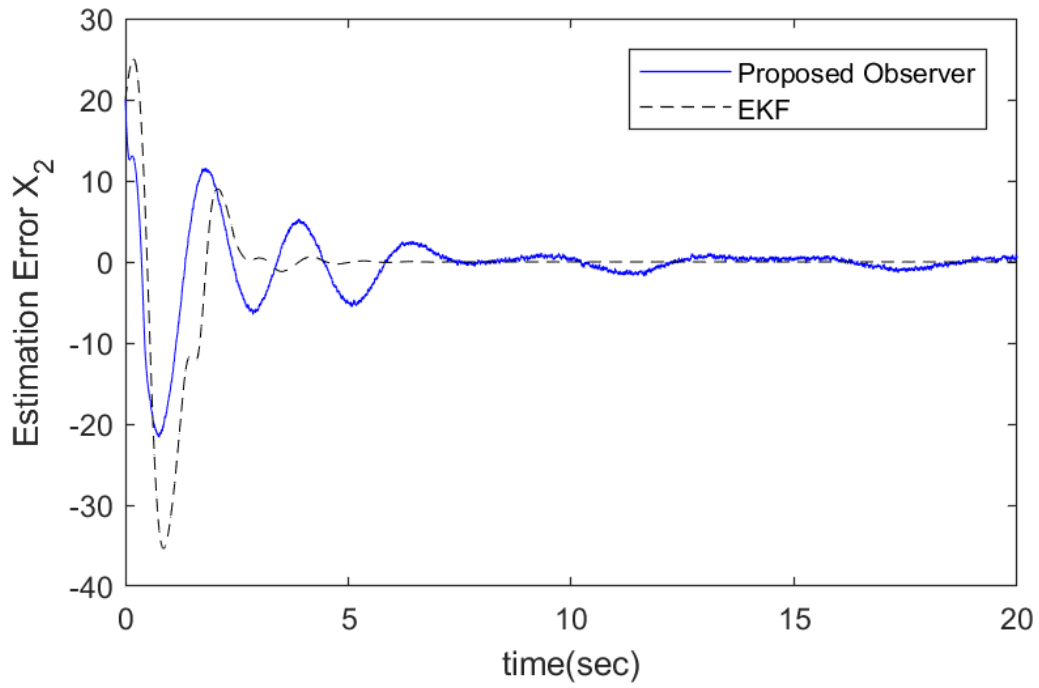


Figure 4.8. Estimation error in state x_2

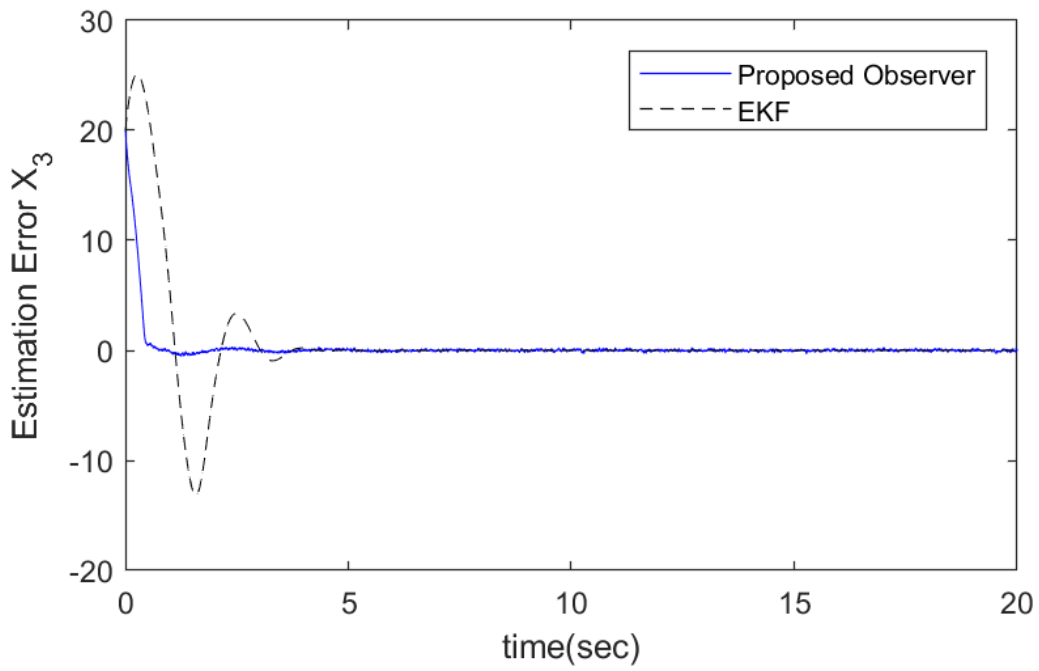


Figure 4.9. Estimation error in state x_3

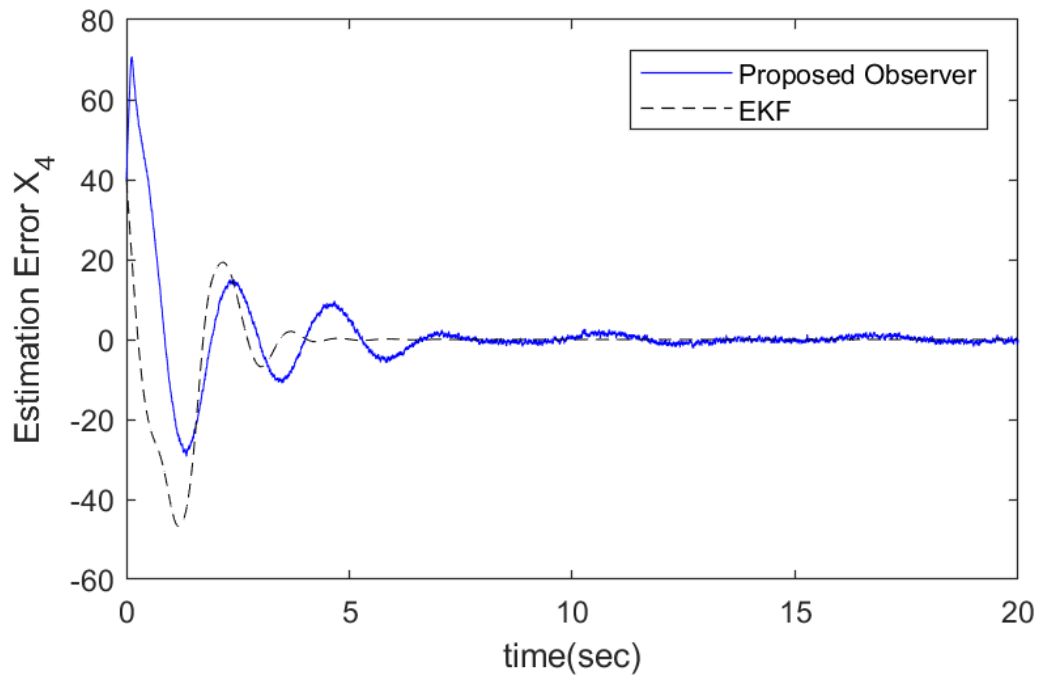


Figure 4.10. Estimation error in state x_4

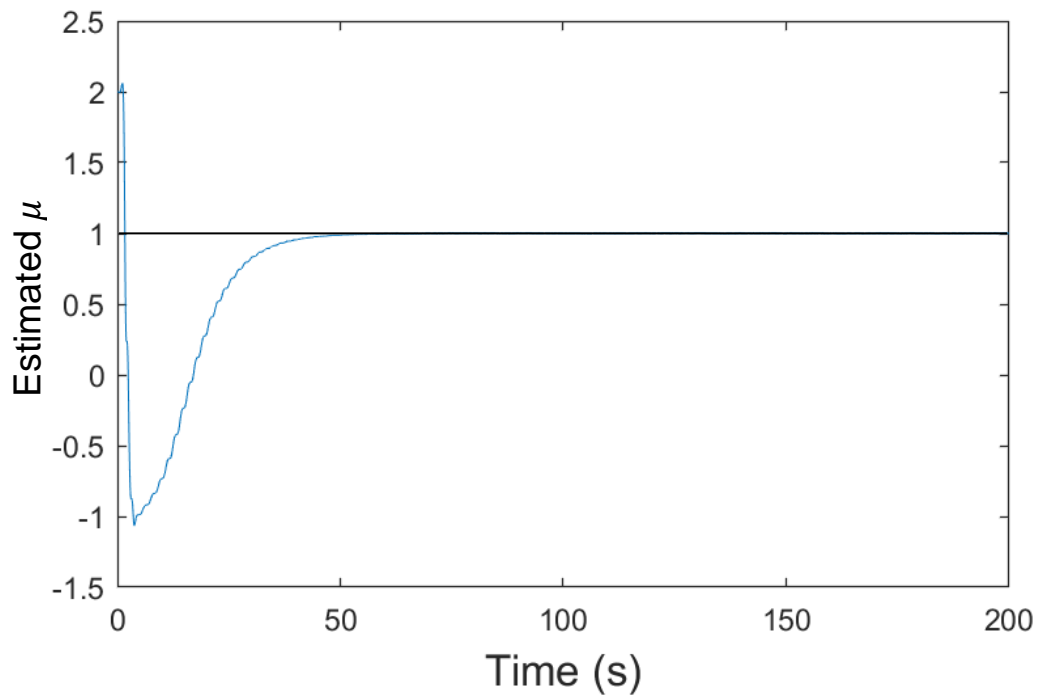


Figure 4.11. Unknown Parameter ' μ ' Estimation using EKF

As seen from the results, the proposed observer outperforms the EKF in terms of initial state estimation errors. Since an EKF demands for the initial state estimates to be close to the true state values, any large deviation in the initial state estimates can strongly influence the convergence rate. As the EKF relies on linearizing the nonlinear system before constructing a linear gain observer for the dynamics, any linearization errors can have an effect on initial estimation error. Hence, the proposed observer converges faster with much smaller initial state estimation errors as seen in Figure 4.7 - Figure 4.10 .

The EKF performs better when it comes to attenuating noise during steady state. However, this is because of the optimal nature of the extended Kalman filter which relies on the availability of precise noise covariance values. Hence, in cases where an accurate noise covariance matrix is unavailable, the EKF would yield poor noise attenuation characteristics. Also, the EKF requires an online solution to the matrix differential Ricatti equation and hence can be computationally intensive.

4.2.4. Dissipative nonlinear case

A dissipative nonlinear system is a specific case of the generalised sector bounded nonlinear system given by

$$(x - \hat{x})^T G(\phi(u, x) - \phi(u, \hat{x}))$$

Where the bounds are given by $\gamma_1 \rightarrow \infty$ and $\gamma_2 = 0$

For the specific case of a dissipative nonlinear system, the LMI can be formulated as follows:

Lemma 4.4: For the system (4.2) in the form (4.6), a stable observer (4.4) exists given a choice of σ' , such that, if $\gamma_2 \geq |D\hat{x}| \geq \gamma_1$, $\max(|(D\hat{x})(D\hat{x})^{-1}|) = \sigma'$, the observer can guarantee a performance

$$J = \frac{\int_0^T \tilde{x}^T W \tilde{x} dt + \int_0^T \tilde{\mu}^T \mathcal{D}_{\hat{x}} W_{\mu} \mathcal{D}_{\hat{x}} \tilde{\mu} dt}{\tilde{x}_0^T P_0 \tilde{x}_0 + \tilde{\mu}_0^T P_{\mu 0} \tilde{\mu}_0 + \int_0^T v^T Q^{-1} v dt + \int_0^T w^T R^{-1} w dt} < \frac{1}{\alpha}$$

$\forall x, \hat{x}$ after a sufficiently large time T , iff $P_{22} > 0$, $\epsilon_i > 0$, and $P_{2\mu}^T$ such that $\forall |\sigma'| \leq \sigma'_{max}$

$$P_{22}E_2 = \epsilon_i * G_2'$$

$$P_{2\mu}^T E_2 = 0$$

$$\begin{bmatrix} M_{11} & M_{12} & M_{13} & M_{14} \\ M_{12}^T & M_{22} & M_{23} & M_{24} \\ M_{13}^T & M_{23}^T & -\epsilon_i & 0 \\ M_{14}^T & M_{24}^T & 0 & R^{-1} \end{bmatrix} < 0$$

Where,

$$M_{11} = P_{22}A_{22} + A_{22}^T P_{22} - A_{12}^T Q^T A_{12} - A_{12}^T Q A_{12} - \mu_{max}^2 \epsilon_i D_2^T D_2$$

$$M_{12} = P_{22}B_2 + A_{22}^T P_{2\mu} - A_{12}^T Q B_1 + \sigma' P_{2\mu}$$

$$M_{13} = P_{22}B_2 - X_2 B_1$$

$$M_{14} = P_{22}F_2 - X_2 F_1$$

$$M_{22} = B_2^T P_{2\mu}^T + P_{2\mu}^T B_2 + 2\sigma' P_{\mu\mu}$$

$$M_{23} = P_{2\mu}^T B_2$$

$$M_{24} = P_{2\mu}^T F_2$$

When the observer gains are chosen as

$$L_2 = [P_{22} - P_{\mu 2}^T P_{\mu\mu}^{-1} P_{\mu 2}]^{-1} A_{12}^T Q$$

$$L_{\mu} = -[P_{22} - P_{\mu 2}^T P_{\mu\mu}^{-1} P_{\mu 2}]^{-1} P_{2\mu} P_{\mu\mu}^{-1} (D_{\hat{x}_2})^{-1} A_{12}^T Q$$

Proof :

Equation (4.4) can be written in terms of $\dot{\hat{x}}_2$ -dynamics ,

$$\begin{aligned}
\dot{\tilde{x}}_2 &= (A_{22} - L_2 A_{12})\tilde{x}_2 + (E_2 - L_2 E_1)\tilde{\Phi}_2 + (B_2 - L_2 B_1) \mathcal{D}_{\tilde{x}_2} \mu \\
&\quad + (B_2 - L_2 B_1) \mathcal{D}_{\tilde{x}_2} \tilde{\mu} + F_2 w - L_2 F_1 w \\
\dot{\tilde{\mu}} &= -L_\mu (A_{12} \tilde{x}_2 + E_1 \tilde{\Phi}_2 + B_1 \mathcal{D}_{\tilde{x}_2} \mu + B_1 \mathcal{D}_{\tilde{x}_2} \tilde{\mu} + F_1 w)
\end{aligned} \tag{4.37}$$

Consider the Lyapunov candidate function,

$$V = \begin{bmatrix} \tilde{x}_2 \\ \tilde{\mu} \end{bmatrix}^T \begin{bmatrix} P_{22} & P_{2\mu} \mathcal{D}_{\tilde{x}_2} \\ P_{2\mu}^T \mathcal{D}_{\tilde{x}_2} & \mathcal{D}_{\tilde{x}_2} P_{\mu\mu} \mathcal{D}_{\tilde{x}_2} \end{bmatrix} \begin{bmatrix} \tilde{x}_2 \\ \tilde{\mu} \end{bmatrix} \tag{4.38}$$

From lemma 1 given in [67], $J_1 < 0$ iff $\exists \varepsilon_i, \eta > 0$ s.t

$$J_2 := J_1 - \int_0^T (\sum \varepsilon_i V_i + \eta V_\phi) dt < 0 \tag{4.39}$$

Assuming $\mu_i < \mu_{i-max}$, on the sliding surface

$$V_i = \mu_i^2 \tilde{x}^T D_i^T D_i \tilde{x} - \mu_{i-max}^2 \tilde{x}^T D_i^T D_i \tilde{x} \leq 0 \tag{4.40}$$

$$V_\phi = 2\tilde{x}^T G \tilde{\Phi} \leq 0 \tag{4.41}$$

Now,

$$\begin{aligned}
\dot{V} &= \begin{bmatrix} \dot{\tilde{x}}_2 \\ \dot{\tilde{\mu}} \end{bmatrix}^T \begin{bmatrix} P_{22} & P_{2\mu} \mathcal{D}_{\tilde{x}_2} \\ P_{2\mu}^T \mathcal{D}_{\tilde{x}_2} & \mathcal{D}_{\tilde{x}_2} P_{\mu\mu} \mathcal{D}_{\tilde{x}_2} \end{bmatrix} \begin{bmatrix} \dot{\tilde{x}}_2 \\ \dot{\tilde{\mu}} \end{bmatrix} \\
&\quad + \begin{bmatrix} \tilde{x}_2 \\ \tilde{\mu} \end{bmatrix}^T \begin{bmatrix} P_{22} & P_{2\mu} \dot{\mathcal{D}}_{\tilde{x}_2} \\ \dot{\mathcal{D}}_{\tilde{x}_2} P_{2\mu}^T & \dot{\mathcal{D}}_{\tilde{x}_2} P_{\mu\mu} \mathcal{D}_{\tilde{x}_2} + \mathcal{D}_{\tilde{x}_2} P_{\mu\mu} \dot{\mathcal{D}}_{\tilde{x}_2} \end{bmatrix} \begin{bmatrix} \tilde{x}_2 \\ \tilde{\mu} \end{bmatrix}
\end{aligned} \tag{4.42}$$

Hence, defining

$$\begin{bmatrix} P_{22} & P_{2\mu} \mathcal{D}_{\tilde{x}_2} \\ P_{2\mu}^T \mathcal{D}_{\tilde{x}_2} & \mathcal{D}_{\tilde{x}_2} P_{\mu\mu} \mathcal{D}_{\tilde{x}_2} \end{bmatrix} \times \begin{bmatrix} L_2 \\ L_\mu \end{bmatrix} = \begin{bmatrix} X_2 \\ X_\mu \end{bmatrix} \tag{4.43}$$

We find

$$\begin{aligned}
\begin{bmatrix} \tilde{x}_2 \\ \tilde{\mu} \end{bmatrix}^T \begin{bmatrix} P_{22} & P_{2\mu} \mathcal{D}_{\hat{x}_2} \\ P_{2\mu}^T \mathcal{D}_{\hat{x}_2} & \mathcal{D}_{\hat{x}_2} P_{\mu\mu} \mathcal{D}_{\hat{x}_2} \end{bmatrix} \begin{bmatrix} \dot{\tilde{x}}_2 \\ \dot{\tilde{\mu}} \end{bmatrix} &= \begin{bmatrix} \tilde{x}_2 \\ \tilde{\mu} \end{bmatrix}^T \begin{bmatrix} P_{22} & P_{2\mu} \mathcal{D}_{\hat{x}_2} \\ P_{2\mu}^T \mathcal{D}_{\hat{x}_2} & \mathcal{D}_{\hat{x}_2} P_{\mu\mu} \mathcal{D}_{\hat{x}_2} \end{bmatrix} \times \\
&\quad \left(\begin{bmatrix} A_{22} & B_2 \mathcal{D}_{\hat{x}_2} \\ 0 & 0 \end{bmatrix} \begin{bmatrix} \tilde{x}_2 \\ \tilde{\mu} \end{bmatrix} + \begin{bmatrix} E_2 \tilde{\Phi}_2 + B_2 \mathcal{D}_{\hat{x}_2} \mu + F_2 w \\ 0 \end{bmatrix} \right) \\
&\quad - \begin{bmatrix} X_2 \\ X_\mu \end{bmatrix} \left\{ \begin{bmatrix} A_{12} & B_1 \mathcal{D}_{\hat{x}_2} \end{bmatrix} \begin{bmatrix} \tilde{x}_2 \\ \tilde{\mu} \end{bmatrix} + E_1 \tilde{\Phi}_2 + B_1 \mathcal{D}_{\hat{x}_2} \mu + F_1 w \right\}
\end{aligned} \tag{4.44}$$

Hence,

$$\begin{aligned}
\begin{bmatrix} \tilde{x}_2 \\ \tilde{\mu} \end{bmatrix}^T \begin{bmatrix} P_{22} & P_{2\mu} \mathcal{D}_{\hat{x}_2} \\ P_{2\mu}^T \mathcal{D}_{\hat{x}_2} & \mathcal{D}_{\hat{x}_2} P_{\mu\mu} \mathcal{D}_{\hat{x}_2} \end{bmatrix} \begin{bmatrix} \dot{\tilde{x}}_2 \\ \dot{\tilde{\mu}} \end{bmatrix} &= \\
\begin{bmatrix} \tilde{x}_2 \\ \mathcal{D}_{\hat{x}_2} \tilde{\mu} \\ \tilde{\Phi}_2 \\ \mathcal{D}_{\hat{x}_2} \mu \\ w \end{bmatrix}^T \begin{bmatrix} P_{22} A_{22} & P_{22} B_2 & P_{22} E_2 & P_{22} B_2 & P_{22} F_2 \\ P_{2\mu}^T A_{22} & P_{2\mu}^T B_2 & P_{2\mu}^T E_2 & P_{2\mu}^T B_2 & P_{2\mu}^T F_2 \\ 0 & 0 & 0 & 0 & 0 \\ 0 & 0 & 0 & 0 & 0 \\ 0 & 0 & 0 & 0 & 0 \end{bmatrix} \begin{bmatrix} \tilde{x}_2 \\ \mathcal{D}_{\hat{x}_2} \tilde{\mu} \\ \tilde{\Phi}_2 \\ \mathcal{D}_{\hat{x}_2} \mu \\ w \end{bmatrix} \\
- \begin{bmatrix} \tilde{x}_2 \\ \mathcal{D}_{\hat{x}_2} \tilde{\mu} \\ \tilde{\Phi}_2 \\ \mathcal{D}_{\hat{x}_2} \mu \\ w \end{bmatrix}^T \begin{bmatrix} X_2 A_{12} & X_2 B_1 & X_2 E_1 & X_2 B_1 & X_2 F_1 \\ X_\mu A_{12} & X_\mu B_1 & X_\mu E_1 & X_\mu B_1 & X_\mu F_1 \\ 0 & 0 & 0 & 0 & 0 \\ 0 & 0 & 0 & 0 & 0 \\ 0 & 0 & 0 & 0 & 0 \end{bmatrix} \begin{bmatrix} \tilde{x}_2 \\ \mathcal{D}_{\hat{x}_2} \tilde{\mu} \\ \tilde{\Phi}_2 \\ \mathcal{D}_{\hat{x}_2} \mu \\ w \end{bmatrix}
\end{aligned} \tag{4.45}$$

Where,

$$X_2 = P_{22} L_2 + P_{2\mu} \mathcal{D}_{\hat{x}_2} L_\mu \text{ and } X_\mu = \mathcal{D}_{\hat{x}_2} P_{2\mu}^T L_2 + \mathcal{D}_{\hat{x}_2} P_{\mu\mu} \mathcal{D}_{\hat{x}_2} L_\mu$$

However, For the dissipative case , $\gamma_2 \geq |D\hat{x}| \geq \gamma_1$, $\max(|(D\hat{x})(D\hat{x})^{-1}|) = \sigma'$ and

$$P_{22} E_2 = \text{eta} * G2' \tag{4.46}$$

$$P_{2\mu}^T E_2 = 0$$

Where $P_{22} > 0$, $\text{eta} > 0$, and $P_{2\mu}^T$ such that $\forall |\sigma'| \leq \sigma'_{max}$

Hence substituting condition (4.46) in

$$(4.45) \text{ and choosing } PL = \begin{bmatrix} X_2 \\ X_\mu \end{bmatrix} = \begin{bmatrix} A_{12}^T \\ 0 \end{bmatrix} Q$$

We get,

$$\begin{bmatrix} \tilde{x}_2 \\ \tilde{\mu} \end{bmatrix}^T \begin{bmatrix} P_{22} & P_{2\mu} \mathcal{D}_{\tilde{x}_2} \\ P_{2\mu}^T \mathcal{D}_{\tilde{x}_2} & \mathcal{D}_{\tilde{x}_2} P_{\mu\mu} \mathcal{D}_{\tilde{x}_2} \end{bmatrix} \begin{bmatrix} \dot{\tilde{x}}_2 \\ \dot{\tilde{\mu}} \end{bmatrix} = \begin{bmatrix} M_{11} & M_{12} & M_{13} & M_{14} \\ M_{12}^T & M_{22} & M_{23} & M_{24} \\ M_{13}^T & M_{23}^T & -\epsilon_i & 0 \\ M_{14}^T & M_{24}^T & 0 & R^{-1} \end{bmatrix} < 0 \quad (4.47)$$

Where,

$$M_{11} = P_{22}A_{22} + A_{22}^T P_{22} - A_{12}^T Q^T A_{12} - A_{12}^T Q A_{12} - \mu_{max}^2 \epsilon_i D_2^T D_2$$

$$M_{12} = P_{22}B_2 + A_{22}^T P_{2\mu} - A_{12}^T Q B_1 + \sigma' P_{2\mu}$$

$$M_{13} = P_{22}B_2 - X_2 B_1$$

$$M_{14} = P_{22}F_2 - X_2 F_1$$

$$M_{22} = B_2^T P_{2\mu}^T + P_{2\mu}^T B_2 + 2\sigma' P_{\mu\mu}$$

$$M_{23} = P_{2\mu}^T B_2$$

$$M_{24} = P_{2\mu}^T F_2$$

Hence, the gains L_2 and L_μ can be calculated from (4.43) by following the same procedure given in the proof of Lemma 4.2.

$$L_2 = [P_{22} - P_{\mu 2}^T P_{\mu\mu}^{-1} P_{\mu 2}]^{-1} A_{12}^T Q \quad (4.48)$$

$$L_{\mu} = -[P_{22} - P_{\mu 2}^T P_{\mu \mu}^{-1} P_{\mu 2}]^{-1} P_{2\mu} P_{\mu \mu}^{-1} (D_{\hat{x}_2})^{-1} A_{12}^T Q \quad (4.49)$$

Where the value of Q can be determined by solving LMI (4.47) .

4.2.5. Example 2: Dissipative nonlinear system

A dissipative nonlinear system consisting of two rotating masses bridged together by a gear train are represented below. The second rotating mass with rotational inertia J_2 , is influenced by a nonlinear viscous drag. Whereas, the linear damping affects both the masses and the gear train .

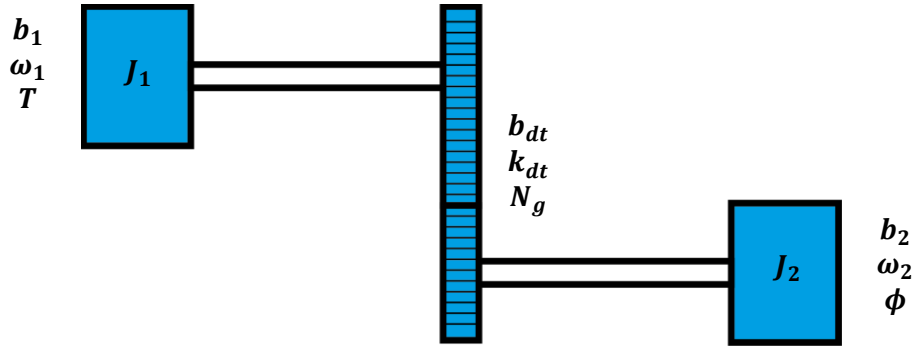


Figure 4.12. Gear train dissipative system

The system dynamics are modeled below

$$J_1 \dot{\omega}_1 = T - k_{dt} \Delta \theta - (b_1 + b_{dt}) \omega_1 + \frac{b_{dt}}{N_g} \omega_2$$

$$J_2 \dot{\omega}_2 = \frac{k_{dt}}{N_g} \Delta \theta + \frac{b_{dt}}{N_g} \omega_1 - \left(b_2 + \frac{b_{dt}}{N_g^2} \right) \omega_2 - \text{sgn}(\omega_2) \times \omega_2^2$$

$$\Delta \dot{\theta} = \omega_1 - \frac{1}{N_g} \omega_2$$

Where,

J_1, J_2 denote the rotational inertia of the two masses

ω_1, ω_2 denote the angular velocities of the two masses

b_1, b_2 denote the linear viscous drag acting on the two masses,

b_{dt} denotes the linear viscous drag at the interface gearbox

k_{dt} denotes the spring constant of the interface gearbox

N_g denotes the gear ratio

The above system is characterized by the following parameters as show in [60],

$$J_1 = J_2 = 1 \text{ kg.m}^2, \quad b_1 = b_2 = 0.1, \quad b_{dt} = 1, \quad k_{dt} = 5 \frac{N}{m}, \quad N_g = 0.5, \quad \omega \sim (0, 0.01),$$

$v \sim (0, 0.04 \times I)$ and represented in its state space form given by:

$$A = \begin{bmatrix} -1.1 & 2 & -5 \\ 2 & -2 & 10 \\ 1 & -2 & 0 \end{bmatrix}, \quad B = \begin{bmatrix} 0 \\ 0 \\ 1 \end{bmatrix}, \quad C = \begin{bmatrix} 1 & 0 & 0 \\ 0 & 1 & 0 \end{bmatrix}, \quad D = [0 \quad 1 \quad 0]$$

$$E = \begin{bmatrix} 0 \\ 1 \\ 0 \end{bmatrix}, \quad H = \begin{bmatrix} 1 \\ 0 \\ 0 \end{bmatrix}, \quad R = 0.001, \quad u = 0.1 \sin(2\pi t), \quad r = 1, \quad \mu = 0.15$$

$$F = \begin{bmatrix} 0.1 \\ 0 \\ 0 \end{bmatrix}, \quad Q = \begin{bmatrix} 0.04 & 0 \\ 0 & 0.04 \end{bmatrix}$$

$$G = [0 \quad 1 \quad 0], \quad \Phi = -\text{sgn}(x_2) \times x_2^2$$

Using an initial condition $x(0) = [5 \quad 5 \quad 5]^T$ and an input $= 0.1 \sin(2\pi t)$, the simulation is performed using MATLAB for a time period of $T_{end} = 10 \text{secs}$. An external disturbance v is also taken into account with a covariance $R = 0.001$ and $Q = 0.004$. The unknown input μ is assumed to have an actual value of $\mu = 0.15$ and the initial value for the μ estimate is taken as $\mu(0) = 0$. The calculations yield the following results:

$$\bar{L}_2 = [-0.1709 \quad 0.0105]$$

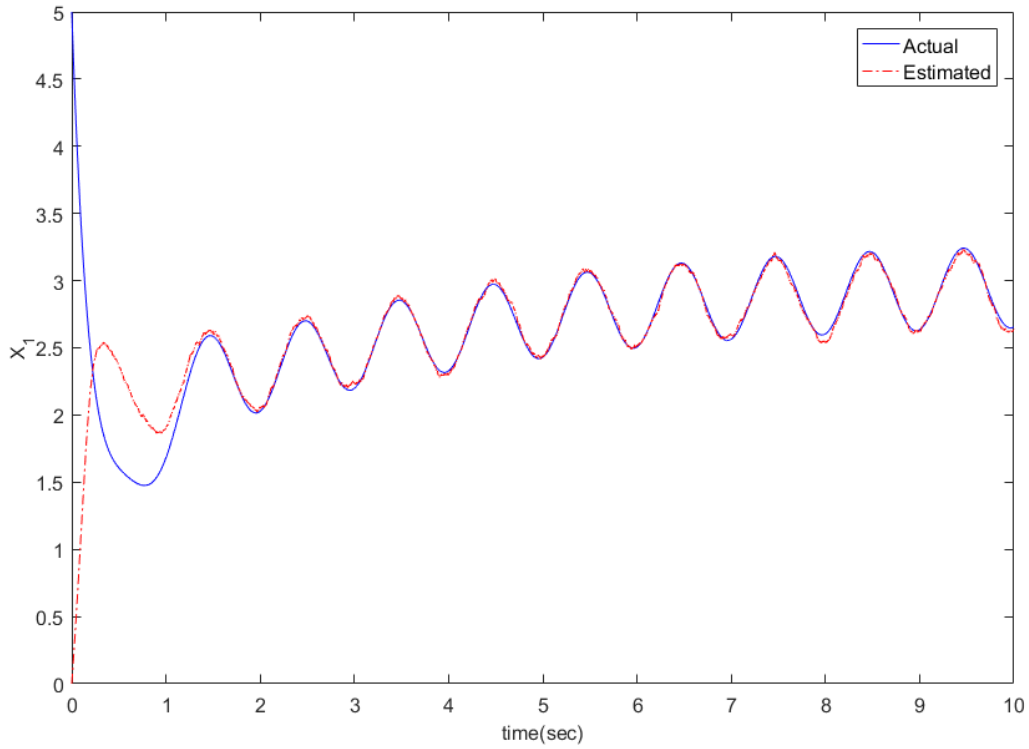


Figure 4.13. Estimation of state X_1

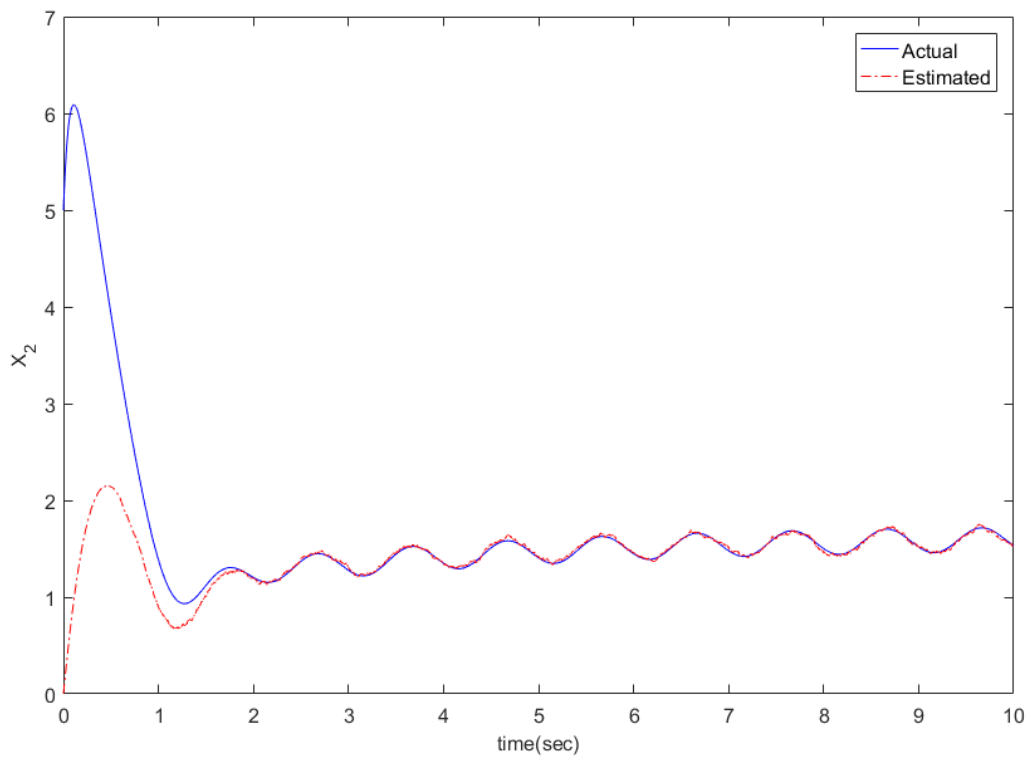


Figure 4.14. Estimation of state X_2

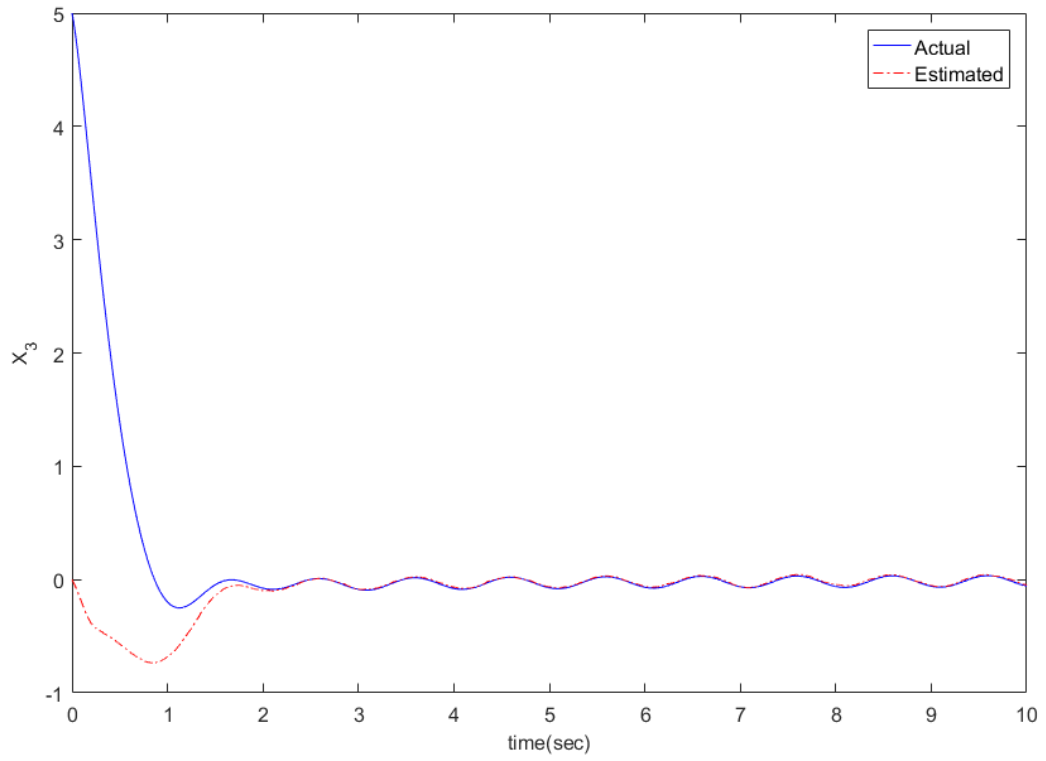


Figure 4.15. Estimation of state X_2

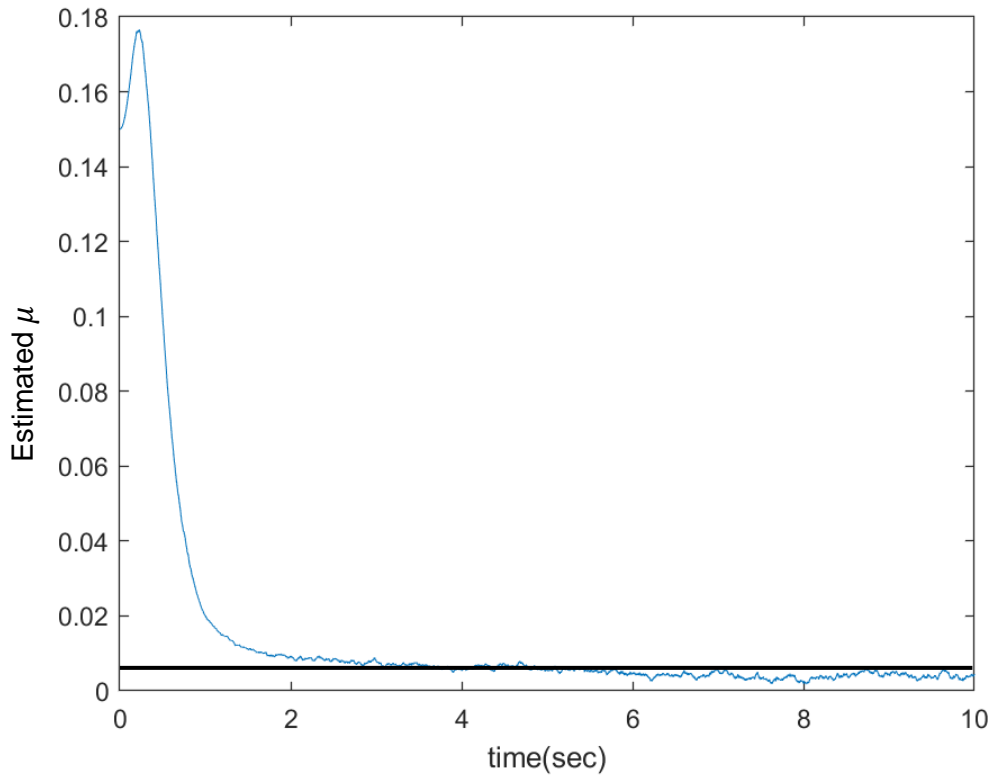


Figure 4.16. Unknown Parameter ' μ ' Estimation

Form the above simulations, we can see that the both the states and the unknown system parameters are estimated and rapidly converge to their true values (For unknown parameter = 0.15). The convergence rate is improved considerably as compared to the rate seen in [60] for the same system with the same parameters as seen above.

Chapter 5.

Conclusion and Future work

Having a highly robust and efficient adaptive observer can be very effective in solving issues related to state and parameter estimation in nonlinear systems. This dissertation presents a sliding mode observer design for wide range of nonlinear systems. With the use of the proposed time averaged Lyapunov functional, the observer design tends to be highly robust against system noise and external disturbances acting on the system.

The time averaged Lyapunov functional is initially used to analyze the choice of covariance and sliding mode gain parameters so that the convergence rate of the estimation error can be improved. The simulation results provide a detailed look at the behaviour of the observed states and the how the system noise affects the convergence rate. For a Lipschitz nonlinear system, the observer design provides an existence condition which is significantly less conservative as compared to linear gain observers given in literature. The results of the proposed observer are compared with those of the linear gain observer to further validate the case. Since the observer design is formulated as a dynamic constrained optimization problem, suitable cost functions are defined to guarantee minimization of the state estimation errors. Hence, the observer is able to accurately estimate the states and efficiently converge to its true state value.

Furthermore, the observer developed for the generalized sector bounded case, successfully predicts an unknown system parameter whilst simultaneously estimating the system states. Since the observer design reduces the size of the \mathcal{D} matrix, it makes it significantly easier to solve mathematically. This can be used as an added advantage to solve mathematically complex systems where the unknown parameter affects multiple states. Later, the design is extended to a dissipative nonlinear case where again the observer performs robustly and estimates both the unknown parameters and states accurately. The design is implemented to both a 4th order nonlinear system and a highly dissipative nonlinear gear train system respectively, where the effect of noise and disturbances on the system model is substantial.

The universality of the nonlinearities considered for the observer design allows us to extend this design to a wide class of physical systems. All the observer existence conditions and gain selection approaches have been presented in the form of Linear Matrix Inequalities (LMIs) which can be explicitly solved offline using commercial LMI solvers (MATLAB). This makes the design computationally less intensive as compared to an EKF which requires an online solution. Also, the proposed observer presents smaller initial state estimation errors as compared to the extended Kalman filter based observer. Furthermore, the observer design doesn't require precise knowledge of noise covariance matrices as compared to Extended Kalman Filters. Overall, the sliding mode observer design presented in this dissertation is very robust to external disturbances and can effectively estimate the unknown parameter and state variables present in the system.

For future research, the following extensions can be made to this work:

- Extending the results for fault detection , estimation and fault tolerant control
- Extending the results to systems with time-varying parameters
- Design the Sliding mode observer using a fractional order super-twisting algorithm to deal with phenomenon the chattering

References

- [1] G. H. Ellis, *Observers in control systems: a practical guide*. 2002.
- [2] C. H. Lien, "Robust observer-based control of systems with state perturbations via LMI approach," *IEEE Trans. Automat. Contr.*, vol. 49, no. 8, pp. 1365–1370, 2004.
- [3] L. Rodrigues and J. P. How, "Observer-based control of piecewise-affine systems," *Proc. IEEE Conf. Decis. Control*, vol. 2, pp. 1366–1371, 2001.
- [4] X. Jin and K. Hirakawa, "Approximations to camera sensor noise," 2013, vol. 8655, p. 86550H.
- [5] Y. Zhang and A. Srivastava, "Accurate Temperature Estimation Using Noisy Thermal Sensors for Gaussian and Non-Gaussian Cases," *IEEE Trans. Very Large Scale Integr. Syst.*, vol. 19, no. 9, pp. 1617–1626, Sep. 2011.
- [6] C. Mitsantisuk, K. Ohishi, S. Urushihara, and S. Katsura, "Kalman Filter-Based Disturbance Observer and its Applications to Sensorless Force Control," *Adv. Robot.*, vol. 25, no. 3–4, pp. 335–353, Jan. 2011.
- [7] V. Sundarapandian, "Exponential observer design for nonlinear systems with real parametric uncertainty," *Math. Comput. Model.*, vol. 37, no. 1–2, pp. 177–190, Jan. 2003.
- [8] J. Deutscher, "Numerical design of nonlinear observers with approximately linear error dynamics," in *Proceedings of the 2006 IEEE Conference on Computer Aided Control Systems Design, CACSD, 2007*, pp. 2985–2990.
- [9] S. P. Banks, "A note on non-linear observers," *Int. J. Control*, vol. 34, no. 1, pp. 185–190, 1981.
- [10] D. Bestle and M. Zeitz, "Canonical form observer design for non-linear time-variable systems," *Int. J. Control*, vol. 38, no. 2, pp. 419–431, 1983.
- [11] Fengjun Yan and Junmin Wang, "In-cylinder oxygen mass fraction cycle-by-cycle

- estimation via a lyapunov-based observer design,” *Proc. 2010 Am. Control Conf.*, pp. 652–657, 2010.
- [12] A. F. Lynch and S. A. Bortoff, “Nonlinear observers with approximately linear error dynamics: The multivariable case,” *IEEE Trans. Automat. Contr.*, vol. 46, no. 6, pp. 927–932, 2001.
- [13] Z. Ding, “Observer design in convergent series for a class of nonlinear systems,” *IEEE Trans. Automat. Contr.*, vol. 57, no. 7, pp. 1849–1854, 2012.
- [14] W. Baumann and W. Rugh, “Feedback control of nonlinear systems by extended linearization,” *IEEE Trans. Automat. Contr.*, vol. 31, no. 1, pp. 40–46, 1986.
- [15] H. Cho, J. Yang, and J. H. Seo, “Geometric characterization of reduced-order dynamic observer error linearization for uncontrolled multi-output systems,” in *Proceedings of the IEEE Conference on Decision and Control*, 2012, pp. 338–343.
- [16] S. Mehta and K. Vijayaraghavan, “Analysis of Sliding Mode Observers using a Novel Time-Averaged Lyapunov Function,” in *ASME 2017 International Design Engineering Technical Conferences and Computers and Information in Engineering Conference IDETC2017*, 2017.
- [17] A. Howell and J. K. Hedrick, “Nonlinear observer design via convex optimization,” in *Am. Control Conf.*, 2002, pp. 2088–2093.
- [18] J. Lei and H. K. Khalil, “High-gain observers in the presence of sensor nonlinearities,” in *American Control Conference (ACC), 2017*, 2017.
- [19] J. Birk and M. Zeitz, “Extended luenberger observer for non-linear multivariable systems,” *Int. J. Control*, vol. 47, no. 6, pp. 1823–1836, 1988.
- [20] S. Raghavan and J. K. Hedrick, “Observer design for a class of nonlinear systems,” *Int. J. Control*, vol. 59, no. 2, pp. 515–528, 1994.
- [21] A. A. Prasov and H. K. Khalil, “A nonlinear high-gain observer for systems with measurement noise in a feedback control framework,” *IEEE Trans. Automat.*

- Contr.*, vol. 58, no. 3, pp. 569–580, 2013.
- [22] N. Kazantzis and C. Kravaris, “Nonlinear observer design using Lyapunov’s auxiliary theorem,” *Proc. 36th IEEE Conf. Decis. Control*, vol. 5, no. June 1997, pp. 241–247, 1997.
- [23] G. I. Bara, A. Zemouche, and M. Boutayeb, “Observer synthesis for Lipschitz discrete-time systems,” in *Proceedings - IEEE International Symposium on Circuits and Systems*, 2005, pp. 3195–3198.
- [24] a. J. Krener and W. Respondek, “Nonlinear observers with linearizable error dynamics,” *J. Control Optim.*, vol. 23, no. 2, pp. 197–216, 1985.
- [25] B. L. Walcott, M. J. Corless, and S. H. ??ak, “Comparative study of non-linear state-observation techniques,” *Int. J. Control*, vol. 45, no. 6, pp. 2109–2132, 1987.
- [26] A. M. Pertew, H. J. Marquez, and Q. Zhao, “LMI-based sensor fault diagnosis for nonlinear Lipschitz systems,” *Automatica*, vol. 43, no. 8, pp. 1464–1469, 2007.
- [27] R. Rajamani, “Observers for Lipschitz nonlinear systems,” *IEEE Trans. Automat. Contr.*, vol. 43, no. 3, pp. 397–401, 1998.
- [28] R. Rajamani and Y. M. Cho, “Existence and design of observers for nonlinear systems: Relation to distance to unobservability,” *Int. J. Control*, vol. 69, no. 5, pp. 717–731, Jan. 1998.
- [29] F. Zhu and Z. Han, “A note on observers for Lipschitz nonlinear systems,” *Autom. Control. IEEE Trans.*, vol. 47, no. 10, pp. 1751–1754, 2002.
- [30] A. Zemouche, M. Boutayeb, and G. I. Bara, “Observers for a class of Lipschitz systems with extension to Hinfinity performance analysis,” *Syst. Control Lett.*, vol. 57, no. 1, pp. 18–27, Jan. 2008.
- [31] J. Huang, Z. Han, X. Cai, and L. Liu, “Adaptive full-order and reduced-order observers for the Lur’e differential inclusion system,” *Commun. Nonlinear Sci. Numer. Simul.*, vol. 16(7), pp. 2869–2879, 2011.
- [32] R. Rajamani and A. Ganguli, “Sensor fault diagnostics for a class of non-linear

systems using linear matrix inequalities,” *Int. J. Control*, vol. 77, no. 10, pp. 920–930, Jul. 2004.

- [33] K. Vijayaraghavan, R. Rajamani, and J. Bokor, “Quantitative fault estimation for a class of nonlinear systems,” *Int. J. Control*, vol. 80, no. 1, pp. 64–74, 2007.
- [34] K. Vijayaraghavan, “Nonlinear observer for simultaneous states and unknown parameter estimation,” *Int. J. Control*, vol. 86, no. 12, pp. 2263–2273, 2013.
- [35] A. Zemouche, R. Rajamani, H. Kheloufi, and F. Bedouhene, “Robust observer-based stabilization of Lipschitz nonlinear uncertain systems via LMIs - discussions and new design procedure,” *Int. J. Robust Nonlinear Control*, vol. 27, no. 11, pp. 1915–1939, 2017.
- [36] G. Phanomchoeng and R. Rajamani, “Observer design for Lipschitz nonlinear systems using Riccati equations,” in *American Control Conference ACC 2010*, 2010, pp. 6060–6065.
- [37] G. Phanomchoeng, R. Rajamani, and D. Piyabongkarn, “Nonlinear Observer for Bounded Jacobian Systems, With Applications to Automotive Slip Angle Estimation,” *IEEE Trans. Automat. Contr.*, vol. 56, no. 5, pp. 1163–1170, May 2011.
- [38] M. Arcak and P. Kokotovic, “Nonlinear observers : a circle criterion design and robustness analysis,” *Automatica*, vol. 37, pp. 1923–1930, 2001.
- [39] X. Fan and M. Arcak, “Observer design for systems with multivariable monotone nonlinearities,” *Syst. Control Lett.*, vol. 50, no. 4, pp. 319–330, 2003.
- [40] F. E. Thau, “Observing the state of non-linear dynamic systems†,” *Int. J. Control*, vol. 17, no. March 2013, pp. 471–479, 1973.
- [41] S. R. Kou, D. L. Elliott, and T. J. Tarn, “Exponential Observers for Nonlinear Dynamic Systems 1,” *Inf. Control*, vol. 29, pp. 204–216, 1975.
- [42] S. R. Kou, D. L. Elliott, and T. J. Tarn, “Exponential Observers for Nonlinear Dynamic Systems 1,” *Inf. Control*, vol. 29, pp. 204–216, 1975.

- [43] T. Meurer, "On the extended luenberger-type observer for semilinear distributed-parameter systems," *IEEE Trans. Automat. Contr.*, vol. 58, no. 7, pp. 1732–1743, 2013.
- [44] a. J. Krener and A. Isidori, "Linearization by output injection and nonlinear observers," *Syst. Control Lett.*, vol. 3, no. 47–52, 1983.
- [45] R. Marino, "Adaptive Observers for Single Output Nonlinear Systems," *IEEE Trans. Automat. Contr.*, vol. 35, no. 9, pp. 1054–1058, 1990.
- [46] H. K. Khalil, *Nonlinear Systems 3rd Edition*. Prentice Hall, 2002.
- [47] H. K. Khalil, "High-gain observers in nonlinear feedback control," in *New Directions in nonlinear observer design*, London: Springer London, 1999, pp. 249–268.
- [48] Z.-P. Jiang and L. Praly, "Iterative designs of adaptive controllers for systems with nonlinear integrators," in *[1991] Proceedings of the 30th IEEE Conference on Decision and Control*, pp. 2482–2487.
- [49] D. Seto, A. M. Annaswamy, and J. Baillieul, "Adaptive control of nonlinear systems with a triangular structure," *IEEE Trans. Automat. Contr.*, vol. 39, no. 7, pp. 1411–1428, Jul. 1994.
- [50] M. M. Polycarpou and P. A. Ioannou, "A robust adaptive nonlinear control design," *Automatica*, vol. 32, no. 3, pp. 423–427, Mar. 1996.
- [51] I. Kanellakopoulos, P. V. Kokotovic, and A. S. Morse, "Systematic Design of Adaptive Controllers for Feedback Linearizable Systems," *IEEE Trans. Automat. Contr.*, vol. 36, no. 11, pp. 1241–1253, 1991.
- [52] M. Krstić, I. Kanellakopoulos, and P. V. Kokotović, "Adaptive nonlinear control without overparametrization," *Syst. Control Lett.*, vol. 19, no. 3, pp. 177–185, 1992.
- [53] G. Bastin and M. R. Gevers, "Stable Adaptive Observers for Nonlinear Timevarying Systems," *IEEE Trans. Automat. Contr.*, vol. 33, no. 7, pp. 650–658,

1988.

- [54] G. Besançon, J. De León-Morales, and O. Huerta-Guevara, "On adaptive observers for state affine systems," *Int. J. Control*, vol. 79, no. 6, pp. 581–591, Jun. 2006.
- [55] J. Jung, K. Huh, H. K. Fathy, and J. L. Stein, "Optimal robust adaptive observer design for a class of nonlinear systems via an H-infinity approach," *Proc. 2006 Am. Control Conf.*, pp. 3637–3642, 2006.
- [56] R. Rajamani and J. K. Hedrick, "Adaptive Observers for Active Automotive Suspensions: Theory and Experiment," *IEEE Trans. Control Syst. Technol.*, vol. 3, no. 1, pp. 86–93, 1995.
- [57] Y. M. Cho and R. Rajamani, "A systematic approach to adaptive observer synthesis for nonlinear systems," *IEEE Trans. Automat. Contr.*, vol. 42, no. 4, pp. 534–537, 1997.
- [58] M. Pourgholi and V. J. Majd, "A nonlinear adaptive resilient observer design for a class of Lipschitz systems using LMI," *Circuits, Syst. Signal Process.*, vol. 30, no. 6, pp. 1401–1415, 2011.
- [59] K. Vijayaraghavan, "Nonlinear observer for simultaneous states and unknown parameter estimation," *Int. J. Control*, vol. 86, no. 12, pp. 2263–2273, Dec. 2013.
- [60] K. Vijayaraghavan and A. Valibeygi, "Adaptive nonlinear observer for state and unknown parameter estimation in noisy systems," *Int. J. Control*, vol. 89, no. July, pp. 1–17, Jan. 2015.
- [61] L.-C. Zai, C. L. DeMarco, and T. A. Lipo, "An extended Kalman filter approach to rotor time constant measurement in PWM induction motor drives," *Ind. Appl. IEEE Trans.*, vol. 28, no. 1, pp. 96–104, 1992.
- [62] T. Kataoka, S. Toda, and Y. Sato, "On-line estimation of induction motor parameters by extended Kalman filter," *Fifth Eur. Conf. Power Electron. Appl.*, vol. 4, pp. 325–329, 1993.

- [63] E. a. A. Wan and R. Van Der Merwe, "The unscented Kalman filter for nonlinear estimation," *Technology*, vol. v, pp. 153–158, 2000.
- [64] S. J. Julier and J. K. Uhlmann, "Unscented Filtering and Nonlinear Estimation," *Proc. IEEE*, vol. 92, no. 3, pp. 401–422, Mar. 2004.
- [65] S. S. Bisht and M. P. Singh, "An adaptive unscented Kalman filter for tracking sudden stiffness changes," *Mech. Syst. Signal Process.*, vol. 49, no. 1–2, pp. 181–195, Dec. 2014.
- [66] C. Moons and B. De Moor, "Parameter identification of induction motor drives," *Automatica*, vol. 31, no. 8, pp. 1137–1147, 1995.
- [67] S. Boyd, L. El Ghaoui, E. Feron, and V. Balakrishnan, *Linear Matrix Inequalities in System and Control Theory SIAM Studies in Applied Mathematics*. SIAM, 1994.
- [68] J. H. Ahrens and H. K. Khalil, "High-gain observers in the presence of measurement noise: A switched-gain approach," *Automatica*, vol. 45, no. 4, pp. 936–943, Apr. 2009.
- [69] F. Esfandiari and H. K. Khalil, "Output feedback stabilization of fully linearizable systems," *Int. J. Control*, vol. 56, no. 5, pp. 1007–1037, 1992.
- [70] H. K. Khalil and L. Praly, "High-gain observers in nonlinear feedback control," *Int. J. Robust Nonlinear Control*, vol. 24, no. 6, pp. 993–1015, Apr. 2014.
- [71] S. V. Drakunov and V. I. Utkin, "Sliding Mode Control in Dynamic Systems," *Int. J. Control*, vol. 55, no. 4, pp. 1029–1037, 1992.
- [72] C. Edwards and S. Spurgeon, *Sliding Mode Control: Theory And Applications*. CRC Press, 1998.
- [73] C. Edwards, S. K. Spurgeon, and R. J. Patton, "Sliding mode observers for fault detection and isolation," *Automatica*, vol. 36, no. 4, pp. 541–553, 2000.
- [74] C. P. Tan and C. Edwards, "Sliding mode observers for detection and reconstruction of sensor faults," *Automatica*, vol. 38, no. 10, pp. 1815–1821, 2002.

- [75] A. Alessandri, "Sliding-mode estimators for a class of non-linear systems affected by bounded disturbances," *Int. J. Control*, vol. 76, no. 3, pp. 226–236, Jan. 2003.
- [76] F. Chen, R. Jiang, K. Zhang, B. Jiang, and G. Tao, "Robust Backstepping Sliding Mode Control and Observer-based Fault Estimation for a Quadrotor UAV," *IEEE Trans. Ind. Electron.*, pp. 1–1, 2016.
- [77] J. He, L. Mi, S. Mao, C. Zhang, and H. Chu, "Fault-Tolerant Control of a Nonlinear System Actuator Fault Based on Sliding Mode Control," *J. Control Sci. Eng.*, vol. 2017, pp. 1–13, 2017.
- [78] R. Galván-Guerra, L. Fridman, and J. Dávila, "High-order sliding-mode observer for linear time-varying systems with unknown inputs," *Int. J. Robust Nonlinear Control*, 2016.
- [79] D. Efimov and L. Fridman, "Global sliding-mode observer with adjusted gains for locally Lipschitz systems," *Automatica*, vol. 47, no. 3, pp. 565–570, Mar. 2011.
- [80] S. K. Spurgeon, "Sliding Mode Observers - A Survey," *Int. J. Syst. Sci. Vol. 39, No. 8, August 2008, pp. 751–764*, vol. 39, No. 8, no. August, pp. 37–41, 2008.
- [81] B. L. Walcott and S. H. Zak, "State observation of nonlinear uncertain dynamical systems," *IEEE Trans. Automat. Contr.*, vol. AC-32, no. 8612207, pp. 166–170, 1987.
- [82] K. C. Veluvolu and Y. C. Soh, "High-gain observers with sliding mode for state and unknown input estimations," *IEEE Trans. Ind. Electron.*, vol. 56, no. 9, pp. 3386–3393, 2009.
- [83] A. N. Michel and L. Hou, "Nonlinear Analysis : Hybrid Systems Stability results involving time-averaged Lyapunov function derivatives," vol. 3, pp. 51–64, 2009.
- [84] V. L. Kharitonov and A. P. Zhabko, "Lyapunov–Krasovskii approach to the robust stability analysis of time-delay systems," *Automatica*, vol. 39, no. 1, pp. 15–20, Jan. 2003.
- [85] F. Mazenc, S. I. Niculescu, and M. Krstic, "Lyapunov-Krasovskii functionals and

- application to input delay compensation for linear time-invariant systems,” *Automatica*, vol. 48, no. 7, pp. 1317–1323, 2012.
- [86] V. Sharma, B. B. Sharma, and R. Nath, “Nonlinear unknown input sliding mode observer based chaotic system synchronization and message recovery scheme with uncertainty,” *Chaos, Solitons & Fractals*, vol. 96, pp. 51–58, 2017.
- [87] O. E. Rössler, “An equation for continuous chaos,” *Phys. Lett. A*, vol. 57, no. 5, pp. 397–398, 1976.
- [88] P. Gaspard, “Rössler Systems,” *Encycl. Nonlinear Sci.*, pp. 808–811, 2005.
- [89] S. S. Delshad, T. Gustafsson, H. R. Karimi, and A. Zemouche, “Observer-based control design for a class of nonlinear systems subject to unknown inputs: LMI approach,” in *2015 15th International Conference on Control, Automation and Systems (ICCAS)*, 2015, pp. 984–989.
- [90] H. K. Khalil, *Nonlinear Systems, Third Edition*. 2002.
- [91] M. W. Spong, “Modeling and Control of Elastic Joint Robots,” *J. Dyn. Syst. Meas. Control*, vol. 109, no. 4, pp. 310–319, 1987.
- [92] K. Vijayaraghavan, “Observer design for generalized sector-bounded noisy nonlinear systems,” *Proc. Inst. Mech. Eng. Part I J. Syst. Control Eng.*, vol. 228, no. 9, pp. 645–657, Sep. 2014.
- [93] G. Phanomchoeng and R. Rajamani, “Observer Design for Lipschitz Nonlinear Systems Using Riccati Equations,” *Proc. Am. Control Conf.*, pp. 6060–6065, 2010.